Variability of Sea Surface Temperature in North-West Pacific Ocean in the Period from January 1990 to December 2022

A Dissertation for

Course code and Course Title: MSC 617-Discipline Specific Dissertation

Credits:16

Submitted in partial fulfilment of Master Degree

(M.Sc.) in Marine Sciences

by

SHLESHMITA SHAILESH PEDNEKAR

Seat Number: 22P0400018

ABC ID: 879785041016

PRN: 201302993

Under the Supervision of

DR. JOSHUA ROSARIO D'MELLO

School of Earth, Ocean and Atmospheric Sciences

Marine Sciences

Goa University

April 2024

SEOAS, GOA UNIVERSITY
TALEIGAO PLATEAU GOA

Examined by:

Seal of the School.

DECLARATION BY STUDENT

I hereby declare that the data presented in this Dissertation entitled "Variability of Sea Surface Temperature in North-West Pacific Ocean in the Period from January 1990 to December 2022" is based on the results of investigation carried out by me in the Marine Sciences at the School of Earth, Ocean and Atmospheric Sciences, Goa University under the Supervision/ Mentor-ship of Dr. Joshua Rosario D'Mello and the same has not been submitted elsewhere for the award of a degree or diploma by me. Further, I understand that Goa University or its authorities will be not be responsible for the correctness of observation / experimental or other finding given the dissertation.

I hereby authorize the university authorities to upload this dissertation on the dissertation repository or anywhere else as the UGC regulations demand and make it available to any one as needed.

Pednekar

(Shleshmita Shailesh Pednekar)

Seat No.:22P0400018

Date: 16/4/2024

Place: Goa University

COMPLETION CERTIFICATE

This is to certify that the dissertation entitled as **"Variability of Sea Surface Temperature in the North-West Pacific Ocean in Period from January 1990 to December 2022."** is a bonafide work carried out by **Ms. Shleshmita Shailesh Pednekar** under my supervision in partial fulfilment of the requirements for the award of the degree of **Master of Science** in the Discipline Marine Sciences at the School of Earth, Ocean and Atmospheric Sciences, Goa University.

16-04-2024

Date: 16th of April 2024

(Dr. Joshua Rosario D'Mello)
School of Earth, Ocean and Atmospheric Sciences,
Goa University

29/4/24

Dean of School of Earth, Ocean and Atmospheric Sciences,
Goa University

SEOAS, GOA UNIVERSITY
TALEIGAO PLATEAU
GOA

School Stamp

Date: 29/4/24

Place: Goa University

CONTENTS

PREFACE

This study intends to explore how the temperature of the sea's surface changes in the north-west Pacific Ocean. The study intends to understand how the temperature changes over time using recently measured data. By analysing data and using computer programs to help us, the study sees patterns in the temperature data. Our goal is to share what we've learned to help others understand more about the ocean and its role in the Earth's climate.

ACKNOWLEDGEMENTS

The success and final outcome of the dissertation required a lot of guidance and assistance from various people, and I am fortunate to have received this along with the completion of the project work.

Firstly, I would like to express my gratitude to God, and I am thankful to my parents and family members for supporting and believing in me.

It gives me pleasure and honour to express my deep gratitude and heartiest thanks to my guide, Dr. Joshua R. D'Mello, Assistant Professor at the School of Earth, Ocean and Atmospheric Sciences, Goa University, for his valuable guidance, his time and constant support he provided during the entire duration of this dissertation.

I express my sincere gratitude to Sr. Prof. Dr. C.U. Rivonker, former Dean of the School of Earth, Ocean and Atmospheric Sciences, Goa University, for his support and provision of necessary facilities during the completion of my work. Furthermore, I would like to also thank to Dr. Sanjeev C. Ghadi, the current Dean of the School of Earth, Ocean and Atmospheric Sciences.

Additionally, I would like to thank the data providers – the data is of Sea Surface Temperature is from HadISST Average Sea Surface Temperature. It is downloaded from the webpage https://coastwatch.pfeg.noaa.gov/erddap/griddap/erdHadISST.html on 7 December 2023.

I wish to acknowledge using the PyFerret program for analysis and graphics in this dissertation work. PyFerret is a product of the National Oceanic and

Atmospheric Administration's (NOAA) Pacific Marine Environmental Laboratory (PMEL) (Information is available at http://ferret.pmel.noaa.gov/Ferret/).

Lastly but not the least, my sincere gratitude to all my friends and classmates for helping me and supporting me throughout my dissertation work.

LIST OF TABLES

LIST OF FIGURES

LIST OF ABBREVIATIONS, SYMBOLS AND UNITS

Abbreviation, Symbol or Unit	Expansion
°	Degree
°C	degree Celsius
°C/decade	degree Celsius per decade
°C/year	degree Celsius per year
%	Percentage
AR5	Fifth Assessment Report
AUVs	Autonomous underwater vehicles
AVHRR	Advanced Very-High-Resolution Radiometer
E	East
ECS	East China Sea
ENSO	El Niño-Southern Oscillation
Eq	Equator
Ft	feet
HadISST	Hadley Centre Sea Ice and Sea Surface Temperature
In	inches
IPCC	Intergovernmental Panel on Climate Change
IPO	Interdecadal Pacific Oscillation
KE	Kuroshio Extension
Km	Kilometre
mm/year	millimetre per year
MODIS	Moderate Resolution Imaging Spectroradiometer

N	North
NCEP	National Centers for Environmental Prediction
NEC	North Equatorial Current
NECC	North Equatorial Counter-current
NIO	North Indian Ocean
NOAA	National Oceanic and Atmospheric Administration
NP-SAFZ	North Pacific subarctic Oceanic Frontal Zones
NP-STFZ	North Pacific subtropical Oceanic Frontal Zones
NWPac	northwest Pacific
OFZ	Oceanic Frontal Zones
OGCM	Ocean General Circulation Model
PDO	Pacific Decadal Oscillation
PMEL	Pacific Marine Environmental Laboratory
PWP	Pacific Warm Pool
R^2	Coefficient of Determination
SCS	South China Sea
SSH	Sea Surface Height
SST	Sea Surface Temperature
Sv	Sverdrup
TC	Tropical Cyclone
W	West
WBCs	Western Boundary Current
WPWP	Western Pacific Warm Pool

LIST OF PROGRAMS

ABSTRACT

This study investigates the variability of Sea Surface Temperature (SST) patterns in the north-west Pacific Ocean from January 1990 to December 2022, focusing on average values and trends at monthly, seasonal and the entire study's time-period. Utilizing data from the Hadley Centre Sea Ice and Sea Surface Temperature (HadISST) dataset, we identify regions with notably high and low SST averages, monthly, seasonally and a long-term average for the entire study period. The average SST map ranges from 13.14 °C to 29.77 °C when averaged for the entire time period. Most of the region shows positive SST trends, indicating overall warming. The basin-averaged SST is 26.17 °C for the entire study-period from January 1990 to December 2022, with monthly basin-averages peaking in August and showing the least values in February. Seasonal variations are evident, with Boreal Autumn exhibiting the highest average and Boreal Spring the lowest. Trendline analysis shows varying rates of change over the various parts of the north-west Pacific Ocean are seen. These findings enhance our understanding of SST variability in the north-west Pacific Ocean and can help improve its application in climate and other studies.

KEYWORDS

Sea surface Temperature (SST);

Variability;

north-west Pacific Ocean (0 °N to 40 °N, 99 °E to 170 °W);

January 1990 to December 2022;

Average;

Trends

CHAPTER 1: INTRODUCTION

1.1 BACKGROUND

The temperature of the water at the ocean's surface, known as sea surface temperature (SST), is an essential physical characteristic of the world's oceans. The surface temperature of the world's seas varies mainly with latitude, with warmest waters around the equator and coldest waters in the Arctic and Antarctic areas *(Minnett, 2014)*.

The SST (SST) or ocean surface temperature is the ocean's temperature near the surface. The precise meaning of the surface depends on how we measure it. It is located between 1 millimetre (0.04 in) and 20 metres (70 ft) below the level of the sea. SST significantly impact air masses in the Earth's atmosphere within a short distance of the shore. Localized patches of heavy snow can form in bands downwind of warm water bodies in an otherwise cold air mass. Warm SSTs can cause and enhance cyclones over the ocean. Experts refer to this process as tropical cyclogenesis. Tropical cyclones can also leave a cold wake *(D'Mello and Prasanna Kumar, 2016)*. This is due to turbulent mixing in the upper 30 meters (100 feet) of the ocean. The sea surface temperature varies during the day. This is similar to the air above it, albeit to a lower degree. The SST varies less on breezy days than on calm days. Ocean currents like the Atlantic Multidecadal Oscillation can have long-term effects on SST. Thermohaline circulation significantly impacts average SST across most of the world's seas. Coastal SSTs can cause offshore winds to produce upwelling, which can dramatically chill or warm neighbouring landmasses, but shallower seas over a continental shelf are often warmer. Onshore winds can induce significant warming even in locations with somewhat consistent upwelling, such as South America's northwest coast. Its values are essential in numerical weather prediction because SST influences the atmosphere above, resulting in the production of sea breezes and fog. It is also used to calibrate data from weather satellites. It is very likely that global mean SST increased by 0.88°C between 1850-1900 and 2011-2020 as a result of global warming, with the majority of that rise (0.60°C) occurring between 1980 and 2020. Land surface temperatures have risen faster than ocean temperatures, as the ocean absorbs around 92% of the surplus heat produced by climate change (https://en.wikipedia.org/wiki/Sea_surface_temperature).

The temperature of the top few millimetres of the ocean is defined as SST. This temperature has an effect on the rate of all physical, chemical, and biological activities in the ocean, either directly or indirectly. Sensors aboard satellites, buoys, ships, ocean reference stations, autonomous underwater vehicles (AUVs), and other technologies monitor SST across the world.

SST monitoring provides key data on the global climate system as well as information on how the ocean and atmosphere interact. This data also helps us predict the commencement of El Niño and La Niña cycles, which are multi-year swings in atmospheric pressure and wind speeds. These variations have an impact on ocean circulation, global weather patterns, and marine ecosystems. Anomalies in SST have been connected to shifting marine resources. Warming temperatures cause fish and other animals to migrate poleward (https://ecowatch.noaa.gov/thematic/sea-surface-temperature) Temperature measurements are accompanied by an indication of the depth of measurement. This is due to significant differences in measurements taken at different depths, particularly during the day when low wind speed and high sunshine conditions may result in the formation of a warm layer at the ocean's surface and strong vertical temperature gradients (a diurnal thermocline). Measurements of SST are limited to the top layer of the ocean, known as the near-surface layer (https://en.wikipedia.org/wiki/Sea_surface_temperature).

SST has been recorded using mercury-in-glass thermometers in buckets containing salt-water gathered by lowering them from ships, as well as thermistors on buoys or in ship engine-cooling-water intakes in recent decades. These thermometers record temperatures at depths ranging from tens of centimetres to a few meters, which is commonly referred to as the "bulk" SST. It has recently become acknowledged that it is preferable to include the depth of the measurement since vertical gradients can exist in the upper few meters of the water column. Remotely sensed SST readings from satellite infrared radiometers are of a temperature very close to the sea surface, sometimes known as skin temperature. The skin temperature is near to the temperature of the ocean in contact with the atmosphere, making it a crucial parameter for controlling heat and gas fluxes between the ocean and the atmosphere (*Minnett ,2014)*.

SST measurements are crucial for understanding and monitoring oceanic conditions, which have significant implications for weather forecasting, climate studies, marine ecosystems, and various other fields. Several techniques are used to measure SST:

1. Infrared Radiometry: One of the primary methods for measuring SST is through infrared radiometry. Satellites equipped with infrared sensors capture

thermal radiation emitted by the ocean's surface in the infrared part of the electromagnetic spectrum. This data allows the calculation of SST based on the temperature-related emissions detected. These sensors are sensitive to the temperature of the water at the very top surface layer.

2. Microwave Radiometry: Microwave sensors on satellites can also be used to measure SST. Unlike infrared sensors, microwave sensors can penetrate through clouds and are operational even under cloudy conditions. However, their spatial resolution might not be as high as infrared sensors.

3. In-situ Measurements: Direct measurements taken in-situ, using buoys, ships, or floats equipped with temperature sensors, are also used to measure SST. These sensors are immersed in the water and can provide high-precision measurements at specific locations.

4. Drifters and Argo Floats: Drifters and Argo floats are automated instruments that periodically collect and transmit oceanic data, including temperature measurements, from various ocean depths. These devices move with ocean currents and provide valuable data for monitoring SST on a broader scale.

5. Satellite Radiometer Sensors: Instruments like the Advanced Very-High-Resolution Radiometer (AVHRR) and the Moderate Resolution Imaging Spectroradiometer (MODIS) onboard various Earth-observing satellites measure SST by detecting the thermal radiation emitted from the ocean surface (https://www.remss.com/measurements/sea-surface-temperature/).

The temperature of the water at the ocean's surface is known as SST, and it is an important physical characteristic of the world's oceans. The surface temperature of the world's seas varies mostly with latitude, with warmest waters around the equator and coldest waters in the Arctic and Antarctic areas. SST rises as the seas absorb more heat and the ocean circulation patterns that carry warm and cold water around the world.

Changes in SST can have a variety of effects on marine ecosystems. Variations in ocean temperature, for example, can affect which plant, animal, and microbe species are present in a given place, modify migration and breeding patterns, endanger delicate ocean life such as corals, and alter the frequency and intensity of destructive algal blooms such as "red tide." Long-term increases in SST may also impair circulation patterns that transport nutrients from the deep sea to the surface. Changes in reef habitat and nutrient supply might drastically alter ocean ecosystems and lead to fish population decreases, affecting those who rely on fishing for food or a living.

As the oceans are constantly interacting with the atmosphere, SST can have a significant impact on global climate. The amount of atmospheric water vapour over the oceans has increased as SST has risen. This water vapour feeds weather systems, increasing the likelihood of heavy rain and snow. Changes in SST can alter storm tracks, perhaps causing droughts in some places. Increases in SST are also projected to increase the growing season for certain bacteria that can taint seafood and cause foodborne diseases, raising the likelihood of adverse health impacts (https://www.epa.gov/climate-indicators/climate-change-indicators-sea-surface-temperature).

The ocean absorbs the majority of the surplus heat from greenhouse gas emissions, resulting in rising ocean temperatures. Increasing ocean temperatures have an impact on marine species and ecosystems, resulting in coral bleaching and the loss of breeding habitats for marine fish and mammals. Rising ocean temperatures have an impact on the benefits that humans derive from the ocean, endangering food security, increasing disease prevalence, creating more extreme weather events, and reducing coastal protection. Achieving the Paris Agreement on Climate Change's mitigation targets and limiting global average temperature rise to well below 2 °C over pre-industrial levels is critical to avoiding the huge, irreversible effects of ocean warming. Establishing marine protected zones and implementing adaptive measures, such as precautionary catch restrictions to avoid overfishing, can protect ocean ecosystems and shield humans from the effects of ocean warming (https://www.iucn.org/resources/issues-brief/ocean-warming). The Pacific Ocean is the largest and deepest of the world's five oceans. It stretches from the Arctic Ocean in the north to the Southern Ocean (or, depending on the definition, Antarctica) in the south and is limited on the west by Asia and Oceania and on the east by the America (https://en.wikipedia.org/wiki/Pacific_Ocean).

The northwest Pacific experiences the highest number of tropical cyclones globally, with an average of 35 each year. Approximately 80% of tropical cyclones will develop into typhoons. Each year, approximately 26 tropical cyclones attain the intensity of tropical storms, making up 31% of global tropical storms and more than double the number of any other location. The substantial interaction between sea and air in this location warrants more investigation into the impact on SST *(Wu et al., 2020)*. Western boundary currents (WBCs) are turbulent zones of water with substantial ocean-atmosphere interaction, poleward heat transport, and ocean-atmosphere heat exchange. The two northern hemisphere WBCs are the Gulf Stream (Atlantic) and the Kuroshio current

(Pacific), whose poleward reach is regulated by the location of the frontal zone where they meet the sub-polar gyre *(Bulgin et al., 2020)*.

The South China Sea and western North Pacific domain (Eq.-40°N, 100°E-180°), where approximately one-third of the world's TCs originate *(Ritchie and Holland, 1999)*. The monsoon trough in the western North Pacific plays a major role in TC genesis. According to Ritchie and Holland's (1999) review of 8-year data, the monsoon trough environment, including the monsoon shear line, confluent zone, and gyre, accounts for around 75% of TCs across the western North Pacific. The monsoon trough is accompanied by low-level cyclonic circulation and modest vertical wind shear, both of which provide ideal dynamic circumstances for TC formation. *(Gray, 1998)* reports high relative humidity in the middle troposphere and SST in the trough zone. Simulating monsoon trough activity is crucial for accurately predicting TC genesis frequencies. This study examines the bias in seasonal TC generation based on simulated trough behaviour.

SSTs have a significant impact on climate and weather. Every 3 to 7 years, for example, a large stretch of the Pacific Ocean along the equator heats by 2 to 3 degrees Celsius. This warming is a symptom of the El Niño climatic phenomenon, which alters rainfall patterns around the world, causing abundant rain in the southern United States and severe drought in Australia, Indonesia, and southern Asia. On a lesser scale, ocean temperatures influence the formation and intensification of tropical cyclones (hurricanes and typhoons), which draw energy from warm ocean waters (https://neo.gsfc.nasa.gov/). The current is widespread and transports warmer water from the subtropics to the subpolar latitudes. The average SST along the North Pacific Current can range from 45°F– 61°F (7.2°C –

16.1°C) in the winter to 64°F– 74°F (17.8°C– 23.3°C) in the summer (https://en.wikipedia.org/wiki/Sea_surface_temperature).

The oceans tend to stratify due to temperature; the bottom waters of the deep regions are extremely cold, with temperatures just above freezing. The thickness of the surface zone, where temperature changes are discernible, is between 330 and 1,000 feet (100 and 300 metres). When compared to the middle and western Pacific, it is more compressed in the temperate eastern Pacific, around the coasts of North and middle America, where cold water occurs at a shallower depth. As the ratio of land to sea areas is greater in the Northern Hemisphere, and because Antarctica and the Southern Ocean also influence water temperature, ocean temperatures in the North Pacific tend to be higher than those in the South Pacific.

Although it is in the Northern Hemisphere, the mean position of the thermal equator (the line on the Earth on which the highest average air temperatures are found; the line migrates latitudinally with changing angular distance from the Equator of the Sun) in the Pacific is closer to the geographic equator than in the Atlantic and Indian oceans. The surface and deep zones of the Pacific have significant temperature and salinity differences. The deep zone, which accounts for around 80% of the volume of the ocean, has rather constant temperature and salinity patterns; its average temperature is 38.3 °F (3.5 °C). (https://www.britannica.com/place/Pacific-Ocean). The Philippine Sea, South China Sea, East China Sea, Sea of Japan, Sea of Okhotsk, Bering Sea, Gulf of Alaska, Mar de Grau, Tasman Sea, and the Coral Sea are all large marginal seas in the western Pacific (https://en.wikipedia.org/wiki/Pacific_Ocean). The Pacific Warm Pool (PWP) is distinguished by a mean SST above 28°C (the minimum surface water temperature required for deep convection), moderate trade winds, and the resulting deep convection, with thunderstorm tops surpassing 15 kilometres. This body of water, which spans the western waters of the equatorial Pacific, contains the warmest seawater in the world. As this warm water area further extends westward into the Indian Ocean, it is also known as the Indo-Pacific Warm Pool. Scientists discovered that, over a two-decade period, the warm pool's average yearly temperatures and dimensions (the area enclosed by the 28-degree Celsius isotherm) increased and then decreased like a softly pulsating beacon.

As the waters are heated enough to transport heat and moisture high into the atmosphere (by convection), the warm pool has a significant impact on the climate of the surrounding area. It has been dubbed the "heat engine of the world" and plays a critical role in climate and monsoon variability for many Asian and African countries, as well as influencing faraway regions and large-scale climate models. The extent and intensity of the warm pool varies with the El Niño-Southern Oscillation (ENSO). During El Niño episodes, the PWP increases horizontally while shrinking vertically. The inverse occurs during La Niña. In recent years, the PWP has grown in both horizontal coverage and vertical depth. This is believed to be a result of global warming (https://skybrary.aero/articles/western-pacific-warm-pool).

1.2 AIM AND OBJECTIVES

The aim of the study is to understand the variability of the SST in north-west Pacific Ocean in the period from January 1990 to December 2022.

The objectives of the study are as follows:

- To study the average monthly, seasonal and annual variability of SST in north-west Pacific Ocean in the period from January 1990 to December 2022
- To study the trends in the monthly, seasonal and annual variability of the SST in the north-west Pacific Ocean in the period from January 1990 to December 2022

1.3 SCOPE

The scope of the study includes studying the variability of the SST in the north-west Pacific Ocean, bounded in the region between the Equator to 40 °N latitudes and from 99 °E to 170 °W longitudes. The period of study is from January 1990 to December 2022, using monthly online freely-available data. In-situ observations of SSTs will not be done. The online data would be downloaded and plotted using freely-available software like NOAA PMEL's PyFerret. Averages and slopes of trendlines of SST would be mapped, and basin-averaged plots would also be made. This would be done for the entire period of study, month-wise and season-wise. The causes for the observed variability of SST will not be studied.

CHAPTER 2: LITERATURE REVIEW

The Kuroshio and Oyashio Currents are the western boundary currents of the North Pacific Ocean's wind-driven subtropical and subarctic circulations. Kuroshio literally means "black stream" ('kuro') in Japanese, owing to the water's blackish ultramarine to cobalt blue tint. The Kuroshio Current's 'blackness' originates from the fact that the downwelling-dominant subtropical North Pacific Ocean has poor biological productivity and is free of debris and other organic material in the surface water. Upwelling, on the other hand, dominates the subarctic North Pacific Ocean. The nutrient-rich upwelled water feeds the Oyashio from the north, giving rise to its appellation, parent ('oya') stream ('shio') *(Qiu, 2001)*. There is a huge geographical area traversed by the Kuroshio Current (see Qiu, 2001): the region upstream of the Tokara Strait, the region south of Japan, and the Kuroshio Extension zone east of the Izu Ridge. The Kuroshio Current has various properties in various geographical areas due to differences in the controlling physics *(Qiu, 2001)*.

Decadal variability in the Kuroshio-Oyashio Extension region is explored using an eddy-resolving quasi-global ocean general circulation model, with a focus on the subarctic (Oyashio) and Kuroshio Extension (KE) fronts. The KE front is deep, with a steep sea surface height (SSH) gradient and a moderate SST gradient. The subarctic front, on the other hand, is shallow and identified as a zone of tight gradient in SST but not SSH. As the decadal scale shifts from a warm phase around 1970 to a cool period in the mid-1980s, the model's fronts travel southward, as observed, and the concomitant dramatic cooling is confined primarily to those frontal zones. The cooling of the mixed layer reflects the peculiar vertical structure of the fronts. Concurrent with their southerly march, the two fronts have intensified on a decadal scale. The cooling in the frontal zones can be attributed to neither direct atmospheric thermal forcing nor the advective effect of the intensified KE, although the advective effect of the intense Oyashio can contribute to the cooling in the subarctic frontal zone. In fact, their time evolution is not totally consistent, implying that their variability is regulated by distinct mechanisms. Decadal SSH variability in the KE frontal zone appears to be substantially explained by the propagation of baroclinic Rossby waves in the central North Pacific caused by anomalous Ekman pumping. This technique cannot completely account for the equivalent variability in the subarctic frontal zone, where eastward propagating SSH anomalies off the Japanese coast seem to be superimposed on the Rossby wave signals *(Nonaka et al., 2005)*.

A temperature front exists north of the Kuroshio Extension, influencing surface and upper-layer atmospheric circulation and supporting the North Pacific storm track *(Ogawa et al., 2012)*. Frequent activities have a significant impact on mid-latitude weather and climate systems, causing heavy rainfall, redistributing heat and momentum between subtropics and mid-latitudes, and maintaining atmospheric circulation *(Luo et al., 2011)*. The Kuroshio Extension has substantial recirculation gyres on its southern side, allowing for flow volumes of up to 130 Sv. The Kuroshio Current originates from the North Equatorial Current and enters the East China Sea via a route east of Taiwan. It eventually reaches the study area in southern Japan after passing through the Tokara Strait at roughly 30°N. The Kuroshio Current flows from 30 to 55 Sv through the Tokara Strait, with the main axis represented by the annual mean SST isotherm at 16 °C *(Qiu, 2001)*.

The Kuroshio Current originates in the tropical western Pacific and is linked to both the North Equatorial Current to the east and the WPWP (western Pacific Warm pool) to the south. Changes in the Northern Equatorial Current and WPWP have a direct impact on hydrology in the Kuroshio Current source region. The North Equatorial Current flows from east to west, driven by northeast trade winds and variations in the North Pacific Subtropical High *(Yasuda et al., 1985)*. The Pacific Ocean equatorial SSTs are higher in the western Pacific Ocean and lower near the equator in the eastern Pacific Ocean *(McPhaden, 1993)*. El Niño-Southern Oscillation (ENSO) is connected with anomalies in the Equatorial Western Pacific, SST, and sea surface height (SSH). SST and SSH anomalies are more intense in the northern hemisphere than in the southern hemisphere *(Hu et al., 2016)*.

Ship and satellite measurements were used to study decadal variations in the North Pacific oceanic frontal zones *(Nakamura and Kazmin, 2003)*. The influence of decadal climate changes on the subarctic and subtropical oceanic frontal zones of the North Pacific is documented. According to research, the western North Pacific region (Kuroshio-Oyashio Extension) is one of the key hotspots for decadal SST variability *(Nakamura et al., 1997; Schneider et al., 2002; Schneider and Cornuelle, 2005)*. Optimum Interpolated SST was used to study the long-term spatiotemporal variability of SST in the northwestern Pacific and China's offshore *(Wu et al., 2020)*. The SST in the north-west Pacific has increased linearly year after year for the last 164 years, with a trend of 0.033 °C/decade. From 1870 to 1910, the SST gradually decreased and remained in the range of 25.2 to 26.0 °C. The warming trend in the northwestern Pacific SST is very significant. The tropical climate in the north-western United States from

1993 to 2009, the North Pacific Ocean, saw a maximum trend of more than 10 mm/year around the boundary of the wind-driven tropical and subtropical gyres *(Qiu and Chen, 2012)*. After leaving Japan's coast, the Kuroshio Current joins the Oyashio Current at 35.7 °N- 38.1 °N and 140 °E to form the Kuroshio Extension in the North Pacific Ocean *(Jia Wang et al., 2020)*. The Kuroshio Extension front is deep and accompanied by a severe sea surface height gradient with a minor SST gradient, whereas the subarctic front is shallow and characterized as a zone of tight SST but not an SSH gradient *(Nonaka et al., 2005)*. The decadal variability in the Kuroshio-Oyashio extension region was explored using the Ocean General Circulation Model (OGCM) Eddy-Resolving model, with a focus on fronts (Oyashio and the Kuroshio Extension) *(Nonaka et al., 2005)*.

The ocean is a key component of the ocean-atmosphere coupling system *(Chelton and Xie, 2010; Wu et al., 2019a, b, 2020)*. In comparison to the atmosphere, the ocean has sluggish change and a high heat capacity *(England et al., 2014)*. Climate change at the interannual, decadal, and longer periods may be closely tied to the ocean due to progressive changes in the ocean *(Trenberth and Hurrell, 1994; Ault et al., 2009)*. The basic parameter interacting between the ocean and the atmosphere is SST *(Wu et al., 2019 a, b)*, which characterizes the combined outcomes of ocean heat content and dynamic activities *(Buckley et al., 2014; Takakura et al., 2018)*. This parameter is crucial for understanding climate change and ocean dynamics, as it measures heat exchange between sea and air. Observations and numerical simulations reveal that large-scale longitude and latitude SST anomalies of more than 20 degrees can produce significant changes in air circulation, such as the El Niño and La Niña phenomena *(Chen et al., 2016; Zheng et al., 2016)*.

During El Niño, the trade winds in the tropical eastern Pacific diminish, and the SST rises dramatically, reaching 3– 5 degrees Celsius above average. As a result, significant changes in atmospheric circulation and ocean circulation have occurred, resulting in global atmospheric and marine environment abnormalities and climate anomalies *(Li et al., 2017)*. El Niño in the eastern Pacific has a significant impact on the northwest Pacific, influencing climate change in China *(Hu et al., 2018)*. On the one hand, climate change produces rising SSTs in the northwestern Pacific, which increases vertical stratification, influences air circulation, and alters the intensity and duration of coastal winds and upwelling. The 10-year periods of the Pacific Decadal Oscillation (PDO) and the El Niño-Southern Oscillation (ENSO) occur every 2 to 7 years on average, resulting in considerable fluctuations in upwelling. All of these factors will have an impact on the marine environment along China's coast, triggering land-based droughts, floods, and climate calamities *(Xiao et al., 2015; Yang et al., 2017; Xue et al., 2018)*.

These factors can affect the marine environment in Chinese coastal areas, resulting in droughts, floods, and climatic disasters *(Xu et al., 2018)*. Climate change has a significant impact on SST in the north-west Pacific and China offshore. The study of SST fluctuations is crucial for understanding global climate change and predicting El Niño events. As a result, it is critical to investigate the impact of climate change on SST in the north-west Pacific and offshore China.

The study of SST variations is essential because it is one of the key factors of global climate change and one of the important characterizations and predictions of El Niño. Previous researchers have done extensive research on the shifting trend of SST. According to the Intergovernmental Panel on Climate Change (IPCC) Fifth Assessment Report (AR5), the global SST warming trend was 0.064 °C/decade between 1880 and 2012 *(Pachauri et al., 2014)*.

In reality, numerous studies have found that Pacific SST anomalies are intimately associated with global and regional climate shifts, with multi-scale temporal variations *(Graham, 1994; Latif, 2006; Shakun and Shaman, 2009; Li et al., 2014)*. ENSO (El Niño-Southern Oscillation) and PDO (Pacific Decadal Oscillation) are closely related to global and regional climate change. As a result, the Pacific has long been one of the important ocean areas investigated by scholars *(Bao and Ren, 2014; Mei et al., 2015; Stuecker et al., 2015; Wills et al., 2018)*.

To date, two types of primary meteorological SST datasets have been obtained: one based on observed mid-resolution 100-year datasets and the other on satellite high-resolution decadal datasets *(Wang et al., 2012; Smith et al., 2014; Huang et al., 2015; Diamond et al., 2015)*. The former has rebuilt a time series of months spanning 150 years, while the later has gathered over 30 years of daily average time series. In terms of time and resolution, existing meteorological datasets already have criteria for the establishment of a natural mode of change in *SST (Liu et al., 2017; Wang et al., 2018)*. The prerequisites for scholars to employ satellite data for short-term climate change studies have been met with the ongoing advancement of ocean observation technology and the accumulation of satellite remote sensing data. In recent years, there has been a great deal of interest in the investigation and discussion of the interannual variation of SST based on satellite remote sensing SST *(Tang et al., 2003; Yang et al., 2013; Zhang et al., 2015; Skirving et al., 2018)*.

Large-area simultaneous measurements with high temporal and spatial precision can be achieved via satellite remote sensing. The remote sensing SST obtained is helpful in gaining a more complete and rapid understanding of oceanographic phenomena that affect the ocean surface, such as El Niño *(Robinson, 2016)*. A collection of SST data has been provided to investigate the conditions for the occurrence and evolution of ocean surface heat change modes throughout time and space. As a result, satellite remote sensing SST has attracted a lot of interest in recent years. Based on satellite remote sensing data, the timelines for researching changes in SST in the north-western Pacific, particularly in China's offshore, are currently primarily under 20 years, which is relatively short for studying climate change *(Song et al., 2018; Pan et al., 2018)*.

The North Pacific Ocean’s SSTs follow a predictable pattern, with temperature anomalies near North America contrasting with those off Japan's coast. Ocean changes impact both fish populations and climate in neighbouring land regions. They use global climate models to study the physical mechanisms underlying SST fluctuation, taking into account interactions between the atmosphere and ocean. Ocean currents and SST change in tandem, and the time it takes for these currents to react to changes in wind patterns contributes to their long-term variability *(Wills et al., 2019)*.

Summers with warm (cold) SST in the north Indian Ocean (NIO) result in fewer (more) TCs forming across the WNP. Specifically, fewer (more) TCs form north of 10°N while more (fewer) TCs form south of 10°N. The warm (cold) SST in the NIO causes anomalous anticyclonic (cyclonic) vorticity north of 10°N and cyclonic (anti-cyclonic) vorticity south of 10°N. This suppresses (promotes) TC genesis north of 10°N and promotes (suppresses) TC genesis south of 10°N *(Zheng et al.,2016)*. Long-term mean climatologies show significant variances near sea ice at high latitudes, as well as differences in spatial resolution of small-scale characteristics like the Gulf Stream and equatorial upwelling. NCEP (National Centers for Environmental Prediction) SST analyses provide superior resolution in these areas *(Hurrell and Trenberth, 1999)*. Between 1981 and 2020, NWPac SST increased by 2.76° ± 0.32°C per century (one standard error), with fluctuations due to interannual and multidecadal variability. We propose that human global warming and internal variability may have contributed to the 2020 event even though the linear trend was minimal prior to 1980, the forced response indicates significant warming since then (2.45° ± 0.12°C per century from 1981 to 2020), consistent with observations *(Hayashi et al., 2021)*.

CHAPTER 3: DATA AND METHODOLOGY

3.1 STUDY AREA

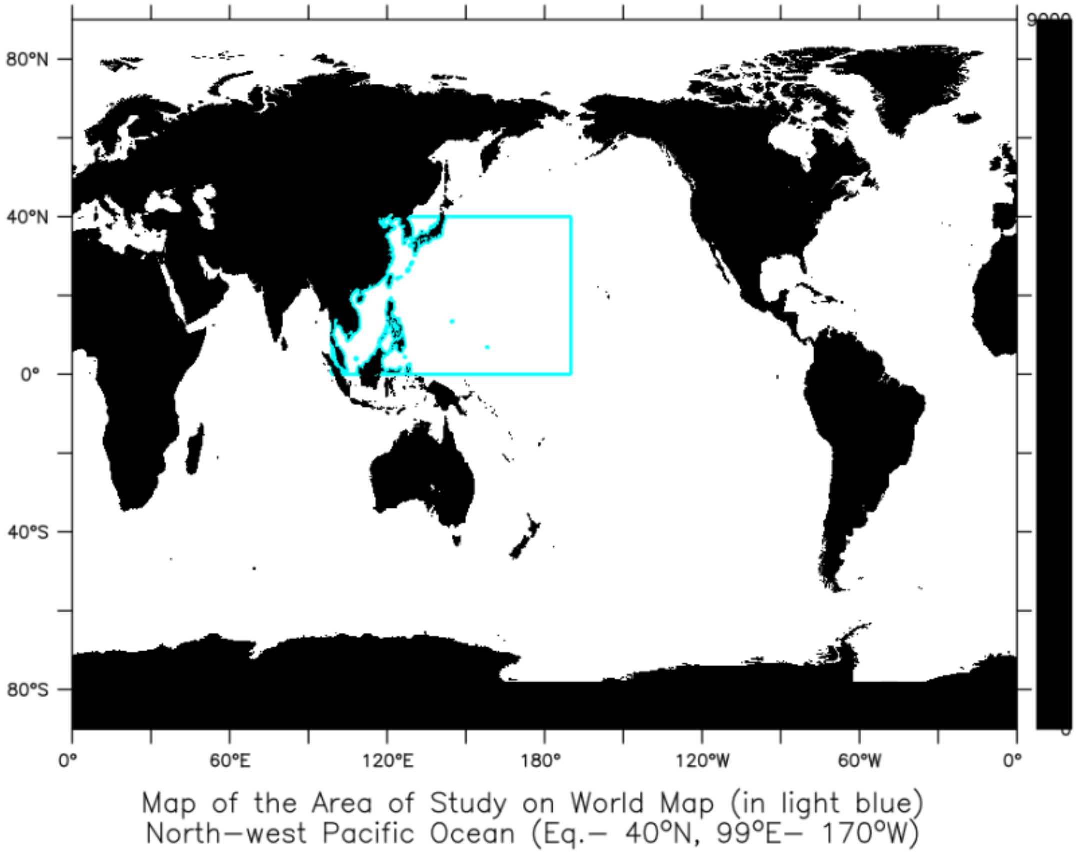

Figure 3.1 Area of study (bounded in light blue) of the north-west Pacific Ocean, shown on the world map

The Pacific Ocean is the largest and deepest of the world's five oceans. It stretches from the Arctic Ocean in the north to the Southern Ocean in the south and is surrounded in the west by Asia and Oceania and in the east by the American landmass (https://en.wikipedia.org/wiki/Pacific_Ocean).The western Pacific region's seaward limit is indicated by a fragmented line of oceanic trenches that runs from the Aleutian Trench in the north to the Kuril and Japan trenches in the south (https://www.britannica.com/place/Pacific-Ocean).

In this work, the area of study is the north-west Pacific Ocean defined by the region between the latitudes 0 °N to 40 °N and the longitudes 99 °E to 170 °W. This study area is shown on a world map, as shown in Figure 3.1, and in detail, it includes some regional seas and neighbouring countries, as shown in Figure 3.2.

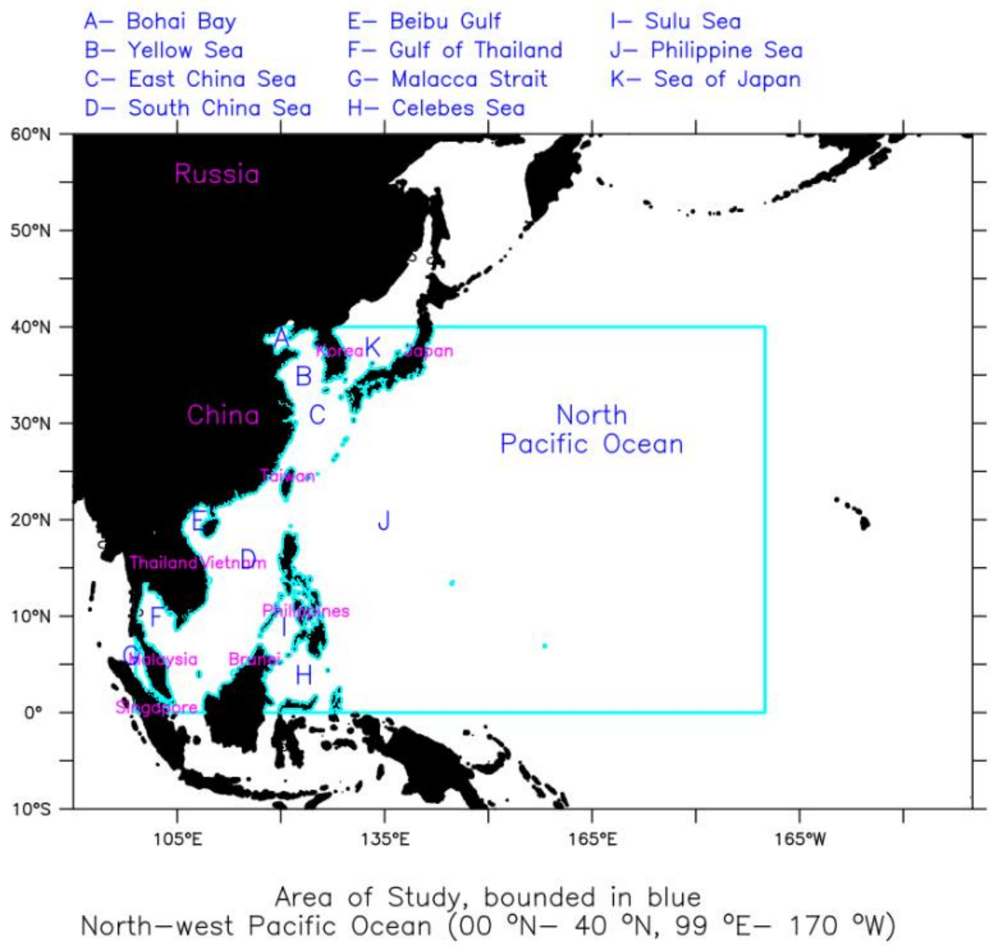

Figure 3.2 Area of study (Eq. to 40 °N, 99 °E to 170 °W) (bounded in light blue) of the north-west Pacific Ocean

3.2 DATA SOURCES

The SST data is available from the Hadley Centre Sea Ice and Sea Surface Temperature (HadISST). It is monthly data and is available in the period from

1870 to present. The data is globally available, and spatial resolution is 1 degree by 1 degree.

3.3 METHODOLOGY

The SST data used is the HADISST dataset. The data was downloaded from the web-page https://coastwatch.pfeg.noaa.gov/erddap/griddap/erdHadISST.html on 7 December 2023. The data downloaded is monthly data for the period from January 1990 to December 2022. The data is downloaded for a 1 degree by 1 degree spatial resolution. The data used is from the Equator to 40 °N and from 99 °E to 170 °W.

The 33 years of SST data was further analysed and plotted using PyFerret software of the Pacific Marine Environmental Laboratory (PMEL) (https://ferret.pmel.noaa.gov/Ferret/). The data was averaged, slopes of trendlines were computed, and images were obtained, indicating the regions with variability in the SST. Images were plotted for the entire period of study, month-wise and also season-wise. Basin-averaged plots were also plotted. The seasons were defined as boreal spring, boreal summer, boreal autumn and boreal winter. Each of the above seasons were averaged from February to April, May to July, August to October and from November to the following January, respectively.

The programs given below were used to plot the various figures in this study.

Program 3.1 Program to plot the study area on a world map and the detailed study area in the north-west Pacific Ocean as shown in Figure 3.1 and Figure 3.2 respectively.

```
! 02 February 2024

! This program plots the study area region, i.e. the north-west Pacific Ocean (00
N- 40 N, 99 E- 170 W), on the world map, to study the SST

! This program also plots the magnified study area, and labels the various areas

SET WINDOW 1

SET Mode verify

SET Region/ x=00E:360E/ y=90S:90N

USE etopo05.cdf

! SET Mode metafile

SHADE/ Level=(0 9000 9000)/ Palette=black/ Nolabel rose

CONTOUR/ Overlay/ Level=(0)/ Colour=11/ Nolabel rose[x=99E:170W,
Y=00N:40N]

GO box 99 190 00 40 11

SHADE/ Overlay/ Level=(1 9000 9000)/ Palette=black/ Nolabel rose


LABEL/Nouser 3.9 -0.7 0 0 0.16 "Map of the Area of Study on World Map (in
light blue)<nl>North-west Pacific Ocean (Eq.- 40^oN, 99^oE- 170^oW)"

! CANCEL Mode metafile

FRAME/ File= Study_Area_North_West_Pacific_Ocean_00N40N099E190E.gif

! sp Fprint - o Study_Area_North_West_Pacific_Ocean_00N40N099E190E.ps -l
cps -p portrait metafile.plt

SET WINDOW 2

SET Region/ x=90E:500W/ y=10S:60N
```

```
USE etopo05.cdf

! SET Mode metafile

! CONTOUR/ Level=(0)/ Title="Area of Study, bounded in blue, in the north-west Pacific Ocean<nl>(00 N- 40 N, 99 E- 170 W)" rose

CONTOUR/ Level=(0)/ Nolab rose

SET Region/ x=99E:170W/ y=00N:40N

CONTOUR/ Overlay/ Level=(0)/ Colour=11/ Nolabel rose

GO box 99 190 00 40 11

SET Region/ x=90E:500W/ y=10S:60N

SHADE/ Overlay/ Level=(0 9000 9000)/ Palette=black/ Nolabel rose


LABEL 150 -20 0 0 0.16 "Area of Study, bounded in blue<nl>North-west Pacific Ocean (00 ^oN- 40 ^oN, 99 ^oE- 170 ^oW)"

! Labels on Sea

LABEL 165 30 0 0 0.16 "@c004North<nl>Pacific Ocean"

! Labels on land

LABEL 117 55 1 0 0.16 "@c006Russia"

LABEL 117 30 1 0 0.16 "@c006China"

LABEL 108 15 1 0 0.10 "@c006Thailand"

LABEL 118 15 1 0 0.10 "@c006Vietnam"

LABEL 108 05 1 0 0.10 "@c006Malaysia"

LABEL 108 00 1 0 0.10 "@c006Singapore"

LABEL 120 05 1 0 0.10 "@c006Brunei"

LABEL 130 10 1 0 0.10 "@c006Philippines"

LABEL 125 24 1 0 0.10 "@c006Taiwan"

LABEL 145 37 1 0 0.10 "@c006Japan"

LABEL 132 37 1 0 0.10 "@c006Korea"

! Other Label with codes
```

LABEL 117 038 -1 0 0.16 "@c004 A"

LABEL 090 071 -1 0 0.13 "@c004 A- Bohai Bay"

LABEL 120 034 -1 0 0.16 "@c004 B"

LABEL 090 068 -1 0 0.13 "@c004 B- Yellow Sea"

LABEL 122 030 -1 0 0.16 "@c004 C"

LABEL 090 065 -1 0 0.13 "@c004 C- East China Sea"

LABEL 112 015 -1 0 0.16 "@c004 D"

LABEL 090 062 -1 0 0.13 "@c004 D- South China Sea"

LABEL 105 019 -1 0 0.16 "@c004 E"

LABEL 128 071 -1 0 0.13 "@c004 E- Beibu Gulf"

LABEL 099 009 -1 0 0.16 "@c004 F"

LABEL 128 068 -1 0 0.13 "@c004 F- Gulf of Thailand"

LABEL 095 005 -1 0 0.16 "@c004 G"

LABEL 128 065 -1 0 0.13 "@c004 G- Malacca Strait"

LABEL 120 003 -1 0 0.16 "@c004 H"

LABEL 128 062 -1 0 0.13 "@c004 H- Celebes Sea"

LABEL 118 008 -1 0 0.16 "@c004 I"

LABEL 166 071 -1 0 0.13 "@c004 I- Sulu Sea"

LABEL 132 019 -1 0 0.16 "@c004 J"

LABEL 166 068 -1 0 0.13 "@c004 J- Philippine Sea"

LABEL 130 037 -1 0 0.16 "@c004 K"

LABEL 166 065 -1 0 0.13 "@c004 K- Sea of Japan"

! CANCEL Mode metafile

FRAME/
File=Study_Area_North_West_Pacific_Ocean_00N40N099E190E_with_labels.gi
f

! sp Fprint -o
Study_Area_North_West_Pacific_Ocean_00N40N099E190E_with_labels.ps

Program 3.2 Program mapping the SST in the north-west Pacific Ocean (Eq. to 40 °N, 99 °E to 170 °W) averaged in the entire period January 1990 to December 2022, and also plotted month-wise and season-wise, and shown from Figure 4.1. to Figure 4.17.

```
! 3 January 2024

! This programme maps the SST, in the North-West Pacific Ocean (00 N to 40 N,
99 E to 170W), averaged in the time period from January 1990 to December 2022.

! The maps are for the entire period, month-wise and season-wise.

!!!!!!!!!!!!!!!!!!!!!!!!!!!!!!!!!!!!!!!!!!!!!!!!!!!!!!!!!!!!!!!!!!!!!!!!!!!!!!!!!!!!!!!!!!!!

! The dataset is HadISST Average Sea Surface Tempezatuze, 1°, Global,
Monthly, 1870-present.

! The datafile SST_ErdHadl_90S90N180W180E_199001_202212.nc was
downloaded from
https://coastwatch.pfeg.noaa.gov/erddap/griddap/erdHadISST.html on 7
December 2023.

! The dataset contains the variable SST

! The SST data is global (90 N to 90 S, 180 W to 180 E), and 1s 1 degree by 1
degree.A stride of 1 was given when downloading this data from the website.

! The SST data is on the sea surface.

! The SST data is monthly and is downloaded in the period from January 1990 to
September 2023. A stride of 1 was given when downloading this data from the
website.

! The SST data is on the sea surface.

! The citation is

! Rayner, N. A., Parker, D. E., Horton, E. B., Folland, C. K., Alexander, L. V.,
Rowell, D. Po, Kent, E. C., Kaplan, A. (2003).

! J. Geophys.Res.Vol.108, No.D14,4407

! d.o.i.: 10.1029/2002JD002670

!!!!!!!!!!!!!!!!!!!!!!!!!!!!!!!!!!!!!!!!!!!!!!!!!!!!!!!!!!!!!!!!!!!!!!!!!!!!!!!!!!!!!!!!!!!!!
```

```
USE SST_ErdHadl_90S90N180W180E_199001_202309.nc
        ! Dataset of SST in the period from January 1990 to September 2023

SHOW Data

KEYMARK 1

LET sst_filled = sst[d=SST_ErdHadl_90S90N180W180E_199001_202309.nc, l=1:405@fln:12]

! Map in the period from January 1990 to December 2022

SET MODE Metafile

SHADE/ Level=(-inf)(10 30 2.5)(inf)/ Palette=ocean_temp/ Title=" " sst_filled[x=99E:170W, y=00N:40N, T="01-Jan-1990":"31-Dec-2022"@ave]

CONTOUR/ Over/ Level=(-10 50 5)/ Nolab sst_filled[x=99E:170W, y=00N:40N, T="01-Jan-1990":"31-Dec-2022"@ave]

LABEL/Nouser 3.9 -0.8 0 0 0.15 "SST (^oC) in the north-west Pacific Ocean (00^oN to 40^oN, 099^oE to 170^oW),<nl>averaged in the period from January 1990 to December 2022"

GO land

USE etopo05.cdf

SHADE/ Overlay/ Palette=black/ Level=(0 9000 9000)/ Nolab rose

CANCEL MODE Metafile

FRAME/File="SST_17_Time_Series_00N40N099E170W_199001_202212.gif"

sp Fprint -o "SST_17_Time_Series_00N40N099E170W_199001_202212.ps" -l cps -p portrait Metafile.plt

! Month-wise plots

LET SST_Jan = sst_filled[l=1:405:12]

LET SST_Feb = sst_filled[l=2:405:12]

LET SST_Mar = sst_filled[l=3:405:12]

LET SST_Apr = sst_filled[l=4:405:12]

LET SST_May = sst_filled[l=5:405:12]

LET SST_Jun = sst_filled[l=6:405:12]
```

```
LET SST_Jul = sst_filled[l=7:405:12]

LET SST_Aug = sst_filled[l=8:405:12]

LET SST_Sep = sst_filled[l=9:405:12]

LET SST_Oct = sst_filled[l=10:405:12]

LET SST_Nov = sst_filled[l=11:405:12]

LET SST_Dec = sst_filled[l=12:405:12]

! SST Map in January

SET MODE Metafile

SHADE/ Level=(-inf)(10 30 2.5)(inf)/ Palette=ocean_temp/ Title=" " SST_Jan[x=99E:170W, y=00N:40N, T="01-Jan-1990":"31-Dec-2022"@ave]

CONTOUR/ Over/ Level=(-10 50 5)/ Nolab SST_Jan[x=99E:170W, y=00N:40N, T="01-Jan-1990":"31-Dec-2022"@ave]

LABEL/Nouser 3.9 -0.8 0 0 0.15 "January SST (^oC) in the north-west Pacific Ocean (00^oN to 40^oN, 099^oE to 170^oW),<nl>averaged in the period from January 1990 to December 2022"

GO land

USE etopo05.cdf

SHADE/ Overlay/ Palette=black/ Level=(0 9000 9000)/ Nolab rose

CANCEL MODE Metafile


FRAME/File="SST_01_Month_Jan_00N40N099E170W_199001_202212.gif"

sp Fprint -o "SST_01_Month_Jan_00N40N099E170W_199001_202212.ps" -l cps -p portrait Metafile.plt

! SST Map in February

SET MODE Metafile

SHADE/ Level=(-inf)(10 30 2.5)(inf)/ Palette=ocean_temp/ Title=" " SST_Feb[x=99E:170W, y=00N:40N, T="01-Jan-1990":"31-Dec-2022"@ave]

CONTOUR/ Over/ Level=(-10 50 5)/ Nolab SST_Feb[x=99E:170W, y=00N:40N, T="01-Jan-1990":"31-Dec-2022"@ave]
```

LABEL/Nouser 3.9 -0.8 0 0 0.15 "February SST (^oC) in the north-west Pacific Ocean (00^oN to 40^oN, 099^oE to 170^oW),<nl>averaged in the period from January 1990 to December 2022"

GO land

USE etopo05.cdf

SHADE/ Overlay/ Palette=black/ Level=(0 9000 9000)/ Nolab rose

CANCEL MODE Metafile

FRAME/File="SST_02_Month_Feb_00N40N099E170W_199001_202212.gif"

sp Fprint -o "SST_02_Month_Feb_00N40N099E170W_199001_202212.ps" -l cps -p portrait Metafile.plt

! SST Map in March

SET MODE Metafile

SHADE/ Level=(-inf)(10 30 2.5)(inf)/ Palette=ocean_temp/ Title=" " SST_Mar[x=99E:170W, y=00N:40N, T="01-Jan-1990":"31-Dec-2022"@ave]

CONTOUR/ Over/ Level=(-10 50 5)/ Nolab SST_Mar[x=99E:170W, y=00N:40N, T="01-Jan-1990":"31-Dec-2022"@ave]

LABEL/Nouser 3.9 -0.8 0 0 0.15 "March SST (^oC) in the north-west Pacific Ocean (00^oN to 40^oN, 099^oE to 170^oW),<nl>averaged in the period from January 1990 to December 2022"

GO land

USE etopo05.cdf

SHADE/ Overlay/ Palette=black/ Level=(0 9000 9000)/ Nolab rose

CANCEL MODE Metafile

FRAME/File="SST_03_Month_Mar_00N40N099E170W_199001_202212.gif"

sp Fprint -o "SST_03_Month_Mar_00N40N099E170W_199001_202212.ps" -l cps -p portrait Metafile.plt

! SST Map in April

SET MODE Metafile

SHADE/ Level=(-inf)(10 30 2.5)(inf)/ Palette=ocean_temp/ Title=" " SST_Apr[x=99E:170W, y=00N:40N, T="01-Jan-1990":"31-Dec-2022"@ave]

CONTOUR/ Over/ Level=(-10 50 5)/ Nolab SST_Apr[x=99E:170W, y=00N:40N, T="01-Jan-1990":"31-Dec-2022"@ave]

LABEL/Nouser 3.9 -0.8 0 0 0.15 "April SST (^oC) in the north-west Pacific Ocean (00^oN to 40^oN, 099^oE to 170^oW),<nl>averaged in the period from January 1990 to December 2022"

GO land

USE etopo05.cdf

SHADE/ Overlay/ Palette=black/ Level=(0 9000 9000)/ Nolab rose

CANCEL MODE Metafile

FRAME/File="SST_04_Month_Apr_00N40N099E170W_199001_202212.gif"

sp Fprint -o "SST_04_Month_Apr_00N40N099E170W_199001_202212.ps" -l cps -p portrait Metafile.plt

! SST Map in May

SET MODE Metafile

SHADE/ Level=(-inf)(10 30 2.5)(inf)/ Palette=ocean_temp/ Title=" " SST_May[x=99E:170W, y=00N:40N, T="01-Jan-1990":"31-Dec-2022"@ave]

CONTOUR/ Over/ Level=(-10 50 5)/ Nolab SST_May[x=99E:170W, y=00N:40N, T="01-Jan-1990":"31-Dec-2022"@ave]

LABEL/Nouser 3.9 -0.8 0 0 0.15 "May SST (^oC) in the north-west Pacific Ocean (00^oN to 40^oN, 099^oE to 170^oW),<nl>averaged in the period from January 1990 to December 2022"

GO land

USE etopo05.cdf

SHADE/ Overlay/ Palette=black/ Level=(0 9000 9000)/ Nolab rose

CANCEL MODE Metafile

FRAME/File="SST_05_Month_May_00N40N099E170W_199001_202212.gif"

sp Fprint -o "SST_05_Month_May_00N40N099E170W_199001_202212.ps" -l cps -p portrait Metafile.plt

! SST Map in June

SET MODE Metafile

SHADE/ Level=(-inf)(10 30 2.5)(inf)/ Palette=ocean_temp/ Title=" " SST_Jun[x=99E:170W, y=00N:40N, T="01-Jan-1990":"31-Dec-2022"@ave]

CONTOUR/ Over/ Level=(-10 50 5)/ Nolab SST_Jun[x=99E:170W, y=00N:40N, T="01-Jan-1990":"31-Dec-2022"@ave]

LABEL/Nouser 3.9 -0.8 0 0 0.15 "June SST (^oC) in the north-west Pacific Ocean (00^oN to 40^oN, 099^oE to 170^oW),<nl>averaged in the period from January 1990 to December 2022"

GO land

USE etopo05.cdf

SHADE/ Overlay/ Palette=black/ Level=(0 9000 9000)/ Nolab rose

CANCEL MODE Metafile

FRAME/File="SST_06_Month_Jun_00N40N099E170W_199001_202212.gif"

sp Fprint -o "SST_06_Month_Jun_00N40N099E170W_199001_202212.ps" -l cps -p portrait Metafile.plt

! SST Map in July

SET MODE Metafile

SHADE/ Level=(-inf)(10 30 2.5)(inf)/ Palette=ocean_temp/ Title=" " SST_Jul[x=99E:170W, y=00N:40N, T="01-Jan-1990":"31-Dec-2022"@ave]

CONTOUR/ Over/ Level=(-10 50 5)/ Nolab SST_Jul[x=99E:170W, y=00N:40N, T="01-Jan-1990":"31-Dec-2022"@ave]

LABEL/Nouser 3.9 -0.8 0 0 0.15 "July SST (^oC) in the north-west Pacific Ocean (00^oN to 40^oN, 099^oE to 170^oW),<nl>averaged in the period from January 1990 to December 2022"

GO land

USE etopo05.cdf

SHADE/ Overlay/ Palette=black/ Level=(0 9000 9000)/ Nolab rose

CANCEL MODE Metafile

FRAME/File="SST_07_Month_Jul_00N40N099E170W_199001_202212.gif" sp Fprint -o "SST_07_Month_Jul_00N40N099E170W_199001_202212.ps" -l cps -p portrait Metafile.plt

! SST Map in August

SET MODE Metafile

SHADE/ Level=(-inf)(10 30 2.5)(inf)/ Palette=ocean_temp/ Title=" " SST_Aug[x=99E:170W, y=00N:40N, T="01-Jan-1990":"31-Dec-2022"@ave]

CONTOUR/ Over/ Level=(-10 50 5)/ Nolab SST_Aug[x=99E:170W, y=00N:40N, T="01-Jan-1990":"31-Dec-2022"@ave]

LABEL/Nouser 3.9 -0.8 0 0 0.15 "August SST (^oC) in the north-west Pacific Ocean (00^oN to 40^oN, 099^oE to 170^oW),<nl>averaged in the period from January 1990 to December 2022"

GO land

USE etopo05.cdf

SHADE/ Overlay/ Palette=black/ Level=(0 9000 9000)/ Nolab rose

CANCEL MODE Metafile

FRAME/File="SST_08_Month_Aug_00N40N099E170W_199001_202212.gif"

sp Fprint -o "SST_08_Month_Aug_00N40N099E170W_199001_202212.ps" -l cps -p portrait Metafile.plt

! SST Map in September

SET MODE Metafile

SHADE/ Level=(-inf)(10 30 2.5)(inf)/ Palette=ocean_temp/ Title=" " SST_Sep[x=99E:170W, y=00N:40N, T="01-Jan-1990":"31-Dec-2022"@ave]

CONTOUR/ Over/ Level=(-10 50 5)/ Nolab SST_Sep[x=99E:170W, y=00N:40N, T="01-Jan-1990":"31-Dec-2022"@ave]

LABEL/Nouser 3.9 -0.8 0 0 0.15 "September SST (^oC) in the north-west Pacific Ocean (00^oN to 40^oN, 099^oE to 170^oW),<nl>averaged in the period from January 1990 to December 2022"

GO land

USE etopo05.cdf

SHADE/ Overlay/ Palette=black/ Level=(0 9000 9000)/ Nolab rose

CANCEL MODE Metafile

```
FRAME/File="SST_09_Month_Sep_00N40N099E170W_199001_202212.gif"

sp Fprint -o "SST_09_Month_Sep_00N40N099E170W_199001_202212.ps" -l cps -p portrait Metafile.plt

! SST Map in October

SET MODE Metafile

SHADE/ Level=(-inf)(10 30 2.5)(inf)/ Palette=ocean_temp/ Title=" " SST_Oct[x=99E:170W, y=00N:40N, T="01-Jan-1990":"31-Dec-2022"@ave]

CONTOUR/ Over/ Level=(-10 50 5)/ Nolab SST_Oct[x=99E:170W, y=00N:40N, T="01-Jan-1990":"31-Dec-2022"@ave]

LABEL/Nouser 3.9 -0.8 0 0 0.15 "October SST (^oC) in the north-west Pacific Ocean (00^oN to 40^oN, 099^oE to 170^oW),<nl>averaged in the period from January 1990 to December 2022"

GO land


USE etopo05.cdf

SHADE/ Overlay/ Palette=black/ Level=(0 9000 9000)/ Nolab rose

CANCEL MODE Metafile

FRAME/File="SST_10_Month_Oct_00N40N099E170W_199001_202212.gif"

sp Fprint -o "SST_10_Month_Oct_00N40N099E170W_199001_202212.ps" -l cps -p portrait Metafile.plt

! SST Map in November

SET MODE Metafile

SHADE/ Level=(-inf)(10 30 2.5)(inf)/ Palette=ocean_temp/ Title=" " SST_Nov[x=99E:170W, y=00N:40N, T="01-Jan-1990":"31-Dec-2022"@ave]

CONTOUR/ Over/ Level=(-10 50 5)/ Nolab SST_Nov[x=99E:170W, y=00N:40N, T="01-Jan-1990":"31-Dec-2022"@ave]

LABEL/Nouser 3.9 -0.8 0 0 0.15 "November SST (^oC) in the north-west Pacific Ocean (00^oN to 40^oN, 099^oE to 170^oW),<nl>averaged in the period from January 1990 to December 2022"

GO land

USE etopo05.cdf
```

SHADE/ Overlay/ Palette=black/ Level=(0 9000 9000)/ Nolab rose

CANCEL MODE Metafile

FRAME/File="SST_11_Month_Nov_00N40N099E170W_199001_202212.gif"

sp Fprint -o "SST_11_Month_Nov_00N40N099E170W_199001_202212.ps" -l cps -p portrait Metafile.plt

! SST Map in December

SET MODE Metafile

SHADE/ Level=(-inf)(10 30 2.5)(inf)/ Palette=ocean_temp/ Title=" " SST_Dec[x=99E:170W, y=00N:40N, T="01-Jan-1990":"31-Dec-2022"@ave]

CONTOUR/ Over/ Level=(-10 50 5)/ Nolab SST_Dec[x=99E:170W, y=00N:40N, T="01-Jan-1990":"31-Dec-2022"@ave]

LABEL/Nouser 3.9 -0.8 0 0 0.15 "December SST (^oC) in the north-west Pacific Ocean (00^oN to 40^oN, 099^oE to 170^oW),<nl>averaged in the period from January 1990 to December 2022"

GO land

USE etopo05.cdf

SHADE/ Overlay/ Palette=black/ Level=(0 9000 9000)/ Nolab rose

CANCEL MODE Metafile

FRAME/File="SST_12_Month_Dec_00N40N099E170W_199001_202212.gif"

sp Fprint -o "SST_12_Month_Dec_00N40N099E170W_199001_202212.ps" -l cps -p portrait Metafile.plt

!!

! Season-wise plots

LET SST_FMA = sst_feb[l=1:33:1] * (28.25/89.25) + sst_mar[l=1:33:1] * (31/89.25) + sst_apr[l=1:33:1] * (30/89.25)   ! Boreal Spring Season

LET SST_MJJ = sst_may[l=1:33:1] * (31/92) + sst_jun[l=1:33:1] * (30/92) + sst_jul[l=1:33:1] * (31/92)   ! Boreal Summer Season

LET SST_ASO = sst_aug[l=1:33:1] * (31/92) + sst_sep[l=1:33:1] * (30/92) + sst_oct[l=1:33:1] * (31/92)   ! Boreal Autumn Season

```
LET SST_NDJ = sst_nov[l=1:32:1] * (30/92) + sst_dec[l=1:32:1] * (31/92) +
sst_jan[l=2:33:1] * (31/92)                    ! Boreal Winter Season

! SST Map in Boreal Spring Season

 SET MODE Metafile

SHADE/ Level=(-inf)(10 30 2.5)(inf)/ Palette=ocean_temp/ Title=" "
SST_FMA[x=99E:170W, y=00N:40N, T="01-Jan-1990":"31-Dec-2022"@ave]

CONTOUR/ Over/ Level=(-10 50 5)/ Nolab SST_FMA[x=99E:170W,
y=00N:40N, T="01-Jan-1990":"31-Dec-2022"@ave]

LABEL/Nouser 3.9 -0.8 0 0 0.15 "Boreal Spring Season SST (^oC) in
the<nl>north-west Pacific Ocean (00^oN to 40^oN, 099^oE to
170^oW),<nl>averaged in the period from January 1990 to December 2022"

GO land

USE etopo05.cdf

SHADE/ Overlay/ Palette=black/ Level=(0 9000 9000)/ Nolab rose

CANCEL MODE Metafile

FRAME/File="SST_13_Season_FMA_00N40N099E170W_199001_202212.gif"

sp Fprint -o "SST_13_Season_FMA_00N40N099E170W_199001_202212.ps" -l
cps -p portrait Metafile.plt

! SST Map in Boreal Summer Season

 SET MODE Metafile

SHADE/ Level=(-inf)(10 30 2.5)(inf)/ Palette=ocean_temp/ Title=" "
SST_MJJ[x=99E:170W, y=00N:40N, T="01-Jan-1990":"31-Dec-2022"@ave]

CONTOUR/ Over/ Level=(-10 50 5)/ Nolab SST_MJJ[x=99E:170W,
y=00N:40N, T="01-Jan-1990":"31-Dec-2022"@ave]

LABEL/Nouser 3.9 -0.8 0 0 0.15 "Boreal Summer Season SST (^oC) in
the<nl>north-west Pacific Ocean (00^oN to 40^oN, 099^oE to
170^oW),<nl>averaged in the period from January 1990 to December 2022"

GO land

USE etopo05.cdf

SHADE/ Overlay/ Palette=black/ Level=(0 9000 9000)/ Nolab rose

CANCEL MODE Metafile
```

FRAME/File="SST_14_Season_MJJ_00N40N099E170W_199001_202212.gif"

sp Fprint -o "SST_14_Season_MJJ_00N40N099E170W_199001_202212.ps" -l cps -p portrait Metafile.plt

! SST Map in Boreal Autumn/ Fall Season

SET MODE Metafile

SHADE/ Level=(-inf)(10 30 2.5)(inf)/ Palette=ocean_temp/ Title=" " SST_ASO[x=99E:170W, y=00N:40N, T="01-Jan-1990":"31-Dec-2022"@ave]

CONTOUR/ Over/ Level=(-10 50 5)/ Nolab SST_ASO[x=99E:170W, y=00N:40N, T="01-Jan-1990":"31-Dec-2022"@ave]

LABEL/Nouser 3.9 -0.8 0 0 0.15 "Boreal Autumn Season SST (^oC) in the<nl>north-west Pacific Ocean (00^oN to 40^oN, 099^oE to 170^oW),<nl>averaged in the period from January 1990 to December 2022"

GO land

USE etopo05.cdf

SHADE/ Overlay/ Palette=black/ Level=(0 9000 9000)/ Nolab rose

CANCEL MODE Metafile

FRAME/File="SST_15_Season_ASO_00N40N099E170W_199001_202212.gif"

sp Fprint -o "SST_15_Season_ASO_00N40N099E170W_199001_202212.ps" -l cps -p portrait Metafile.plt

! SST Map in Boreal Winter Season

SET MODE Metafile

SHADE/ Level=(-inf)(10 30 2.5)(inf)/ Palette=ocean_temp/ Title=" " SST_NDJ[x=99E:170W, y=00N:40N, T="01-Jan-1990":"31-Dec-2022"@ave]

CONTOUR/ Over/ Level=(-10 50 5)/ Nolab SST_NDJ[x=99E:170W, y=00N:40N, T="01-Jan-1990":"31-Dec-2022"@ave]

LABEL/Nouser 3.9 -0.8 0 0 0.15 "Boreal Winter Season SST (^oC) in the<nl>north-west Pacific Ocean (00^oN to 40^oN, 099^oE to 170^oW),<nl>averaged in the period from January 1990 to December 2022"

GO land

USE etopo05.cdf

```
SHADE/ Overlay/ Palette=black/ Level=(0 9000 9000)/ Nolab rose

CANCEL MODE Metafile

FRAME/File="SST_16_Season_NDJ_00N40N099E170W_199001_202212.gif"

sp Fprint -o "SST_16_Season_NDJ_00N40N099E170W_199001_202212.ps" -l
cps -p portrait Metafile.plt
```

Program 3.3 Program mapping the slopes of the trendlines of the SST in the north-west Pacific Ocean (Eq. to 40 °N, 99 °E to 170 °W) averaged in the entire period from January 1990 to December 2022, and also month-wise and season-wise, shown from Figure 4.18 to Figure 4.34.

```
! 23 January 2024

! This program plots the SST trendlines from January 1990 to December 2022

! The SST data used was downloaded from the webpage
https://coastwatch.pfeg.noaa.gov/erddap/griddap/erdHadISST.html on 7
December 2023.

! The data is of SST,from HadISST Average Sea Surface Temperature, 1°, Global,
Monthly, 1870-present.

! The data is from the Equator to 40 °N and 99 °E to 170 °W, downloaded every
1.0 degree

SET Mode verify

USE SST_ErdHadl_90S90N180W180E_199001_202309.nc
        ! Dataset of SST in the period from January 1990 to September 2023

SHOW Data

KEYMARK 1

LET sst_filled = sst[d=SST_ErdHadl_90S90N180W180E_199001_202309.nc,
l=1:405@fln:12]

! Months

LET SST_Jan = sst_filled[l=1:405:12]
```

```
LET SST_Feb = sst_filled[l=2:405:12]

LET SST_Mar = sst_filled[l=3:405:12]

LET SST_Apr = sst_filled[l=4:405:12]

LET SST_May = sst_filled[l=5:405:12]

LET SST_Jun = sst_filled[l=6:405:12]

LET SST_Jul = sst_filled[l=7:405:12]

LET SST_Aug = sst_filled[l=8:405:12]

LET SST_Sep = sst_filled[l=9:405:12]

LET SST_Oct = sst_filled[l=10:405:12]

LET SST_Nov = sst_filled[l=11:405:12]

LET SST_Dec = sst_filled[l=12:405:12]

! Seasons

LET SST_FMA = sst_feb[l=1:33:1] * (28.25/89.25) + sst_mar[l=1:33:1] *
(31/89.25) + sst_apr[l=1:33:1] * (30/89.25)   ! Boreal Spring Season

LET SST_MJJ = sst_may[l=1:33:1] * (31/92) + sst_jun[l=1:33:1] * (30/92) +
sst_jul[l=1:33:1] * (31/92)                   ! Boreal Summer Season

LET SST_ASO = sst_aug[l=1:33:1] * (31/92) + sst_sep[l=1:33:1] * (30/92) +
sst_oct[l=1:33:1] * (31/92)                   ! Boreal Autumn Season

LET SST_NDJ = sst_nov[l=1:32:1] * (30/92) + sst_dec[l=1:32:1] * (31/92) +
sst_jan[l=2:33:1] * (31/92)                   ! Boreal Winter Season

! Trendline plots

! For the entire period

KEYMARK 1

SET Mode metafile

LET p = t[d=SST_ErdHadl_90S90N180W180E_199001_202309.nc, gl=1:396:1]

LET q = sst_filled[d=SST_ErdHadl_90S90N180W180E_199001_202309.nc,
x=99E:170W, y=00N:40N, l=1:396:1]

SET GRID q

GO regresst
```

```
! The variable "slope" which is calculated by "Ferret" is in (°C/s)

! The variable "slope" is converted in units to (°C/year) by multiplying below

LET Slope_per_year = Slope*60*60*24*365.25

SHADE/ Level=(-inf)(-0.04 0.04 0.02)(inf)/ Palette=no_green/ Nolabel Slope_per_year

CONTOUR/ Overlay/ Level=(0)/ Nolabel Slope_per_year[x=99E:170W, y=00N:40N]

CONTOUR/ Overlay/ Level=(0 1 0.25)/ Colour=3/ Nolabel Rsquare

GO land 7

LABEL/Nouser 3.9 -0.8 0 0 0.15 "Slopes of trendlines of SSTs (^oC/year),<nl>averaged in the period from January 1990 to December 2022.<nl>Coefficient of Determination (R^2) is contoured every 0.25 interval."

use etopo05.cdf

Shade/ overlay/Palette=black/ Level=(0 9000 9000)/ Nolab rose

CANCEL MODE Metafile

FRAME/File="SST_Trendline_Slope_00N40N099E170W_199001_202212.gif"

sp Fprint -o "SST_Trendline_Slope_00N40N099E170W_199001_202212.ps" -l cps -p portrait metafile.plt

! Trendlines month-wise

! January

KEYMARK 1

SET Mode metafile

LET p = t[d=SST_ErdHadl_90S90N180W180E_199001_202309.nc, gl=1:33:1]

LET q = SST_Jan[x=99E:170W, y=00N:40N, l=1:33:1]

SET GRID q

GO regresst

! The variable "slope" which is calculated by "Ferret" is in (°C/s)

! The variable "slope" is converted in units to (°C/year) by multiplying below

LET Slope_per_year = Slope*60*60*24*365.25
```

```
SHADE/ Level=(-inf)(-0.04 0.04 0.02)(inf)/ Palette=no_green/ Nolabel Slope_per_year

CONTOUR/ Overlay/ Level=(0)/ Nolabel Slope_per_year[x=99E:170W, y=00N:40N]

CONTOUR/ Overlay/ Level=(0 1 0.25)/ Colour=3/ Nolabel Rsquare

GO land 7

LABEL/Nouser 3.9 -0.8 0 0 0.15 "Slopes of trendlines of SSTs (^oC/year) in January,<nl>averaged in the period from January 1990 to December 2022.<nl>Coefficient of Determination (R^2) is contoured every 0.25 interval."

use etopo05.cdf

Shade/ overlay/Palette=black/ Level=(0 9000 9000)/ Nolab rose

CANCEL MODE Metafile

FRAME/File="SST_Trendline_Slope_01_Jan_00N40N099E170W_199001_202212.gif"

sp Fprint -o "SST_Trendline_Slope_01_Jan_00N40N099E170W_199001_202212.ps" -l cps -p portrait metafile.plt

! February

KEYMARK 1

SET Mode metafile

LET p = t[d=SST_ErdHadl_90S90N180W180E_199001_202309.nc, gl=1:33:1]

LET q = SST_Feb[x=99E:170W, y=00N:40N, l=1:33:1]

SET GRID q

GO regresst

! The variable "slope" which is calculated by "Ferret" is in (°C/s)

! The variable "slope" is converted in units to (°C/year) by multiplying below

LET Slope_per_year = Slope*60*60*24*365.25

SHADE/ Level=(-inf)(-0.04 0.04 0.02)(inf)/ Palette=no_green/ Nolabel Slope_per_year
```

```
CONTOUR/ Overlay/ Level=(0)/ Nolabel Slope_per_year[x=99E:170W, y=00N:40N]

CONTOUR/ Overlay/ Level=(0 1 0.25)/ Colour=3/ Nolabel Rsquare

GO land 7

LABEL/Nouser 3.9 -0.8 0 0 0.15 "Slopes of trendlines of SSTs (^oC/year) in February,<nl>averaged in the period from January 1990 to December 2022.<nl>Coefficient of Determination (R^2) is contoured every 0.25 interval."

use etopo05.cdf

Shade/ overlay/Palette=black/ Level=(0 9000 9000)/ Nolab rose

CANCEL MODE Metafile

FRAME/File="SST_Trendline_Slope_02_Feb_00N40N099E170W_199001_202212.gif"

sp Fprint -o "SST_Trendline_Slope_02_Feb_00N40N099E170W_199001_202212.ps" -l cps -p portrait metafile.plt

! March

KEYMARK 1

SET Mode metafile

LET p = t[d=SST_ErdHadl_90S90N180W180E_199001_202309.nc, gl=1:33:1]

LET q = SST_Mar[x=99E:170W, y=00N:40N, l=1:33:1]

SET GRID q

GO regresst

! The variable "slope" which is calculated by "Ferret" is in (°C/s)

! The variable "slope" is converted in units to (°C/year) by multiplying below

LET Slope_per_year = Slope*60*60*24*365.25

SHADE/ Level=(-inf)(-0.04 0.04 0.02)(inf)/ Palette=no_green/ Nolabel Slope_per_year

CONTOUR/ Overlay/ Level=(0)/ Nolabel Slope_per_year[x=99E:170W, y=00N:40N]

CONTOUR/ Overlay/ Level=(0 1 0.25)/ Colour=3/ Nolabel Rsquare
```

```
GO land 7

LABEL/Nouser 3.9 -0.8 0 0 0.15 "Slopes of trendlines of SSTs (^oC/year) in
March,<nl>averaged in the period from January 1990 to December
2022.<nl>Coefficient of Determination (R^2) is contoured every 0.25 interval."

use etopo05.cdf

Shade/ overlay/Palette=black/ Level=(0 9000 9000)/ Nolab rose

CANCEL MODE Metafile

FRAME/File="SST_Trendline_Slope_03_March_00N40N099E170W_199001_2
02212.gif"

sp Fprint -o
"SST_Trendline_Slope_03_March_00N40N099E170W_199001_202212.ps" -l
cps -p portrait metafile.plt

! April

KEYMARK 1

SET Mode metafile

LET p = t[d=SST_ErdHadl_90S90N180W180E_199001_202309.nc, gl=1:33:1]

LET q = SST_Apr[x=99E:170W, y=00N:40N, l=1:33:1]

SET GRID q

GO regresst

! The variable "slope" which is calculated by "Ferret" is in (°C/s)

! The variable "slope" is converted in units to (°C/year) by multiplying below

LET Slope_per_year = Slope*60*60*24*365.25


SHADE/ Level=(-inf)(-0.04 0.04 0.02)(inf)/ Palette=no_green/ Nolabel
Slope_per_year

CONTOUR/ Overlay/ Level=(0)/ Nolabel Slope_per_year[x=99E:170W,
y=00N:40N]

CONTOUR/ Overlay/ Level=(0 1 0.25)/ Colour=3/ Nolabel Rsquare

GO land 7
```

```
LABEL/Nouser 3.9 -0.8 0 0 0.15 "Slopes of trendlines of SSTs (^oC/year) in April,<nl>averaged in the period from January 1990 to December 2022.<nl>Coefficient of Determination (R^2) is contoured every 0.25 interval."

use etopo05.cdf

Shade/ overlay/Palette=black/ Level=(0 9000 9000)/ Nolab rose

CANCEL MODE Metafile

FRAME/File="SST_Trendline_Slope_04_Apr_00N40N099E170W_199001_202212.gif"

sp Fprint -o "SST_Trendline_Slope_04_Apr_00N40N099E170W_199001_202212.ps" -l cps -p portrait metafile.plt

! May

KEYMARK 1

SET Mode metafile

LET p = t[d=SST_ErdHadl_90S90N180W180E_199001_202309.nc, gl=1:33:1]

LET q = SST_May[x=99E:170W, y=00N:40N, l=1:33:1]

SET GRID q

GO regresst

! The variable "slope" which is calculated by "Ferret" is in (°C/s)

! The variable "slope" is converted in units to (°C/year) by multiplying below

LET Slope_per_year = Slope*60*60*24*365.25

SHADE/ Level=(-inf)(-0.04 0.04 0.02)(inf)/ Palette=no_green/ Nolabel Slope_per_year

CONTOUR/ Overlay/ Level=(0)/ Nolabel Slope_per_year[x=99E:170W, y=00N:40N]

CONTOUR/ Overlay/ Level=(0 1 0.25)/ Colour=3/ Nolabel Rsquare

GO land 7

LABEL/Nouser 3.9 -0.8 0 0 0.15 "Slopes of trendlines of SSTs (^oC/year) in May,<nl>averaged in the period from January 1990 to December 2022.<nl>Coefficient of Determination (R^2) is contoured every 0.25 interval."
```

```
use etopo05.cdf

Shade/ overlay/Palette=black/ Level=(0 9000 9000)/ Nolab rose

CANCEL MODE Metafile

FRAME/File="SST_Trendline_Slope_05_May_00N40N099E170W_199001_202212.gif"

sp Fprint -o "SST_Trendline_Slope_05_May_00N40N099E170W_199001_202212.ps" -l cps -p portrait metafile.plt

! June

KEYMARK 1

SET Mode metafile

LET p = t[d=SST_ErdHadl_90S90N180W180E_199001_202309.nc, gl=1:33:1]

LET q = SST_Jun[x=99E:170W, y=00N:40N, l=1:33:1]

SET GRID q

GO regresst

! The variable "slope" which is calculated by "Ferret" is in (°C/s)

! The variable "slope" is converted in units to (°C/year) by multiplying below

LET Slope_per_year = Slope*60*60*24*365.25

SHADE/ Level=(-inf)(-0.04 0.04 0.02)(inf)/ Palette=no_green/ Nolabel Slope_per_year

CONTOUR/ Overlay/ Level=(0)/ Nolabel Slope_per_year[x=99E:170W, y=00N:40N]

CONTOUR/ Overlay/ Level=(0 1 0.25)/ Colour=3/ Nolabel Rsquare

GO land 7

LABEL/Nouser 3.9 -0.8 0 0 0.15 "Slopes of trendlines of SSTs (^oC/year) in June,<nl>averaged in the period from January 1990 to December 2022.<nl>Coefficient of Determination (R^2) is contoured every 0.25 interval."

use etopo05.cdf

Shade/ overlay/Palette=black/ Level=(0 9000 9000)/ Nolab rose

CANCEL MODE Metafile
```

FRAME/File="SST_Trendline_Slope_06_Jun_00N40N099E170W_199001_202212.gif"

sp Fprint -o "SST_Trendline_Slope_06_Jun_00N40N099E170W_199001_202212.ps" -l cps -p portrait metafile.plt

! July

KEYMARK 1

SET Mode metafile

LET p = t[d=SST_ErdHadl_90S90N180W180E_199001_202309.nc, gl=1:33:1]

LET q = SST_Jul[x=99E:170W, y=00N:40N, l=1:33:1]

SET GRID q

GO regresst

! The variable "slope" which is calculated by "Ferret" is in (°C/s)

! The variable "slope" is converted in units to (°C/year) by multiplying below

LET Slope_per_year = Slope*60*60*24*365.25

SHADE/ Level=(-inf)(-0.04 0.04 0.02)(inf)/ Palette=no_green/ Nolabel Slope_per_year

CONTOUR/ Overlay/ Level=(0)/ Nolabel Slope_per_year[x=99E:170W, y=00N:40N]

CONTOUR/ Overlay/ Level=(0 1 0.25)/ Colour=3/ Nolabel Rsquare

GO land 7

LABEL/Nouser 3.9 -0.8 0 0 0.15 "Slopes of trendlines of SSTs (^oC/year) in July,<nl>averaged in the period from January 1990 to December 2022.<nl>Coefficient of Determination (R^2) is contoured every 0.25 interval."

use etopo05.cdf

Shade/ overlay/Palette=black/ Level=(0 9000 9000)/ Nolab rose

CANCEL MODE Metafile

FRAME/File="SST_Trendline_Slope_07_Jul_00N40N099E170W_199001_202212.gif"

```
sp Fprint -o "SST_Trendline_Slope_07_Jul_00N40N099E170W_199001_202212.ps" -l cps -p portrait metafile.plt

! August

KEYMARK 1

SET Mode metafile

LET p = t[d=SST_ErdHadl_90S90N180W180E_199001_202309.nc, gl=1:33:1]

LET q = SST_Aug[x=99E:170W, y=00N:40N, l=1:33:1]

SET GRID q

GO regresst

! The variable "slope" which is calculated by "Ferret" is in (°C/s)

! The variable "slope" is converted in units to (°C/year) by multiplying below

LET Slope_per_year = Slope*60*60*24*365.25

SHADE/ Level=(-inf)(-0.04 0.04 0.02)(inf)/ Palette=no_green/ Nolabel Slope_per_year

CONTOUR/ Overlay/ Level=(0)/ Nolabel Slope_per_year[x=99E:170W, y=00N:40N]

CONTOUR/ Overlay/ Level=(0 1 0.25)/ Colour=3/ Nolabel Rsquare

GO land 7

LABEL/Nouser 3.9 -0.8 0 0 0.15 "Slopes of trendlines of SSTs (^oC/year) in August,<nl>averaged in the period from January 1990 to December 2022.<nl>Coefficient of Determination (R^2) is contoured every 0.25 interval."

use etopo05.cdf

Shade/ overlay/Palette=black/ Level=(0 9000 9000)/ Nolab rose

CANCEL MODE Metafile

FRAME/File="SST_Trendline_Slope_08_Aug_00N40N099E170W_199001_202212.gif"

sp Fprint -o "SST_Trendline_Slope_08_Aug_00N40N099E170W_199001_202212.ps" -l cps -p portrait metafile.plt
```

! September

KEYMARK 1

SET Mode metafile

LET p = t[d=SST_ErdHadl_90S90N180W180E_199001_202309.nc, gl=1:33:1]

LET q = SST_Sep[x=99E:170W, y=00N:40N, l=1:33:1]

SET GRID q

GO regresst

! The variable "slope" which is calculated by "Ferret" is in (°C/s)

! The variable "slope" is converted in units to (°C/year) by multiplying below

LET Slope_per_year = Slope*60*60*24*365.25

SHADE/ Level=(-inf)(-0.04 0.04 0.02)(inf)/ Palette=no_green/ Nolabel Slope_per_year

CONTOUR/ Overlay/ Level=(0)/ Nolabel Slope_per_year[x=99E:170W, y=00N:40N]

CONTOUR/ Overlay/ Level=(0 1 0.25)/ Colour=3/ Nolabel Rsquare

GO land 7

LABEL/Nouser 3.9 -0.8 0 0 0.15 "Slopes of trendlines of SSTs (^oC/year) in September,<nl>averaged in the period from January 1990 to December 2022.<nl>Coefficient of Determination (R^2) is contoured every 0.25 interval."

use etopo05.cdf

Shade/ overlay/Palette=black/ Level=(0 9000 9000)/ Nolab rose

CANCEL MODE Metafile

FRAME/File="SST_Trendline_Slope_09_Sep_00N40N099E170W_199001_202212.gif"

sp Fprint -o "SST_Trendline_Slope_09_Sep_00N40N099E170W_199001_202212.ps" -l cps -p portrait metafile.plt

! October

KEYMARK 1

SET Mode metafile

```
LET p = t[d=SST_ErdHadl_90S90N180W180E_199001_202309.nc, gl=1:33:1]

LET q = SST_Oct[x=99E:170W, y=00N:40N, l=1:33:1]

SET GRID q

GO regresst

! The variable "slope" which is calculated by "Ferret" is in (°C/s)

! The variable "slope" is converted in units to (°C/year) by multiplying below

LET Slope_per_year = Slope*60*60*24*365.25

SHADE/ Level=(-inf)(-0.04 0.04 0.02)(inf)/ Palette=no_green/ Nolabel
Slope_per_year

CONTOUR/ Overlay/ Level=(0)/ Nolabel Slope_per_year[x=99E:170W,
y=00N:40N]

CONTOUR/ Overlay/ Level=(0 1 0.25)/ Colour=3/ Nolabel Rsquare

GO land 7

LABEL/Nouser 3.9 -0.8 0 0 0.15 "Slopes of trendlines of SSTs (^oC/year) in
October,<nl>averaged in the period from January 1990 to December
2022.<nl>Coefficient of Determination (R^2) is contoured every 0.25 interval."

use etopo05.cdf

Shade/ overlay/Palette=black/ Level=(0 9000 9000)/ Nolab rose

CANCEL MODE Metafile

FRAME/File="SST_Trendline_Slope_10_Oct_00N40N099E170W_199001_202
212.gif"

sp Fprint -o
"SST_Trendline_Slope_10_Oct_00N40N099E170W_199001_202212.ps" -l cps -
p portrait metafile.plt

! November

KEYMARK 1

SET Mode metafile

LET p = t[d=SST_ErdHadl_90S90N180W180E_199001_202309.nc, gl=1:33:1]

LET q = SST_Nov[x=99E:170W, y=00N:40N, l=1:33:1]

SET GRID q
```

```
GO regresst

! The variable "slope" which is calculated by "Ferret" is in (°C/s)

! The variable "slope" is converted in units to (°C/year) by multiplying below

LET Slope_per_year = Slope*60*60*24*365.25

SHADE/ Level=(-inf)(-0.04 0.04 0.02)(inf)/ Palette=no_green/ Nolabel
Slope_per_year

CONTOUR/ Overlay/ Level=(0)/ Nolabel Slope_per_year[x=99E:170W,
y=00N:40N]

CONTOUR/ Overlay/ Level=(0 1 0.25)/ Colour=3/ Nolabel Rsquare

GO land 7

LABEL/Nouser 3.9 -0.8 0 0 0.15 "Slopes of trendlines of SSTs (^oC/year) in
November,<nl>averaged in the period from January 1990 to December
2022.<nl>Coefficient of Determination (R^2) is contoured every 0.25 interval."

use etopo05.cdf

Shade/ overlay/Palette=black/ Level=(0 9000 9000)/ Nolab rose

CANCEL MODE Metafile

FRAME/File="SST_Trendline_Slope_11_Nov_00N40N099E170W_199001_202
212.gif"

sp Fprint -o
"SST_Trendline_Slope_11_Nov_00N40N099E170W_199001_202212.ps" -l cps
-p portrait metafile.plt

! December

KEYMARK 1

SET Mode metafile

LET p = t[d=SST_ErdHadl_90S90N180W180E_199001_202309.nc, gl=1:33:1]

LET q = SST_Dec[x=99E:170W, y=00N:40N, l=1:33:1]

SET GRID q

GO regresst

! The variable "slope" which is calculated by "Ferret" is in (°C/s)

! The variable "slope" is converted in units to (°C/year) by multiplying below
```

```
LET Slope_per_year = Slope*60*60*24*365.25

SHADE/ Level=(-inf)(-0.04 0.04 0.02)(inf)/ Palette=no_green/ Nolabel Slope_per_year

CONTOUR/ Overlay/ Level=(0)/ Nolabel Slope_per_year[x=99E:170W, y=00N:40N]

CONTOUR/ Overlay/ Level=(0 1 0.25)/ Colour=3/ Nolabel Rsquare

GO land 7

LABEL/Nouser 3.9 -0.8 0 0 0.15 "Slopes of trendlines of SSTs (^oC/year) in December,<nl>averaged in the period from January 1990 to December 2022.<nl>Coefficient of Determination (R^2) is contoured every 0.25 interval."

use etopo05.cdf

Shade/ overlay/Palette=black/ Level=(0 9000 9000)/ Nolab rose

CANCEL MODE Metafile

FRAME/File="SST_Trendline_Slope_12_Dec_00N40N099E170W_199001_202212.gif"

sp Fprint -o "SST_Trendline_Slope_12_Dec_00N40N099E170W_199001_202212.ps" -l cps -p portrait metafile.plt

! Season-wise plots

! SST Map in Boreal Spring Season

KEYMARK 1

SET Mode metafile

LET p = t[d=SST_ErdHadl_90S90N180W180E_199001_202309.nc, gl=1:33:1]

LET q = SST_FMA[x=99E:170W, y=00N:40N, l=1:33:1]

SET GRID q

GO regresst

! The variable "slope" which is calculated by "Ferret" is in (°C/s)

! The variable "slope" is converted in units to (°C/year) by multiplying below


LET Slope_per_year = Slope*60*60*24*365.25
```

```
SHADE/ Level=(-inf)(-0.04 0.04 0.02)(inf)/ Palette=no_green/ Nolabel Slope_per_year

CONTOUR/ Overlay/ Level=(0)/ Nolabel Slope_per_year[x=99E:170W, y=00N:40N]

CONTOUR/ Overlay/ Level=(0 1 0.25)/ Colour=3/ Nolabel Rsquare

GO land 7

LABEL/Nouser 3.9 -0.8 0 0 0.15 "Slopes of trendlines of SSTs (^oC/year) in Boreal Spring Season,<nl>averaged in the period from January 1990 to December 2022.<nl>Coefficient of Determination (R^2) is contoured every 0.25 interval."

use etopo05.cdf

Shade/ overlay/Palette=black/ Level=(0 9000 9000)/ Nolab rose

CANCEL MODE Metafile

FRAME/File="SST_Trendline_Slope_13_Season_FMA_00N40N099E170W_199001_202212.gif"

sp Fprint -o "SST_Trendline_Slope_13_Season_FMA_00N40N099E170W_199001_202212.ps" -l cps -p portrait metafile.plt

! SST Map in Boreal Summer Season

KEYMARK 1

SET Mode metafile

LET p = t[d=SST_ErdHadl_90S90N180W180E_199001_202309.nc, gl=1:33:1]

LET q = SST_MJJ[x=99E:170W, y=00N:40N, l=1:33:1]

SET GRID q

GO regresst

! The variable "slope" which is calculated by "Ferret" is in (°C/s)

! The variable "slope" is converted in units to (°C/year) by multiplying below

LET Slope_per_year = Slope*60*60*24*365.25

SHADE/ Level=(-inf)(-0.04 0.04 0.02)(inf)/ Palette=no_green/ Nolabel Slope_per_year
```

```
CONTOUR/ Overlay/ Level=(0)/ Nolabel Slope_per_year[x=99E:170W, y=00N:40N]

CONTOUR/ Overlay/ Level=(0 1 0.25)/ Colour=3/ Nolabel Rsquare

GO land 7

LABEL/Nouser 3.9 -0.8 0 0 0.15 "Slopes of trendlines of SSTs (^oC/year) in Boreal Summer Season,<nl>averaged in the period from January 1990 to December 2022.<nl>Coefficient of Determination (R^2) is contoured every 0.25 interval."

use etopo05.cdf

Shade/ overlay/Palette=black/ Level=(0 9000 9000)/ Nolab rose

CANCEL MODE Metafile


FRAME/File="SST_Trendline_Slope_14_Season_MJJ_00N40N099E170W_199001_202212.gif"

sp Fprint -o "SST_Trendline_Slope_14_Season_MJJ_00N40N099E170W_199001_202212.ps" -l cps -p portrait metafile.plt

! SST Map in Boreal Autumn Season

KEYMARK 1

SET Mode metafile

LET p = t[d=SST_ErdHadl_90S90N180W180E_199001_202309.nc, gl=1:33:1]

LET q = SST_ASO[x=99E:170W, y=00N:40N, l=1:33:1]

SET GRID q

GO regresst

! The variable "slope" which is calculated by "Ferret" is in (°C/s)

! The variable "slope" is converted in units to (°C/year) by multiplying below

LET Slope_per_year = Slope*60*60*24*365.25

SHADE/ Level=(-inf)(-0.04 0.04 0.02)(inf)/ Palette=no_green/ Nolabel Slope_per_year
```

```
CONTOUR/ Overlay/ Level=(0)/ Nolabel Slope_per_year[x=99E:170W,
y=00N:40N]

CONTOUR/ Overlay/ Level=(0 1 0.25)/ Colour=3/ Nolabel Rsquare

GO land 7

LABEL/Nouser 3.9 -0.8 0 0 0.15 "Slopes of trendlines of SSTs (^oC/year) in
Boreal Autumn Season,<nl>averaged in the period from January 1990 to
December 2022.<nl>Coefficient of Determination (R^2) is contoured every 0.25
interval."

use etopo05.cdf

Shade/ overlay/Palette=black/ Level=(0 9000 9000)/ Nolab rose

CANCEL MODE Metafile

FRAME/File="SST_Trendline_Slope_15_Season_ASO_00N40N099E170W_199
001_202212.gif"

sp Fprint -o
"SST_Trendline_Slope_15_Season_ASO_00N40N099E170W_199001_202212.p
s" -l cps -p portrait metafile.plt

! SST Map in Boreal Winter Season

KEYMARK 1

SET Mode metafile

LET p = t[d=SST_ErdHadl_90S90N180W180E_199001_202309.nc, gl=1:32:1]

LET q = SST_NDJ[x=99E:170W, y=00N:40N, l=1:32:1]

SET GRID q

GO regresst

! The variable "slope" which is calculated by "Ferret" is in (°C/s)

! The variable "slope" is converted in units to (°C/year) by multiplying below

LET Slope_per_year = Slope*60*60*24*365.25

SHADE/ Level=(-inf)(-0.04 0.04 0.02)(inf)/ Palette=no_green/ Nolabel
Slope_per_year

CONTOUR/ Overlay/ Level=(0)/ Nolabel Slope_per_year[x=99E:170W,
y=00N:40N]
```

```
CONTOUR/ Overlay/ Level=(0 1 0.25)/ Colour=3/ Nolabel Rsquare

GO land 7

LABEL/Nouser 3.9 -0.8 0 0 0.15 "Slopes of trendlines of SSTs (^oC/year) in Boreal Winter Season,<nl>averaged in the period from January 1990 to December 2022.<nl>Coefficient of Determination (R^2) is contoured every 0.25 interval."

use etopo05.cdf

Shade/ overlay/Palette=black/ Level=(0 9000 9000)/ Nolab rose

CANCEL MODE Metafile

FRAME/File="SST_Trendline_Slope_16_Season_NDJ_00N40N099E170W_199001_202212.gif"

sp Fprint -o "SST_Trendline_Slope_16_Season_NDJ_00N40N099E170W_199001_202212.ps" -l cps -p portrait metafile.plt
```

Program 3.4 Program line-plotting the basin-averaged SST and its trendlines for the north-west Pacific Ocean (Eq. to 40 °N, 99 °E to 170 °W) for the entire period from January 1990 to December 2022, and also month-wise and season-wise, and shown from Figure 4.35 to Figure 4.51.

```
! 22 February 2024

! This program plots the sea surface temperature and its trendlines, basin-averaged in the region (00 N to 40 N, 99 E to 170W), in the period from January 1990 to December 2022.

! The sea surface temperature data used was downloaded from the webpage https://coastwatch.pfeg.noaa.gov/erddap/griddap/erdHadISST.html on 7 December 2023.

! The data is of SST, from HadISST Average Sea Surface Temperature, 1°, Global, Monthly, 1870-present.

! The data downloaded is from January 1990 to September 2023.
```

```
SET Mode verify

USE SST_ErdHadl_90S90N180W180E_199001_202309.nc
        ! Dataset of SST in the period from January 1990 to September 2023

SET REGION/ X=99E:170W/ Y=00N:40N
                ! North-west Pacific Ocean

SHOW Data

LET sst_filled = sst[d=SST_ErdHadl_90S90N180W180E_199001_202309.nc,
l=1:405@fln:12]              ! Time-period from January 1990 to September
2023

! SET Mode metafile

LET p = t[d=SST_ErdHadl_90S90N180W180E_199001_202309.nc, gl=1:396:1]

LET q = sst_filled[d=SST_ErdHadl_90S90N180W180E_199001_202309.nc,
x=99E:170W, y=00N:40N, l=1:396:1]              ! Time-period from January
1990 to December 2022

SET GRID q

GO regresst

LET Slope_per_year = Slope*60*60*24*365.25

LET Slope_per_year_NW_Pacific = FLOATSTR(Slope[x=99E:170W@ave,
y=00N:40N@ave]*60*60*24*365.25, "(f9.4)" )

LET Intercept_NW_Pacific = FLOATSTR(intercep[x=99E:170W@ave,
y=00N:40N@ave], "(f6.2)" )

LET Coeff_Determination = FLOATSTR(rsquare[x=@ave, y=@ave], "(f7.3)" )

LET SST_ave_NW_Pacific =  FLOATSTR(sst_filled[x=99E:170W@ave,
y=00N:40N@ave, l=1:396@ave], "(f7.3)")

PLOT/ Nolab sst_filled[x=99E:170W@ave, y=0:40N@ave, t="01-Jan-1990":"31-
Dec-2022"]

PLOT/vs/ Over/ Line/ Title= "Trendline" p, qhat[x=@ave,y=@ave]

LABEL/Nouser 3.9 -0.8 0 0 0.15 "Basin-averaged Sea Surface Temperature in the
north-west Pacific Ocean region<nl>(0^oN-40^oN, 99^oE-170^oW) averaged in
the period from January 1990 to<nl>December 2022 (in black). The trendline
(^oC/year) is plotted in red."
```

```
LABEL/Nouser 0 6.8 -1 0 0.15 "y = `Slope_per_year_NW_Pacific` x + `Intercept_NW_Pacific`"

LABEL/Nouser 3.5 6.8 -1 0 0.15 "Coefficient of Determination (R^2) = `Coeff_Determination`"

LABEL/Nouser 0 6.3 -1 0 0.15 "SST_a_v = `SST_ave_NW_Pacific` ^oC"

! CANCEL Mode Metafile

FRAME/ File="SST_Trendline_Slope_basin_averaged_00N40N099E170W_199001_202212.gif"

sp Fprint -o "SST_Trendline_Slope_basin_averaged_00N40N099E170W_199001_202212.ps" -l cps -p portrait metafile.plt

! Monthwise and seasonwise

LET SST_Jan = sst_filled[l=1:405:12]

LET SST_Feb = sst_filled[l=2:405:12]

LET SST_Mar = sst_filled[l=3:405:12]

LET SST_Apr = sst_filled[l=4:405:12]

LET SST_May = sst_filled[l=5:405:12]

LET SST_Jun = sst_filled[l=6:405:12]

LET SST_Jul = sst_filled[l=7:405:12]

LET SST_Aug = sst_filled[l=8:405:12]

LET SST_Sep = sst_filled[l=9:405:12]

LET SST_Oct = sst_filled[l=10:405:12]

LET SST_Nov = sst_filled[l=11:405:12]

LET SST_Dec = sst_filled[l=12:405:12]

! Seasons

LET SST_FMA = sst_feb[l=1:33:1] * (28.25/89.25) + sst_mar[l=1:33:1] * (31/89.25) + sst_apr[l=1:33:1] * (30/89.25)   ! Boreal Spring Season

LET SST_MJJ = sst_may[l=1:33:1] * (31/92) + sst_jun[l=1:33:1] * (30/92) + sst_jul[l=1:33:1] * (31/92)                         ! Boreal Summer Season
```

```
LET SST_ASO = sst_aug[l=1:33:1] * (31/92) + sst_sep[l=1:33:1] * (30/92) + sst_oct[l=1:33:1] * (31/92)                    ! Boreal Autumn Season

LET SST_NDJ = sst_nov[l=1:32:1] * (30/92) + sst_dec[l=1:32:1] * (31/92) + sst_jan[l=2:33:1] * (31/92)                    ! Boreal Winter Season

! Monthwise

! January

! SET Mode metafile

LET p = t[d=SST_ErdHadl_90S90N180W180E_199001_202309.nc, gl=1:33:1]

LET q = SST_Jan[d=SST_ErdHadl_90S90N180W180E_199001_202309.nc, x=99E:170W, y=00N:40N, l=1:33:1]

SET GRID q

GO regresst

LET Slope_per_year = Slope*60*60*24*365.25

LET Slope_per_year_NW_Pacific = FLOATSTR(Slope[x=99E:170W@ave, y=00N:40N@ave]*60*60*24*365.25, "(f9.4)" )

LET Intercept_NW_Pacific = FLOATSTR(intercep[x=99E:170W@ave, y=00N:40N@ave], "(f6.2)" )

LET Coeff_Determination = FLOATSTR(rsquare[x=@ave, y=@ave], "(f7.3)" )

LET SST_ave_NW_Pacific =  FLOATSTR(SST_Jan[x=99E:170W@ave, y=00N:40N@ave, l=1:33@ave], "(f7.3)")

PLOT/ Nolab SST_Jan[x=99E:170W@ave, y=0:40N@ave, t="01-Jan-1990":"31-Dec-2022"]

PLOT/vs/ Over/ Line/ Title= "Trendline" p, qhat[x=@ave,y=@ave]

LABEL/Nouser 3.9 -0.8 0 0 0.13 "Basin-averaged Sea Surface Temperature in the north-west Pacific Ocean region<nl>(0^oN-40^oN, 99^oE-170^oW) averaged in the month of January in the period from January 1990 to<nl>December 2022 (in black). The trendline (^oC/year) is plotted in red."

LABEL/Nouser 0 6.8 -1 0 0.15 "y = `Slope_per_year_NW_Pacific` x + `Intercept_NW_Pacific`"

LABEL/Nouser 3.5 6.8 -1 0 0.15 "Coefficient of Determination (R^2) = `Coeff_Determination`"

LABEL/Nouser 0 6.3 -1 0 0.15 "SST_a_v = `SST_ave_NW_Pacific` ^oC"
```

```
! CANCEL Mode Metafile

FRAME/ File="SST_Trendline_Slope_basin_averaged_01_Jan_00N40N099E170W_199001_202212.gif"

sp Fprint -o "SST_Trendline_Slope_basin_averaged_01_Jan_00N40N099E170W_199001_202212.ps" -l cps -p portrait metafile.plt

! Febuary

! SET Mode metafile

LET p = t[d=SST_ErdHadl_90S90N180W180E_199001_202309.nc, gl=1:33:1]

LET q = SST_Feb[d=SST_ErdHadl_90S90N180W180E_199001_202309.nc, x=99E:170W, y=00N:40N, l=1:33:1]

SET GRID q

GO regresst

LET Slope_per_year = Slope*60*60*24*365.25

LET Slope_per_year_NW_Pacific = FLOATSTR(Slope[x=99E:170W@ave, y=00N:40N@ave]*60*60*24*365.25, "(f9.4)" )

LET Intercept_NW_Pacific = FLOATSTR(intercep[x=99E:170W@ave, y=00N:40N@ave], "(f6.2)" )

LET Coeff_Determination = FLOATSTR(rsquare[x=@ave, y=@ave], "(f7.3)" )

LET SST_ave_NW_Pacific =  FLOATSTR(SST_Feb[x=99E:170W@ave, y=00N:40N@ave, l=1:33@ave], "(f7.3)")

PLOT/ Nolab SST_Feb[x=99E:170W@ave, y=0:40N@ave, t="01-Jan-1990":"31-Dec-2022"]

PLOT/vs/ Over/ Line/ Title= "Trendline" p, qhat[x=@ave,y=@ave]

LABEL/Nouser 3.9 -0.8 0 0 0.13 "Basin-averaged Sea Surface Temperature in the north-west Pacific Ocean region<nl>(0^oN-40^oN, 99^oE-170^oW) averaged in the month of February in the period from January 1990 to<nl>December 2022 (in black). The trendline (^oC/year) is plotted in red."

LABEL/Nouser 0 6.8 -1 0 0.15 "y = `Slope_per_year_NW_Pacific` x + `Intercept_NW_Pacific`"
```

LABEL/Nouser 3.5 6.8 -1 0 0.15 "Coefficient of Determination (R^2) = `Coeff_Determination`"

LABEL/Nouser 0 6.3 -1 0 0.15 "SST_a_v = `SST_ave_NW_Pacific` ^oC"

! CANCEL Mode Metafile

FRAME/ File="SST_Trendline_Slope_basin_averaged_02_Feb_00N40N099E170W_199001_202212.gif"

sp Fprint -o "SST_Trendline_Slope_basin_averaged_02_Feb_00N40N099E170W_199001_202212.ps" -l cps -p portrait metafile.plt

! March

! SET Mode metafile

LET p = t[d=SST_ErdHadl_90S90N180W180E_199001_202309.nc, gl=1:33:1]

LET q = SST_Mar[d=SST_ErdHadl_90S90N180W180E_199001_202309.nc, x=99E:170W, y=00N:40N, l=1:33:1]

SET GRID q

GO regresst

LET Slope_per_year = Slope*60*60*24*365.25

LET Slope_per_year_NW_Pacific = FLOATSTR(Slope[x=99E:170W@ave, y=00N:40N@ave]*60*60*24*365.25, "(f9.4)")

LET Intercept_NW_Pacific = FLOATSTR(intercep[x=99E:170W@ave, y=00N:40N@ave], "(f6.2)")

LET Coeff_Determination = FLOATSTR(rsquare[x=@ave, y=@ave], "(f7.3)")

LET SST_ave_NW_Pacific = FLOATSTR(SST_Mar[x=99E:170W@ave, y=00N:40N@ave, l=1:33@ave], "(f7.3)")

PLOT/ Nolab SST_Mar[x=99E:170W@ave, y=0:40N@ave, t="01-Jan-1990":"31-Dec-2022"]

PLOT/vs/ Over/ Line/ Title= "Trendline" p, qhat[x=@ave,y=@ave]

LABEL/Nouser 3.9 -0.8 0 0 0.13 "Basin-averaged Sea Surface Temperature in the north-west Pacific Ocean region<nl>(0^oN-40^oN, 99^oE-170^oW) averaged in the month of March in the period from January 1990 to<nl>December 2022 (in black). The trendline (^oC/year) is plotted in red."

```
LABEL/Nouser 0 6.8 -1 0 0.15 "y = `Slope_per_year_NW_Pacific` x + `Intercept_NW_Pacific`"

LABEL/Nouser 3.5 6.8 -1 0 0.15 "Coefficient of Determination (R^2) = `Coeff_Determination`"

LABEL/Nouser 0 6.3 -1 0 0.15 "SST_a_v = `SST_ave_NW_Pacific` ^oC"

! CANCEL Mode Metafile

FRAME/ File="SST_Trendline_Slope_basin_averaged_03_Mar_00N40N099E170W_199001_202212.gif"

sp Fprint -o "SST_Trendline_Slope_basin_averaged_03_Mar_00N40N099E170W_199001_202212.ps" -l cps -p portrait metafile.plt

! April

! SET Mode metafile

LET p = t[d=SST_ErdHadl_90S90N180W180E_199001_202309.nc, gl=1:33:1]

LET q = SST_Apr[d=SST_ErdHadl_90S90N180W180E_199001_202309.nc, x=99E:170W, y=00N:40N, l=1:33:1]

SET GRID q

GO regresst

LET Slope_per_year = Slope*60*60*24*365.25

LET Slope_per_year_NW_Pacific = FLOATSTR(Slope[x=99E:170W@ave, y=00N:40N@ave]*60*60*24*365.25, "(f9.4)" )

LET Intercept_NW_Pacific = FLOATSTR(intercep[x=99E:170W@ave, y=00N:40N@ave], "(f6.2)" )

LET Coeff_Determination = FLOATSTR(rsquare[x=@ave, y=@ave], "(f7.3)" )

LET SST_ave_NW_Pacific =  FLOATSTR(SST_Apr[x=99E:170W@ave, y=00N:40N@ave, l=1:33@ave], "(f7.3)")

PLOT/ Nolab SST_Apr[x=99E:170W@ave, y=0:40N@ave, t="01-Jan-1990":"31-Dec-2022"]

PLOT/vs/ Over/ Line/ Title= "Trendline" p, qhat[x=@ave,y=@ave]

LABEL/Nouser 3.9 -0.8 0 0 0.13 "Basin-averaged Sea Surface Temperature in the north-west Pacific Ocean region<nl>(0^oN-40^oN, 99^oE-170^oW) averaged in
```

the month of April in the period from January 1990 to<nl>December 2022 (in black). The trendline (^oC/year) is plotted in red."

LABEL/Nouser 0 6.8 -1 0 0.15 "y = `Slope_per_year_NW_Pacific` x + `Intercept_NW_Pacific`"

LABEL/Nouser 3.5 6.8 -1 0 0.15 "Coefficient of Determination (R^2) = `Coeff_Determination`"

LABEL/Nouser 0 6.3 -1 0 0.15 "SST_a_v = `SST_ave_NW_Pacific` ^oC"

! CANCEL Mode Metafile

FRAME/ File="SST_Trendline_Slope_basin_averaged_04_Apr_00N40N099E170W_199001_202212.gif"

sp Fprint -o "SST_Trendline_Slope_basin_averaged_04_Apr_00N40N099E170W_199001_202212.ps" -l cps -p portrait metafile.plt

! May

! SET Mode metafile

LET p = t[d=SST_ErdHadl_90S90N180W180E_199001_202309.nc, gl=1:33:1]

LET q = SST_May[d=SST_ErdHadl_90S90N180W180E_199001_202309.nc, x=99E:170W, y=00N:40N, l=1:33:1]

SET GRID q

GO regresst

LET Slope_per_year = Slope*60*60*24*365.25

LET Slope_per_year_NW_Pacific = FLOATSTR(Slope[x=99E:170W@ave, y=00N:40N@ave]*60*60*24*365.25, "(f9.4)")

LET Intercept_NW_Pacific = FLOATSTR(intercep[x=99E:170W@ave, y=00N:40N@ave], "(f6.2)")

LET Coeff_Determination = FLOATSTR(rsquare[x=@ave, y=@ave], "(f7.3)")

LET SST_ave_NW_Pacific = FLOATSTR(SST_May[x=99E:170W@ave, y=00N:40N@ave, l=1:33@ave], "(f7.3)")

PLOT/ Nolab SST_May[x=99E:170W@ave, y=0:40N@ave, t="01-Jan-1990":"31-Dec-2022"]

PLOT/vs/ Over/ Line/ Title= "Trendline" p, qhat[x=@ave,y=@ave]

```
LABEL/Nouser 3.9 -0.8 0 0 0.13 "Basin-averaged Sea Surface Temperature in the north-west Pacific Ocean region<nl>(0^oN-40^oN, 99^oE-170^oW) averaged in the month of May in the period from January 1990 to<nl>December 2022 (in black). The trendline (^oC/year) is plotted in red."

LABEL/Nouser 0 6.8 -1 0 0.15 "y = `Slope_per_year_NW_Pacific` x + `Intercept_NW_Pacific`"

LABEL/Nouser 3.5 6.8 -1 0 0.15 "Coefficient of Determination (R^2) = `Coeff_Determination`"

LABEL/Nouser 0 6.3 -1 0 0.15 "SST_a_v = `SST_ave_NW_Pacific` ^oC"

! CANCEL Mode Metafile

FRAME/ File="SST_Trendline_Slope_basin_averaged_05_May_00N40N099E170W_199001_202212.gif"

sp Fprint -o "SST_Trendline_Slope_basin_averaged_05_May_00N40N099E170W_199001_202212.ps" -l cps -p portrait metafile.plt


! June

! SET Mode metafile

LET p = t[d=SST_ErdHadl_90S90N180W180E_199001_202309.nc, gl=1:33:1]

LET q = SST_Jun[d=SST_ErdHadl_90S90N180W180E_199001_202309.nc, x=99E:170W, y=00N:40N, l=1:33:1]

SET GRID q

GO regresst

LET Slope_per_year = Slope*60*60*24*365.25

LET Slope_per_year_NW_Pacific = FLOATSTR(Slope[x=99E:170W@ave, y=00N:40N@ave]*60*60*24*365.25, "(f9.4)" )

LET Intercept_NW_Pacific = FLOATSTR(intercep[x=99E:170W@ave, y=00N:40N@ave], "(f6.2)" )

LET Coeff_Determination = FLOATSTR(rsquare[x=@ave, y=@ave], "(f7.3)" )

LET SST_ave_NW_Pacific =  FLOATSTR(SST_Jun[x=99E:170W@ave, y=00N:40N@ave, l=1:33@ave], "(f7.3)")
```

```
PLOT/ Nolab SST_Jun[x=99E:170W@ave, y=0:40N@ave, t="01-Jan-1990":"31-Dec-2022"]

PLOT/vs/ Over/ Line/ Title= "Trendline" p, qhat[x=@ave,y=@ave]

LABEL/Nouser 3.9 -0.8 0 0 0.13 "Basin-averaged Sea Surface Temperature in the north-west Pacific Ocean region<nl>(0^oN-40^oN, 99^oE-170^oW) averaged in the month of June in the period from January 1990 to<nl>December 2022 (in black). The trendline (^oC/year) is plotted in red."

LABEL/Nouser 0 6.8 -1 0 0.15 "y = `Slope_per_year_NW_Pacific` x + `Intercept_NW_Pacific`"

LABEL/Nouser 3.5 6.8 -1 0 0.15 "Coefficient of Determination (R^2) = `Coeff_Determination`"

LABEL/Nouser 0 6.3 -1 0 0.15 "SST_a_v = `SST_ave_NW_Pacific` ^oC"

! CANCEL Mode Metafile

FRAME/ File="SST_Trendline_Slope_basin_averaged_06_Jun_00N40N099E170W_199001_202212.gif"

sp Fprint -o "SST_Trendline_Slope_basin_averaged_06_Jun_00N40N099E170W_199001_202212.ps" -l cps -p portrait metafile.plt

! July

! SET Mode metafile

LET p = t[d=SST_ErdHadl_90S90N180W180E_199001_202309.nc, gl=1:33:1]

LET q = SST_Jul[d=SST_ErdHadl_90S90N180W180E_199001_202309.nc, x=99E:170W, y=00N:40N, l=1:33:1]

SET GRID q

GO regresst

LET Slope_per_year = Slope*60*60*24*365.25

LET Slope_per_year_NW_Pacific = FLOATSTR(Slope[x=99E:170W@ave, y=00N:40N@ave]*60*60*24*365.25, "(f9.4)" )

LET Intercept_NW_Pacific = FLOATSTR(intercep[x=99E:170W@ave, y=00N:40N@ave], "(f6.2)" )

LET Coeff_Determination = FLOATSTR(rsquare[x=@ave, y=@ave], "(f7.3)" )
```

```
LET SST_ave_NW_Pacific =  FLOATSTR(SST_Jul[x=99E:170W@ave,
y=00N:40N@ave, l=1:33@ave], "(f7.3)")

PLOT/ Nolab SST_Jul[x=99E:170W@ave, y=0:40N@ave, t="01-Jan-1990":"31-
Dec-2022"]

PLOT/vs/ Over/ Line/ Title= "Trendline" p, qhat[x=@ave,y=@ave]

LABEL/Nouser 3.9 -0.8 0 0 0.13 "Basin-averaged Sea Surface Temperature in the
north-west Pacific Ocean region<nl>(0^oN-40^oN, 99^oE-170^oW) averaged in
the month of July in the period from January 1990 to<nl>December 2022 (in
black). The trendline (^oC/year) is plotted in red."

LABEL/Nouser 0 6.8 -1 0 0.15 "y = `Slope_per_year_NW_Pacific` x +
`Intercept_NW_Pacific`"

LABEL/Nouser 3.5 6.8 -1 0 0.15 "Coefficient of Determination (R^2) =
`Coeff_Determination`"

LABEL/Nouser 0 6.3 -1 0 0.15 "SST_a_v = `SST_ave_NW_Pacific` ^oC"

! CANCEL Mode Metafile

FRAME/
File="SST_Trendline_Slope_basin_averaged_07_Jul_00N40N099E170W_19900
1_202212.gif"

sp Fprint -o
"SST_Trendline_Slope_basin_averaged_07_Jul_00N40N099E170W_199001_20
2212.ps" -l cps -p portrait metafile.plt

! August

! SET Mode metafile

LET p = t[d=SST_ErdHadl_90S90N180W180E_199001_202309.nc, gl=1:33:1]

LET q = SST_Aug[d=SST_ErdHadl_90S90N180W180E_199001_202309.nc,
x=99E:170W, y=00N:40N, l=1:33:1]

SET GRID q

GO regresst

LET Slope_per_year = Slope*60*60*24*365.25

LET Slope_per_year_NW_Pacific = FLOATSTR(Slope[x=99E:170W@ave,
y=00N:40N@ave]*60*60*24*365.25, "(f9.4)" )
```

```
LET Intercept_NW_Pacific = FLOATSTR(intercep[x=99E:170W@ave, y=00N:40N@ave], "(f6.2)" )

LET Coeff_Determination = FLOATSTR(rsquare[x=@ave, y=@ave], "(f7.3)" )

LET SST_ave_NW_Pacific =  FLOATSTR(SST_Aug[x=99E:170W@ave, y=00N:40N@ave, l=1:33@ave], "(f7.3)")

PLOT/ Nolab SST_Aug[x=99E:170W@ave, y=0:40N@ave, t="01-Jan-1990":"31-Dec-2022"]

PLOT/vs/ Over/ Line/ Title= "Trendline" p, qhat[x=@ave,y=@ave]

LABEL/Nouser 3.9 -0.8 0 0 0.13 "Basin-averaged Sea Surface Temperature in the north-west Pacific Ocean region<nl>(0^oN-40^oN, 99^oE-170^oW) averaged in the month of August in the period from January 1990 to<nl>December 2022 (in black). The trendline (^oC/year) is plotted in red."

LABEL/Nouser 0 6.8 -1 0 0.15 "y = `Slope_per_year_NW_Pacific` x + `Intercept_NW_Pacific`"

LABEL/Nouser 3.5 6.8 -1 0 0.15 "Coefficient of Determination (R^2) = `Coeff_Determination`"

LABEL/Nouser 0 6.3 -1 0 0.15 "SST_a_v = `SST_ave_NW_Pacific` ^oC"

! CANCEL Mode Metafile

FRAME/ File="SST_Trendline_Slope_basin_averaged_08_Aug_00N40N099E170W_199001_202212.gif"

sp Fprint -o "SST_Trendline_Slope_basin_averaged_08_Aug_00N40N099E170W_199001_202212.ps" -l cps -p portrait metafile.plt

! September

! SET Mode metafile

LET p = t[d=SST_ErdHadl_90S90N180W180E_199001_202309.nc, gl=1:33:1]

LET q = SST_Sep[d=SST_ErdHadl_90S90N180W180E_199001_202309.nc, x=99E:170W, y=00N:40N, l=1:33:1]

SET GRID q

GO regresst

LET Slope_per_year = Slope*60*60*24*365.25
```

```
LET Slope_per_year_NW_Pacific = FLOATSTR(Slope[x=99E:170W@ave, y=00N:40N@ave]*60*60*24*365.25, "(f9.4)" )

LET Intercept_NW_Pacific = FLOATSTR(intercep[x=99E:170W@ave, y=00N:40N@ave], "(f6.2)" )

LET Coeff_Determination = FLOATSTR(rsquare[x=@ave, y=@ave], "(f7.3)" )

LET SST_ave_NW_Pacific =  FLOATSTR(SST_Sep[x=99E:170W@ave, y=00N:40N@ave, l=1:33@ave], "(f7.3)")

PLOT/ Nolab SST_Sep[x=99E:170W@ave, y=0:40N@ave, t="01-Jan-1990":"31-Dec-2022"]

PLOT/vs/ Over/ Line/ Title= "Trendline" p, qhat[x=@ave,y=@ave]

LABEL/Nouser 3.9 -0.8 0 0 0.13 "Basin-averaged Sea Surface Temperature in the north-west Pacific Ocean region<nl>(0^oN-40^oN, 99^oE-170^oW) averaged in the month of September in the period from January 1990 to<nl>December 2022 (in black). The trendline (^oC/year) is plotted in red."

LABEL/Nouser 0 6.8 -1 0 0.15 "y = `Slope_per_year_NW_Pacific` x + `Intercept_NW_Pacific`"

LABEL/Nouser 3.5 6.8 -1 0 0.15 "Coefficient of Determination (R^2) = `Coeff_Determination`"

LABEL/Nouser 0 6.3 -1 0 0.15 "SST_a_v = `SST_ave_NW_Pacific` ^oC"

! CANCEL Mode Metafile

FRAME/ File="SST_Trendline_Slope_basin_averaged_09_Sep_00N40N099E170W_199001_202212.gif"

sp Fprint -o "SST_Trendline_Slope_basin_averaged_09_Sep_00N40N099E170W_199001_202212.ps" -l cps -p portrait metafile.plt

! October

! SET Mode metafile

LET p = t[d=SST_ErdHadl_90S90N180W180E_199001_202309.nc, gl=1:33:1]

LET q = SST_Oct[d=SST_ErdHadl_90S90N180W180E_199001_202309.nc, x=99E:170W, y=00N:40N, l=1:33:1]

SET GRID q
```

```
GO regresst

LET Slope_per_year = Slope*60*60*24*365.25

LET Slope_per_year_NW_Pacific = FLOATSTR(Slope[x=99E:170W@ave,
y=00N:40N@ave]*60*60*24*365.25, "(f9.4)" )

LET Intercept_NW_Pacific = FLOATSTR(intercep[x=99E:170W@ave,
y=00N:40N@ave], "(f6.2)" )

LET Coeff_Determination = FLOATSTR(rsquare[x=@ave, y=@ave], "(f7.3)" )

LET SST_ave_NW_Pacific =  FLOATSTR(SST_Oct[x=99E:170W@ave,
y=00N:40N@ave, l=1:33@ave], "(f7.3)")

PLOT/ Nolab SST_Oct[x=99E:170W@ave, y=0:40N@ave, t="01-Jan-1990":"31-
Dec-2022"]

PLOT/vs/ Over/ Line/ Title= "Trendline" p, qhat[x=@ave,y=@ave]

LABEL/Nouser 3.9 -0.8 0 0 0.13 "Basin-averaged Sea Surface Temperature in the
north-west Pacific Ocean region<nl>(0^oN-40^oN, 99^oE-170^oW) averaged in
the month of October in the period from January 1990 to<nl>December 2022 (in
black). The trendline (^oC/year) is plotted in red."

LABEL/Nouser 0 6.8 -1 0 0.15 "y = `Slope_per_year_NW_Pacific` x +
`Intercept_NW_Pacific`"

LABEL/Nouser 3.5 6.8 -1 0 0.15 "Coefficient of Determination (R^2) =
`Coeff_Determination`"

LABEL/Nouser 0 6.3 -1 0 0.15 "SST_a_v = `SST_ave_NW_Pacific` ^oC"

! CANCEL Mode Metafile

FRAME/
File="SST_Trendline_Slope_basin_averaged_10_Oct_00N40N099E170W_1990
01_202212.gif"

sp Fprint -o
"SST_Trendline_Slope_basin_averaged_10_Oct_00N40N099E170W_199001_20
2212.ps" -l cps -p portrait metafile.plt

! November

! SET Mode metafile

LET p = t[d=SST_ErdHadl_90S90N180W180E_199001_202309.nc, gl=1:33:1]
```

```
LET q = SST_Nov[d=SST_ErdHadl_90S90N180W180E_199001_202309.nc, x=99E:170W, y=00N:40N, l=1:33:1]

SET GRID q

GO regresst

LET Slope_per_year = Slope*60*60*24*365.25

LET Slope_per_year_NW_Pacific = FLOATSTR(Slope[x=99E:170W@ave, y=00N:40N@ave]*60*60*24*365.25, "(f9.4)" )

LET Intercept_NW_Pacific = FLOATSTR(intercep[x=99E:170W@ave, y=00N:40N@ave], "(f6.2)" )

LET Coeff_Determination = FLOATSTR(rsquare[x=@ave, y=@ave], "(f7.3)" )

LET SST_ave_NW_Pacific =  FLOATSTR(SST_Nov[x=99E:170W@ave, y=00N:40N@ave, l=1:33@ave], "(f7.3)")


PLOT/ Nolab SST_Nov[x=99E:170W@ave, y=0:40N@ave, t="01-Jan-1990":"31-Dec-2022"]

PLOT/vs/ Over/ Line/ Title= "Trendline" p, qhat[x=@ave,y=@ave]

LABEL/Nouser 3.9 -0.8 0 0 0.13 "Basin-averaged Sea Surface Temperature in the north-west Pacific Ocean region<nl>(0^oN-40^oN, 99^oE-170^oW) averaged in the month of November in the period from January 1990 to<nl>December 2022 (in black). The trendline (^oC/year) is plotted in red."

LABEL/Nouser 0 6.8 -1 0 0.15 "y = `Slope_per_year_NW_Pacific` x + `Intercept_NW_Pacific`"

LABEL/Nouser 3.5 6.8 -1 0 0.15 "Coefficient of Determination (R^2) = `Coeff_Determination`"

LABEL/Nouser 0 6.3 -1 0 0.15 "SST_a_v = `SST_ave_NW_Pacific` ^oC"

! CANCEL Mode Metafile

FRAME/ File="SST_Trendline_Slope_basin_averaged_11_Nov_00N40N099E170W_199001_202212.gif"

sp Fprint -o "SST_Trendline_Slope_basin_averaged_11_Nov_00N40N099E170W_199001_202212.ps" -l cps -p portrait metafile.plt
```

```
! December

! SET Mode metafile

LET p = t[d=SST_ErdHadl_90S90N180W180E_199001_202309.nc, gl=1:33:1]

LET q = SST_Dec[d=SST_ErdHadl_90S90N180W180E_199001_202309.nc, x=99E:170W, y=00N:40N, l=1:33:1]

SET GRID q

GO regresst

LET Slope_per_year = Slope*60*60*24*365.25

LET Slope_per_year_NW_Pacific = FLOATSTR(Slope[x=99E:170W@ave, y=00N:40N@ave]*60*60*24*365.25, "(f9.4)" )

LET Intercept_NW_Pacific = FLOATSTR(intercep[x=99E:170W@ave, y=00N:40N@ave], "(f6.2)" )

LET Coeff_Determination = FLOATSTR(rsquare[x=@ave, y=@ave], "(f7.3)" )

LET SST_ave_NW_Pacific =  FLOATSTR(SST_Dec[x=99E:170W@ave, y=00N:40N@ave, l=1:33@ave], "(f7.3)")

PLOT/ Nolab SST_Dec[x=99E:170W@ave, y=0:40N@ave, t="01-Jan-1990":"31-Dec-2022"]

PLOT/vs/ Over/ Line/ Title= "Trendline" p, qhat[x=@ave,y=@ave]

LABEL/Nouser 3.9 -0.8 0 0 0.13 "Basin-averaged Sea Surface Temperature in the north-west Pacific Ocean region<nl>(0^oN-40^oN, 99^oE-170^oW) averaged in the month of December in the period from January 1990 to<nl>December 2022 (in black). The trendline (^oC/year) is plotted in red."

LABEL/Nouser 0 6.8 -1 0 0.15 "y = `Slope_per_year_NW_Pacific` x + `Intercept_NW_Pacific`"

LABEL/Nouser 3.5 6.8 -1 0 0.15 "Coefficient of Determination (R^2) = `Coeff_Determination`"

LABEL/Nouser 0 6.3 -1 0 0.15 "SST_a_v = `SST_ave_NW_Pacific` ^oC"

! CANCEL Mode Metafile

FRAME/ File="SST_Trendline_Slope_basin_averaged_12_Dec_00N40N099E170W_199001_202212.gif"
```

sp Fprint -o "SST_Trendline_Slope_basin_averaged_12_Dec_00N40N099E170W_199001_202212.ps" -l cps -p portrait metafile.plt

! Boreal Spring

! SET Mode metafile

LET p = t[d=SST_ErdHadl_90S90N180W180E_199001_202309.nc, gl=1:33:1]

LET q = SST_FMA[d=SST_ErdHadl_90S90N180W180E_199001_202309.nc, x=99E:170W, y=00N:40N, l=1:33:1]

SET GRID q

GO regresst

LET Slope_per_year = Slope*60*60*24*365.25

LET Slope_per_year_NW_Pacific = FLOATSTR(Slope[x=99E:170W@ave, y=00N:40N@ave]*60*60*24*365.25, "(f9.4)")

LET Intercept_NW_Pacific = FLOATSTR(intercep[x=99E:170W@ave, y=00N:40N@ave], "(f6.2)")

LET Coeff_Determination = FLOATSTR(rsquare[x=@ave, y=@ave], "(f7.3)")

LET SST_ave_NW_Pacific = FLOATSTR(SST_FMA[x=99E:170W@ave, y=00N:40N@ave, l=1:33@ave], "(f7.3)")

PLOT/ Nolab SST_FMA[x=99E:170W@ave, y=0:40N@ave, t="01-Jan-1990":"31-Dec-2022"]

PLOT/vs/ Over/ Line/ Title= "Trendline" p, qhat[x=@ave,y=@ave]

LABEL/Nouser 3.9 -0.8 0 0 0.13 "Basin-averaged Sea Surface Temperature in the north-west Pacific Ocean region<nl>(0^oN-40^oN, 99^oE-170^oW) averaged in Boreal Spring Season for the period from January 1990 to<nl>December 2022 (in black). The trendline (^oC/year) is plotted in red."

LABEL/Nouser 0 6.8 -1 0 0.15 "y = `Slope_per_year_NW_Pacific` x + `Intercept_NW_Pacific`"

LABEL/Nouser 3.5 6.8 -1 0 0.15 "Coefficient of Determination (R^2) = `Coeff_Determination`"

LABEL/Nouser 0 6.3 -1 0 0.15 "SST_a_v = `SST_ave_NW_Pacific` ^oC"

! CANCEL Mode Metafile

```
FRAME/ File="SST_Trendline_Slope_basin_averaged_13_Season_FMA_00N40N099E170W_199001_202212.gif"

sp Fprint -o "SST_Trendline_Slope_basin_averaged_13_Season_FMA_00N40N099E170W_199001_202212.ps" -l cps -p portrait metafile.plt

! Boreal Summer

! SET Mode metafile

LET p = t[d=SST_ErdHadl_90S90N180W180E_199001_202309.nc, gl=1:33:1]

LET q = SST_MJJ[d=SST_ErdHadl_90S90N180W180E_199001_202309.nc, x=99E:170W, y=00N:40N, l=1:33:1]

SET GRID q

GO regresst

LET Slope_per_year = Slope*60*60*24*365.25

LET Slope_per_year_NW_Pacific = FLOATSTR(Slope[x=99E:170W@ave, y=00N:40N@ave]*60*60*24*365.25, "(f9.4)" )

LET Intercept_NW_Pacific = FLOATSTR(intercep[x=99E:170W@ave, y=00N:40N@ave], "(f6.2)" )

LET Coeff_Determination = FLOATSTR(rsquare[x=@ave, y=@ave], "(f7.3)" )

LET SST_ave_NW_Pacific =  FLOATSTR(SST_MJJ[x=99E:170W@ave, y=00N:40N@ave, l=1:33@ave], "(f7.3)")

PLOT/ Nolab SST_MJJ[x=99E:170W@ave, y=0:40N@ave, t="01-Jan-1990":"31-Dec-2022"]

PLOT/vs/ Over/ Line/ Title= "Trendline" p, qhat[x=@ave,y=@ave]

LABEL/Nouser 3.9 -0.8 0 0 0.13 "Basin-averaged Sea Surface Temperature in the north-west Pacific Ocean region<nl>(0^oN-40^oN, 99^oE-170^oW) averaged in Boreal Summer Season for the period from January 1990 to<nl>December 2022 (in black). The trendline (^oC/year) is plotted in red."

LABEL/Nouser 0 6.8 -1 0 0.15 "y = `Slope_per_year_NW_Pacific` x + `Intercept_NW_Pacific`"

LABEL/Nouser 3.5 6.8 -1 0 0.15 "Coefficient of Determination (R^2) = `Coeff_Determination`"
```

```
LABEL/Nouser 0 6.3 -1 0 0.15 "SST_a_v = `SST_ave_NW_Pacific` ^oC"

! CANCEL Mode Metafile

FRAME/
File="SST_Trendline_Slope_basin_averaged_14_Season_MJJ_00N40N099E170
W_199001_202212.gif"

sp Fprint -o
"SST_Trendline_Slope_basin_averaged_14_Season_MJJ_00N40N099E170W_19
9001_202212.ps" -l cps -p portrait metafile.plt


! Boreal Autumn

! SET Mode metafile

LET p = t[d=SST_ErdHadl_90S90N180W180E_199001_202309.nc, gl=1:33:1]

LET q = SST_ASO[d=SST_ErdHadl_90S90N180W180E_199001_202309.nc,
x=99E:170W, y=00N:40N, l=1:33:1]

SET GRID q

GO regresst

LET Slope_per_year = Slope*60*60*24*365.25

LET Slope_per_year_NW_Pacific = FLOATSTR(Slope[x=99E:170W@ave,
y=00N:40N@ave]*60*60*24*365.25, "(f9.4)" )

LET Intercept_NW_Pacific = FLOATSTR(intercep[x=99E:170W@ave,
y=00N:40N@ave], "(f6.2)" )

LET Coeff_Determination = FLOATSTR(rsquare[x=@ave, y=@ave], "(f7.3)" )

LET SST_ave_NW_Pacific =  FLOATSTR(SST_ASO[x=99E:170W@ave,
y=00N:40N@ave, l=1:33@ave], "(f7.3)")

PLOT/ Nolab SST_ASO[x=99E:170W@ave, y=0:40N@ave, t="01-Jan-
1990":"31-Dec-2022"]

PLOT/vs/ Over/ Line/ Title= "Trendline" p, qhat[x=@ave,y=@ave]


LABEL/Nouser 3.9 -0.8 0 0 0.13 "Basin-averaged Sea Surface Temperature in the
north-west Pacific Ocean region<nl>(0^oN-40^oN, 99^oE-170^oW) averaged in
Boreal Autumn Season for the period from January 1990 to<nl>December 2022
(in black). The trendline (^oC/year) is plotted in red."
```

```
LABEL/Nouser 0 6.8 -1 0 0.15 "y = `Slope_per_year_NW_Pacific` x + `Intercept_NW_Pacific`"

LABEL/Nouser 3.5 6.8 -1 0 0.15 "Coefficient of Determination (R^2) = `Coeff_Determination`"

LABEL/Nouser 0 6.3 -1 0 0.15 "SST_a_v = `SST_ave_NW_Pacific` ^oC"

! CANCEL Mode Metafile

FRAME/ File="SST_Trendline_Slope_basin_averaged_15_Season_ASO_00N40N099E170W_199001_202212.gif"

sp Fprint -o "SST_Trendline_Slope_basin_averaged_15_Season_ASO_00N40N099E170W_199001_202212.ps" -l cps -p portrait metafile.plt

! Boreal Winter

! SET Mode metafile

LET p = t[d=SST_ErdHadl_90S90N180W180E_199001_202309.nc, gl=1:32:1]

LET q = SST_NDJ[d=SST_ErdHadl_90S90N180W180E_199001_202309.nc, x=99E:170W, y=00N:40N, l=1:32:1]

SET GRID q

GO regresst

LET Slope_per_year = Slope*60*60*24*365.25

LET Slope_per_year_NW_Pacific = FLOATSTR(Slope[x=99E:170W@ave, y=00N:40N@ave]*60*60*24*365.25, "(f9.4)" )

LET Intercept_NW_Pacific = FLOATSTR(intercep[x=99E:170W@ave, y=00N:40N@ave], "(f6.2)" )

LET Coeff_Determination = FLOATSTR(rsquare[x=@ave, y=@ave], "(f7.3)" )

LET SST_ave_NW_Pacific =  FLOATSTR(SST_NDJ[x=99E:170W@ave, y=00N:40N@ave, l=1:32@ave], "(f7.3)")

PLOT/ Nolab SST_NDJ[x=99E:170W@ave, y=0:40N@ave, t="01-Jan-1990":"31-Dec-2022"]

PLOT/vs/ Over/ Line/ Title= "Trendline" p, qhat[x=@ave,y=@ave]

LABEL/Nouser 3.9 -0.8 0 0 0.13 "Basin-averaged Sea Surface Temperature in the north-west Pacific Ocean region<nl>(0^oN-40^oN, 99^oE-170^oW) averaged in
```

Boreal Winter Season for the period from January 1990 to<nl>December 2022 (in black). The trendline (^oC/year) is plotted in red."

LABEL/Nouser 0 6.8 -1 0 0.15 "y = `Slope_per_year_NW_Pacific` x + `Intercept_NW_Pacific`"

LABEL/Nouser 3.5 6.8 -1 0 0.15 "Coefficient of Determination (R^2) = `Coeff_Determination`"

LABEL/Nouser 0 6.3 -1 0 0.15 "SST_a_v = `SST_ave_NW_Pacific` ^oC"

! CANCEL Mode Metafile

FRAME/ File="SST_Trendline_Slope_basin_averaged_16_Season_NDJ_00N40N099E170W_199001_202212.gif"

sp Fprint -o "SST_Trendline_Slope_basin_averaged_16_Season_NDJ_00N40N099E170W_199001_202212.ps" -l cps -p portrait metafile.plt

.

CHAPTER 4: OBSERVATIONS

4.1 AVERAGE OF SEA SURFACE TEMPERATURE

4.1.1 The SST Average in the Period from January 1990 to December 2022

The SST map in the north-west Pacific Ocean (0 °N to 40 °N, 99 °E to 170 °W), averaged in the period from January 1990 to December 2022, is shown in Figure 4.1.

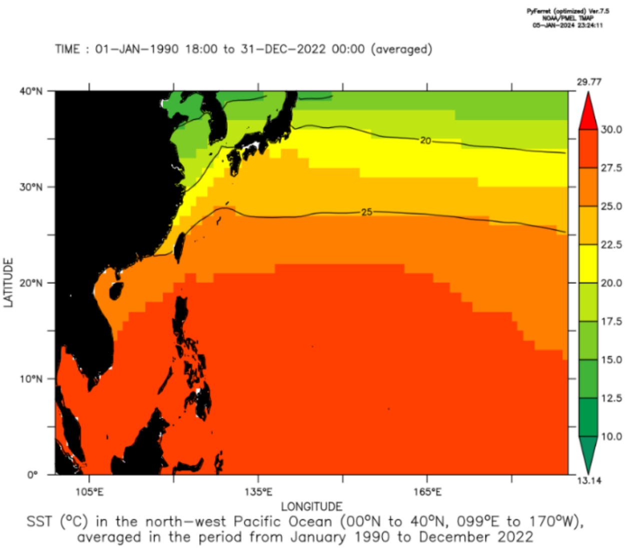

Figure 4.1. SST (°C) map in the north-west Pacific Ocean (0 °N to 40 °N, 99 °E to 170 °W), averaged in the period from January 1990 to December 2022

The SSTs have a minimum value of 13.14 °C and a maximum value of 29.77 °C. The difference between the maximum SST and minimum SST is 16.63 °C**.** The SSTs are highest in the equatorial regions, with values in the range of above 27.5 °C. Such values are seen in the Malacca Strait, Gulf of Thailand, southern parts of South China Sea, Sulu Sea, Celebes Sea, Philippines Sea and nearly in the entire zonal band to the south of 15 °N. The temperatures reduce meridionally, away from the Equator. Temperatures in the range from 25 °C to

27.5 °C are seen from Vietnam to Taiwan. Temperatures further reduce in the East China Sea, decreasing further in the Yellow Sea and the Sea of Japan. Temperatures below 15 °C are seen in the Bohai Sea and parts of the Sea of Japan and to the east of Japan at 40 °N.

4.1.2 The Month-wise SST Average in the Period from January 1990 to December 2022

a. *January:*

The SST (°C) map in the north-west Pacific Ocean (0 °N to 40 °N, 99 °E to 170 °W), averaged in January for the period from January 1990 to December 2022, is shown in Figure 4.2.

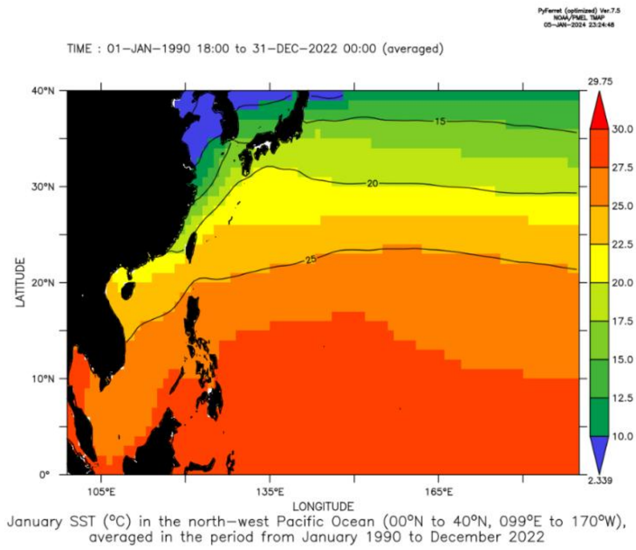

Figure 4.2 SST (°C) map in the north-west Pacific Ocean (0 °N to 40 °N, 99 °E to 170 °W), averaged in January for the period from January 1990 to December 2022.

The SSTs have a minimum value of 2.339 °C and a maximum value of 29.75 °C. The difference between the maximum SST and minimum SST is 27.41

°C. The SSTs have the highest values in the range above 27.5 °C. Such values are seen in the Malacca Strait, Gulf of Thailand, Sulu Sea, Celebes Sea, Bohol Sea and in the equatorial Pacific region. The temperatures reduce meridionally from the Equator towards the north. Temperatures in the range from 25 °C to 27.5 °C are seen extending from the southern regions of the South China Sea to northern parts of the Philippine Sea and then further extending eastward in the zonal band between 10 °N to 20 °N at 170 °W. Temperatures further reduce in the East China Sea, decreasing further in the Yellow Sea and the Sea of Japan. Temperatures below 10 °C are seen in the Bohai Sea and in parts of the Sea of Japan.

b. *February:*

The SST (°C) map in the north-west Pacific Ocean (0 °N to 40 °N, 99 °E to 170 °W), averaged in February for the period from January 1990 to December 2022, is shown in Figure 4.3.

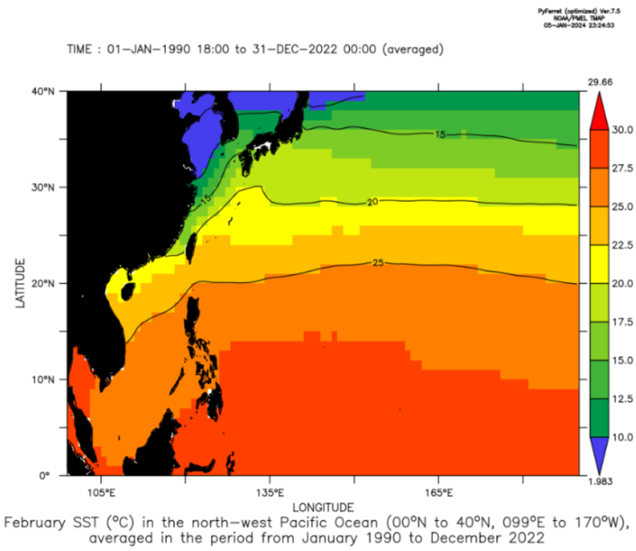

Figure 4.3 SST (°C) map in the north-west Pacific Ocean (0 °N to 40 °N, 99 °E to 170 °W), averaged in February for the period from January 1990 to December 2022.

The SSTs have a minimum value of 1.983 °C and a maximum value of 29.66 °C. The difference between the maximum SST and minimum SST is 27.68 °C. The highest SST values are in the range of above 27.5 °C. Such values are seen in the Malacca Strait, Gulf of Thailand, and Celebes Sea and extend further eastward in the tropical Pacific, between approximately 0 °N and 10 °N. The temperatures reduce meridionally from the Equator northwards. Temperatures range from 25 °C to 27.5 °C in the South China Sea, Sulu Sea, and parts of the Philippine Sea, and they extend eastward to between 10 °N and 20 °N at 170 °W. Temperatures further reduce in the East China Sea, further decreasing in the Yellow Sea and the Sea of Japan. Temperatures below 10 °C are seen in the Yellow Sea and parts of the Sea of Japan. Temperatures are below 5 °C in the Bohai Sea.

c. *March:*

The SST (°C) map in the north-west Pacific Ocean (0 °N to 40 °N, 99 °E to 170 °W), averaged in March for the period from January 1990 to December 2022, is shown in Figure 4.4. The SSTs show a minimum value of 3.216 °C and a maximum value of 29.77 °C. The difference between the maximum SST and minimum SST is 26.55 °C. The SSTs are highest in the equatorial regions, with values ranging above 27.5 °C. Such values are seen in the Malacca Strait, the Gulf of Thailand, the south-eastern parts of the South China Sea, the Sulu Sea, the Celebes Sea, and southern parts of the Philippines Sea. Temperatures in the range from 25 °C to 27.5 °C are seen from the northern parts of the South China Sea to the northern part of the Philippines Sea. Temperatures further reduce near Hong Kong and also Taiwan. Temperatures below 15 °C are seen in parts of the East China Sea and in the Sea of Japan. Further reduced temperatures are seen in the

Yellow Sea, in the Bohai Sea and near the Korean Peninsula. The SST isotherms migrate northward away from the Equator, from the month of March.

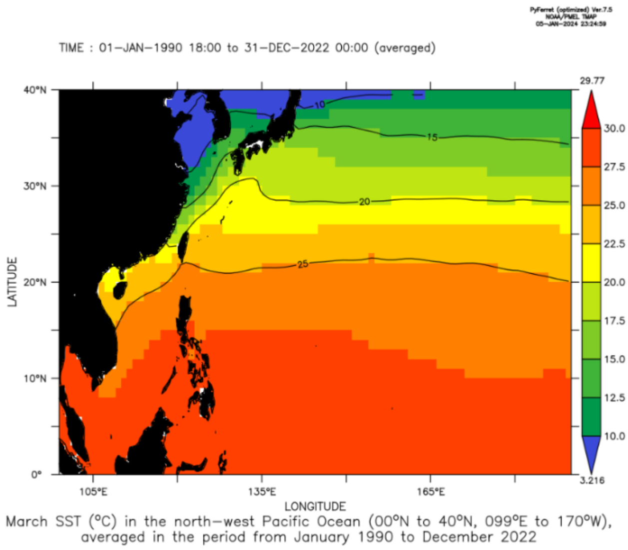

Figure 4.4 SST (°C) map in the north-west Pacific Ocean (0 °N to 40 °N, 99 °E to 170 °W), averaged in March for the period from January 1990 to December 2022.

d. *April:*

The SST (°C) map in the north-west Pacific Ocean (0 °N to 40 °N, 99 °E to 170 °W), averaged in April for the period from January 1990 to December 2022, is shown in Figure 4.5. The SSTs show a minimum value of 6.805 °C and a maximum value of 30.12 °C. The difference between the maximum SST and minimum SST is 23.32 °C. The SST are highest having red patches with values in the range of above 30.0 °C as seen in northern parts of the Gulf of Thailand. The SSTs in the equatorial regions have values in the range of above 27.5 °C. Such values are seen in the Malacca Strait, southern parts of the Gulf of Thailand, southern parts of the South China Sea, Sulu Sea, Celebes Sea, Philippine Sea and nearly in the entire zonal band to the south of 15 °N. The temperatures reduce meridionally, away from the Equator. Temperatures in the range from 25 °C to

27.5 °C are seen from Vietnam to southern parts of Taiwan. Temperatures further reduce in the East China Sea, decreasing further in the Yellow Sea. Temperatures below 10 °C are seen in the Bohai Sea and in parts of the Sea of Japan.

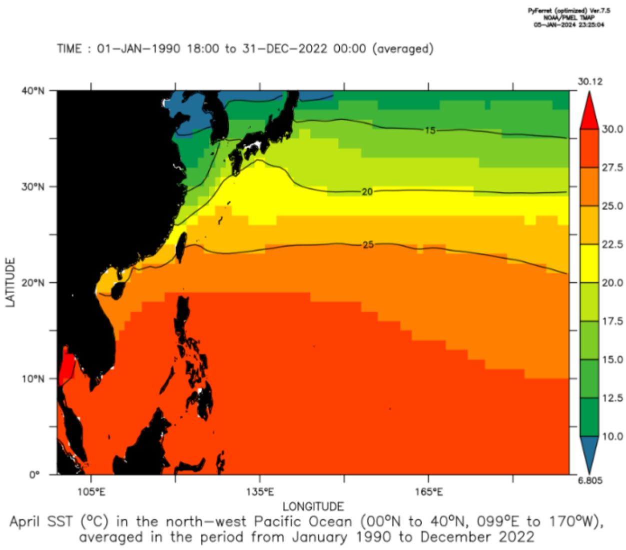

Figure 4.5 SST (°C) map in the north-west Pacific Ocean (0 °N to 40 °N, 99 °E to 170 °W), averaged in April for the period from January 1990 to December 2022.

e. May:

The SST (°C) map in the north-west Pacific Ocean (0 °N to 40 °N, 99 °E to 170 °W), averaged in May for the period from January 1990 to December 2022, is shown in Figure 4.6. The SSTs show a minimum value of 11.64 °C and a maximum value of 30.5 °C. The difference between the maximum SST and minimum SST is 18.86 °C. The highest SSTs have values in the range above 30.0 °C. Such values are seen in the Malacca Strait, the Gulf of Thailand and the southern parts of the South China Sea. The SSTs with values in the range between 27.5 °C and 30 °C are seen in the Sulu Sea, Celebes Sea, Philippine Sea, northern parts of the South China Sea and nearly in the entire zonal band to the south of 15 °N. The temperatures reduce meridionally, away from the Equator. Temperatures in the range from 25 °C to 27.5 °C are seen near Beibu Gulf, near Taiwan and extending zonally further in the western Pacific Ocean. Temperatures reduce meriodionally northwards, reaching temperatures below 15 °C in the Bohai Sea and parts of the Sea of Japan and zonally to the north of about 36 °N.

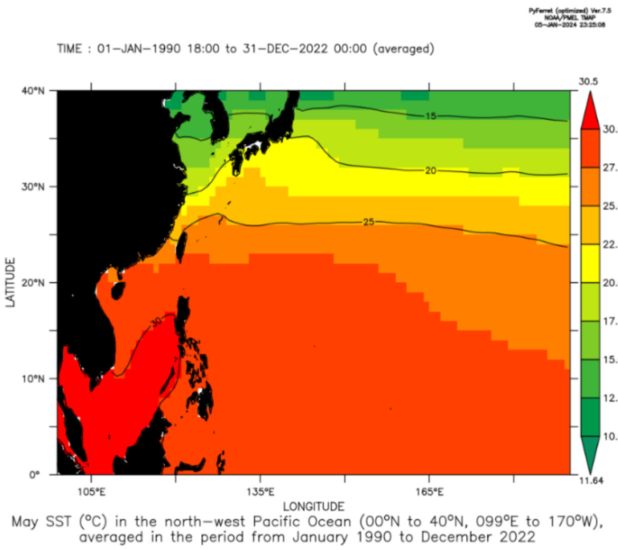

Figure 4.6 SST (°C) map in the north-west Pacific Ocean (0 °N to 40 °N, 99 °E to 170 °W), averaged in May for the period from January 1990 to December 2022.

f. ***June:***

The SST (°C) map in the north-west Pacific Ocean (0 °N to 40 °N, 99 °E to 170 °W), averaged in June for the period from January 1990 to December 2022, is shown in Figure 4.7. The SSTs show a minimum value of 14.57 °C and a maximum value of 30.18 °C. The difference between the maximum SST and minimum SST is 15.61 °C. The SSTs are highest with values in the range of above 30°C. Such values are seen in the Malacca Strait, around Riau Islands and parts of the coast of Sarawak on the island of Borneo and around northern parts of the Philippines, near the island of Luzon. The SSTs with values in the range of above 27.5 °C are seen in the Gulf of Thailand, South China Sea, Sulu Sea, Celebes Sea, Philippine Sea, near southern Taiwan and nearly in the entire zonal band to the south of 20 °N. The temperatures reduce meridionally, away from the Equator. Temperatures in the range from 25 °C to 27.5 °C are seen in the East China Sea, and they extend zonally into the western Pacific to the south of 30 °N. Temperatures reduce meridionally northwards. Regions with SSTs below 20 °C are seen in the Bohai Sea, parts of the Yellow Sea, parts of the Sea of Japan, and are seen also extending zonally to the north of about 35 °N latitude in the north-western Pacific Ocean.

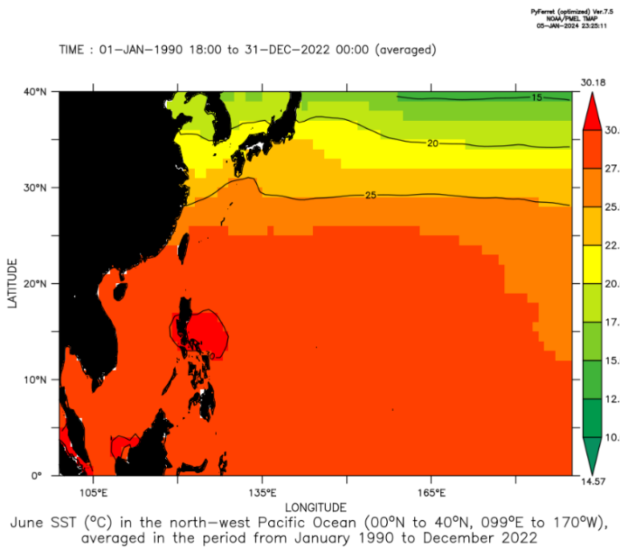

Figure 4.7 SST (°C) map in the north-west Pacific Ocean (0 °N to 40 °N, 99 °E to 170 °W), averaged in June for the period from January 1990 to December 2022.

g. July:

The SST (°C) map in the north-west Pacific Ocean (0 °N to 40 °N, 99 °E to 170 °W), averaged in July for the period from January 1990 to December 2022, is shown in Figure 4.8. The SSTs show a minimum value of 18.08 °C and a maximum value of 29.95 °C. The difference between the maximum SST and minimum SST is 11.87 °C. The SSTs are highest in the equatorial regions, with values ranging above 27.5 °C. Such values are seen in the Malacca Strait, Gulf of Thailand, South China Sea, Sulu Sea, Celebes Sea, Philippine Sea and nearly in the entire zonal band to the south of 25 °N. Temperatures in the range from 25 °C to 27.5 °C are seen some parts of the East China Sea, decreasing further in the Yellow Sea, Bohai Sea and the Sea of Japan. The least SSTs are lesser than 20 °C. These temperatures are seen to the east of Japan, extending in the east-west direction, around 40 °N latitude.

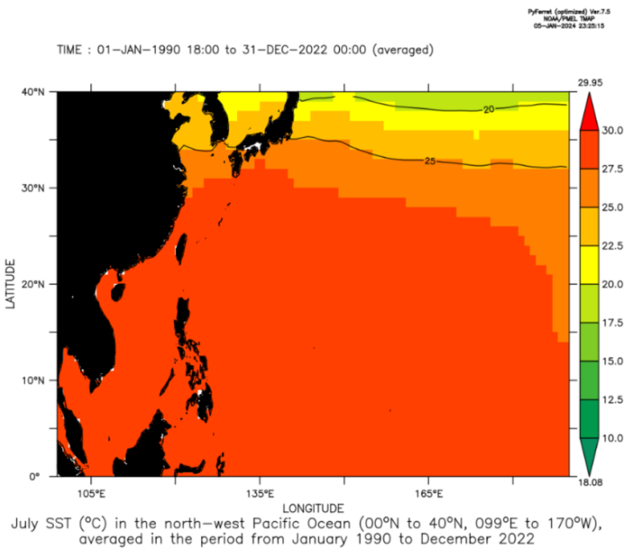

Figure 4.8 SST (°C) map in the north-west Pacific Ocean (0 °N to 40 °N, 99 °E to 170 °W), averaged in July for the period from January 1990 to December 2022.

h. August:

The SST (°C) map in the north-west Pacific Ocean (0 °N to 40 °N, 99 °E to 170 °W), averaged in August for the period from January 1990 to December 2022, is shown in Figure 4.9. The SSTs show a minimum value of 21.66 °C and a maximum value of 29.82 °C. The difference between the maximum SST and minimum SST is 8.16 °C. The SSTs are highest in the equatorial regions, with values in the range of above 27.5 °C. Such values are seen in the Malacca Strait, Gulf of Thailand, South China Sea, Sulu Sea, Celebes Sea, Philippine Sea, East China Sea, the southern coast of Japan and nearly in the entire zonal band to the south of 25 °N. Temperatures below 25 °C are seen in parts of the Korea Bay and parts of the Sea of Japan and to the east of Japan, extending zonally at around 35 °N. SSTs below 22.5 °C, are seen extending zonally, to the east of around 155 °E longitude, at around 40 °N latitude.

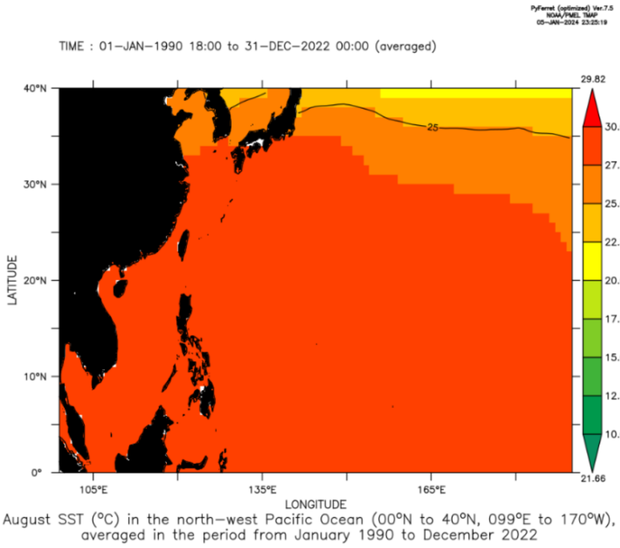

Figure 4.9 SST (°C) map in the north-west Pacific Ocean (0 °N to 40 °N, 99 °E to 170 °W), averaged in August for the period from January 1990 to December 2022.

i. *September:*

The SST (°C) map in the north-west Pacific Ocean (0 °N to 40 °N, 99 °E to 170 °W), averaged in September for the period from January 1990 to December 2022, is shown in Figure 4.10. The SSTs show a minimum value of 20.78 °C and a maximum value of 29.95 °C. The difference between the maximum SST and minimum SST is 9.17 °C. The SSTs are highest in the equatorial regions, with values in the range of above 27.5 °C. Such values are seen in the Malacca Strait, Gulf of Thailand, South China Sea, Sulu Sea, Celebes Sea, Philippine Sea, part of the south coasts of the islands of Kyushu, Shikoku and Honshu, all in Japan. These warm temperatures are also seen in nearly in the entire zonal band to the south of 30 °N. Temperatures in the range from 25 °C to 27.5 °C are seen in the East China Sea Temperatures below 25 °C are seen in the Bohai Sea, Yellow Sea and Sea of Japan. The SST isotherms migrate southward towards the Equator, from the month of September.

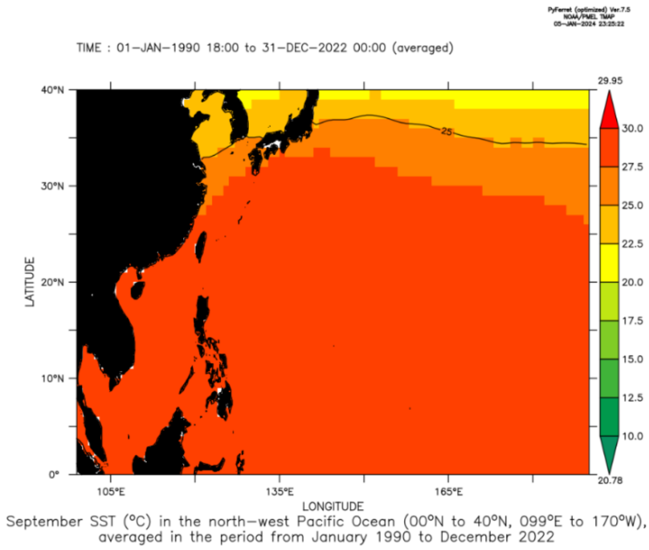

Figure 4.10 SST (°C) map in the north-west Pacific Ocean (0 °N to 40 °N, 99 °E to 170 °W), averaged in September for the period from January 1990 to December 2022.

j. October:

The SST (°C) map in the north-west Pacific Ocean (0 °N to 40 °N, 99 °E to 170 °W), averaged in October for the period from January 1990 to December 2022, is shown in Figure 4.11. The SSTs show a minimum value of 17.78 °C and a maximum value of 29.86 °C. The difference between the maximum SST and minimum SST is 12.08 °C. The SSTs are highest in the equatorial regions, with values in the range of above 27.5 °C. Such values are seen in the Malacca Strait, Gulf of Thailand, South China Sea, Sulu Sea, Celebes Sea, Philippine Sea and nearly in the entire zonal band to the south of 20 °N. Temperatures in the range from 25 °C to 27.5 °C are seen from the island of Hainan to the island of Taiwan, further extending zonally eastwards between 25 °N and 30 °N latitudes approximately. Temperatures further reduce in the East China Sea, decreasing further in the Yellow Sea. Temperatures below 22.5 °C are seen in the Bohai Sea and in the Sea of Japan.

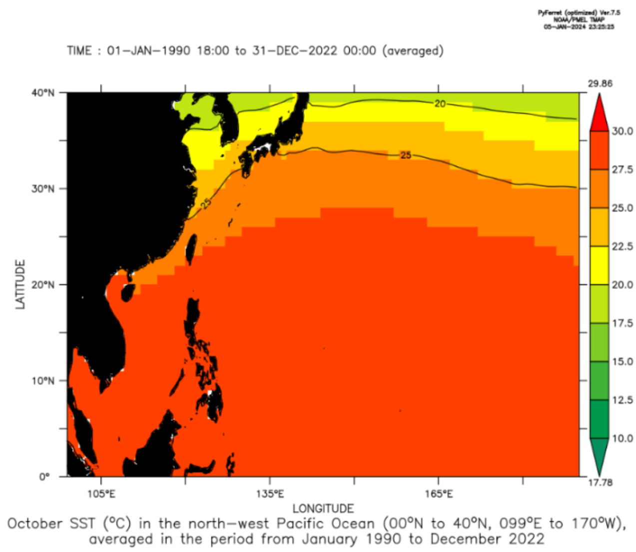

Figure 4.11 SST (°C) map in the north-west Pacific Ocean (0 °N to 40 °N, 99 °E to 170 °W), averaged in October for the period from January 1990 to December 2022.

k. November:

The SST (°C) map in the north-west Pacific Ocean (0 °N to 40 °N, 99 °E to 170 °W), averaged in November for the period from January 1990 to December 2022, is shown in Figure 4.12. The SSTs show a minimum value of 13.05 °C and a maximum value of 30.01 °C. The difference between the maximum SST and minimum SST is 16.96 °C. The SSTs are highest in the equatorial regions, with values just above 30.0 °C. Such values are seen near (1 °N, 149 °E). The SSTs with values in the range of above 27.5 °C are seen in the Malacca Strait, Gulf of Thailand, southern parts of South China Sea, Sulu Sea, Celebes Sea, Philippine Sea and nearly in the entire zonal band to the south of 15 °N.

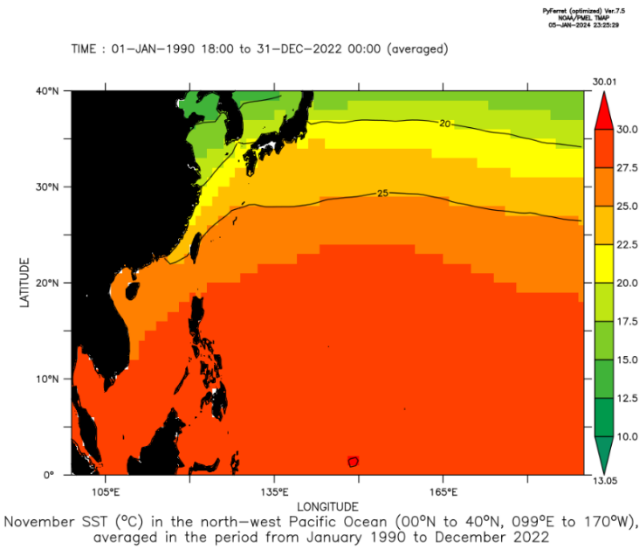

Figure 4.12 SST (°C) map in the north-west Pacific Ocean (0 °N to 40 °N, 99 °E to 170 °W), averaged in November for the period from January 1990 to December 2022.

Temperatures in the range from 25 °C to 27.5 °C are seen from the coastal waters off southern Vietnam to Taiwan and then seen further extending zonally eastward into the Pacific Ocean in the latitudinal band between approximately 20 °N to 25 °N. Temperatures further reduce in the East China Sea, decreasing further in the Yellow Sea and the Sea of Japan. Temperatures below 15 °C are seen in the Bohai Sea and in parts of the Sea of Japan.

l. December:

The SST (°C) map in the north-west Pacific Ocean (0 °N to 40 °N, 99 °E to 170 °W), averaged in December for the period from January 1990 to December 2022, is shown in Figure 4.13.

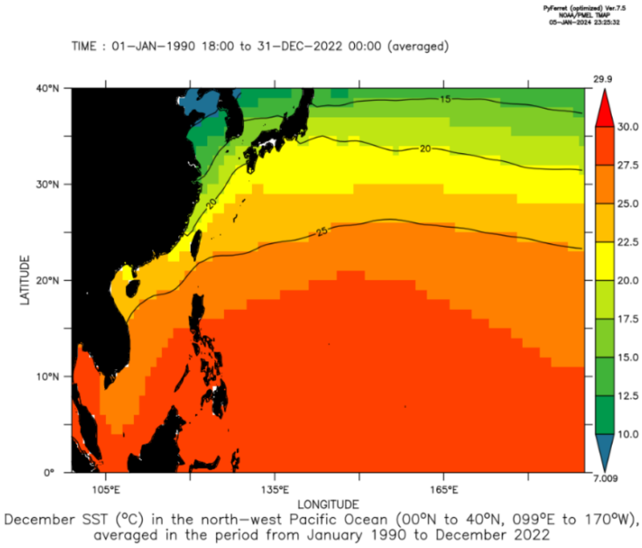

Figure 4.13 SST (°C) map in the north-west Pacific Ocean (0 °N to 40 °N, 99 °E to 170 °W), averaged in December for the period from January 1990 to December 2022.

The SSTs show a minimum value of 7.009 °C and a maximum value of 29.9 °C. The difference between the maximum SST and minimum SST is 22.891 °C. The SSTs are highest in the equatorial regions, with values in the range of above 27.5 °C. Such values are seen in the Malacca Strait, parts of the Gulf of Thailand, Sulu Sea, the Celebes Sea, parts of the Philippine Sea and parts of the tropical north Pacific Ocean. The regions mainly to the south of 15 °N generally show the temperatures of above 27 °C. Temperatures in the range from 25 °C to 27.5 °C are seen in a small part of the Gulf of Thailand, parts of the South China Sea, extending eastwards to the northern parts Philippine Sea and then extending zonally eastwards and covering a latitudinal range between around 12 °N to 23 °N at 170 °W meridian. Temperatures further reduce in the East China Sea, decreasing further in the Yellow Sea and the Sea of Japan. Temperatures below 10 °C are seen in the Bohai Sea, Korea Bay and in parts of the Sea of Japan.

4.1.3 The Season-wise SST Average in the Period from January 1990 to December 2022

a. ***Boreal Spring Season:***

The SST (°C) map in the north-west Pacific Ocean (0 °N to 40 °N, 99 °E to 170 °W), averaged in Boreal Spring for the period from January 1990 to December 2022, is shown in Figure 4.14. The SSTs show a minimum value of 4.129 °C and a maximum value of 29.75 °C.

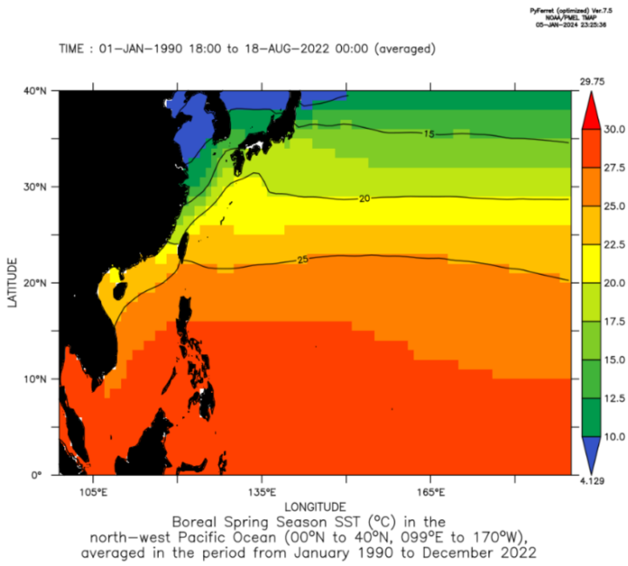

Figure 4.14 SST (°C) map in the north-west Pacific Ocean (0 °N to 40 °N, 99 °E to 170 °W), averaged in Boreal Spring Season for the period from January 1990 to December 2022.

The difference between the maximum SST and minimum SST is 25.621 °C. The SSTs are highest in the equatorial regions, with values in the range of above 27.5 °C. Such values are seen in the Malacca Strait, Gulf of Thailand, south-eastern parts of South China Sea, Sulu Sea, Celebes Sea, southern parts of the Philippine Sea and extends eastwards into the Pacific Ocean, covering almost the entire region equatorward of 10 °N. Temperatures in the range from 25 °C to 27.5 °C are seen from northern parts of South China Sea to northern parts of Philippine Sea and then extending eastward into the Pacific Ocean covering a latitudinal range between 10 °N to 20 °N at 170 °W longitude. Temperatures further reduce in the East China Sea, decreasing further in the Yellow Sea and the Sea of Japan. Temperatures below 10 °C are seen in the Bohai Sea, some other parts of the Yellow Sea and parts of the Sea of Japan. The lowest temperatures are seen in the Bohai Sea, where temperatures drop to less than 5 °C.

b. *Boreal Summer Season:*

The SST (°C) map in the north-west Pacific Ocean (0 °N to 40 °N, 99 °E to 170 °W), averaged in Boreal Summer for the period from January 1990 to December 2022, is shown in Figure 4.15. The SSTs show a minimum value of 15.04 °C and a maximum value of 30.03 °C. The difference between the maximum SST and minimum SST is 14.99 °C. The SSTs are highest with values in the range of above 30 °C. Such values are seen in parts of the Malacca Strait. The SSTs with values in the range of above 27.5 °C are seen in the Gulf of Thailand, most parts of South China Sea, Sulu Sea, Celebes Sea, Philippine Sea and nearly in the entire zonal band to the south of 20 °N. Temperatures in the range from 25 °C to 27.5 °C are seen in parts of the East China Sea and extending zonally eastward into the Pacific Ocean, reaching a latitudinal range between 12

°N to 27 °N at 170 °W longitude. Temperatures further reduce in the northward regions of the East China Sea, decreasing further in the Yellow Sea and in the Sea of Japan. Temperatures in the range between 15 °C to 17.5 °C are seen near the 40 °N latitude.

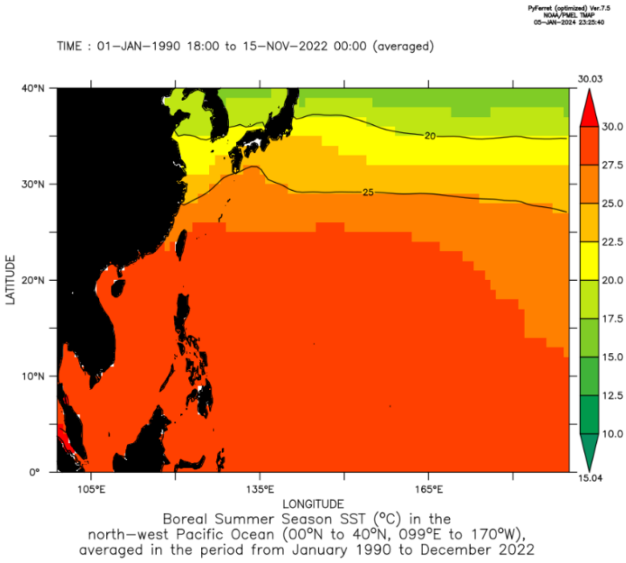

Figure 4.15 SST (°C) map in the north-west Pacific Ocean (0 °N to 40 °N, 99 °E to 170 °W), averaged in Boreal Summer Season for the period from January 1990 to December 2022.

c. *Boreal Autumn Season:*

The SST (°C) map in the north-west Pacific Ocean (0 °N to 40 °N, 99 °E to 170 °W), averaged in Boreal Autumn for the period from January 1990 to December 2022, is shown in Figure 4.16. The SSTs show a minimum value of 20.19 °C and a maximum value of 29.76 °C. The difference between the maximum SST and minimum SST is 9.57 °C. The SSTs are highest in the tropical regions, with values in the range of above 27.5 °C in almost the entire region to the south of 25 °N. Such values are seen in the Malacca Strait, Gulf of Thailand, most parts of the South China Sea, Sulu Sea, Celebes Sea, Philippine Sea and nearly in the entire zonal band to equatorward of 25 °N. Temperatures in the range from 25 °C to 27.5 °C are seen from the northern parts of the Taiwan Strait, parts of the East China Sea, off the southern coast of Japan and extending zonally eastward and covering a latitudinal range between around 24 °N to 33 °N at 170 °W longitude. Temperatures below 25 °C are seen in the most of the Yellow Sea, Bohai Sea, parts of the Sea of Japan and in the latitudinal range northward of about 35 °N in the north-west Pacific Ocean. The lowest SSTs, i.e. in the range between 20 °C to 22.5 °C, are seen extending zonally at around 40 °N latitude.

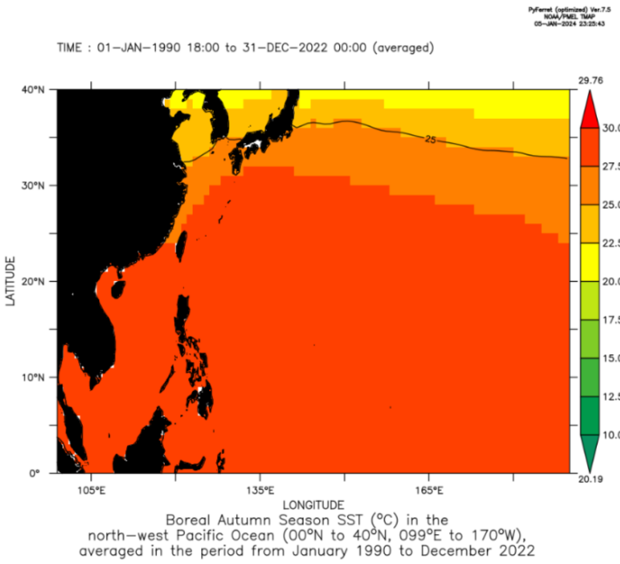

Figure 4.16 SST (°C) map in the north-west Pacific Ocean (0 °N to 40 °N, 99 °E to 170 °W), averaged in Boreal Autumn Season for the period from January 1990 to December 2022.

d. Boreal Winter Season:

The SST (°C) map in the north-west Pacific Ocean (0 °N to 40 °N, 99 °E to 170 °W), averaged in Boreal Winter for the period from January 1990 to December 2022, is shown in Figure 4.17.

The SSTs show a minimum value of 7.477 °C and a maximum value of 29.86 °C. The difference between the maximum SST and minimum SST is 22.383 °C. The SSTs are highest in the tropical regions, with values in the range of above 27.5 °C. Such values are seen in the Malacca Strait, most of the Gulf of Thailand, Sulu Sea, Celebes Sea and most of the Philippine Sea. These higher temperatures then extend zonally into the north Pacific Ocean, reaching northwards up to 20 °N at around 145 °E longitude and then arching towards the south-east and extending northward upto 12 °N at 170 °W longitude.

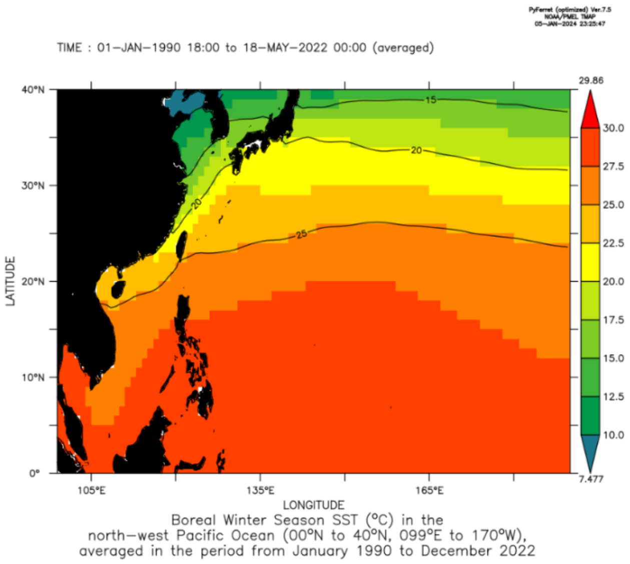

Figure 4.17 SST (°C) map in the north-west Pacific Ocean (0 °N to 40 °N, 99 °E to 170 °W), averaged in Boreal Winter Season for the period from January 1990 to December 2022.

The temperatures reduce meridionally towards the north in general. Temperatures in the range from 25 °C to 27.5 °C are seen in parts of South China Sea and then extending zonally eastward into the Pacific Ocean and having a latitudinal range between around 12 °N to 24 °N at 170 °W longitude. Temperatures further reduce in the Taiwan Strait, decreasing further in the East

China Sea. The temperatures further reduce northwards, reaching temperatures below 15 °C in the most parts of the Yellow Sea, Bohai Sea, parts of the Sea of Japan and in the Pacific Ocean near 40 °N latitude. The lowest temperatures are below 10 °C, and are seen in the Korea Bay and the Bohai Sea.

4.2 SLOPES OF TRENDLINES OF SEA SURFACE TEMPERATURE

4.2.1 The Slopes of the Trendlines of SST in the Period from January 1990 to December 2022

The map of the slopes of the trendlines of SSTs (°C/year) in the north-west Pacific Ocean (0 °N to 40 °N, 99 °E to 170 °W), averaged in the period from January 1990 to December 2022, is shown in Figure 4.18.

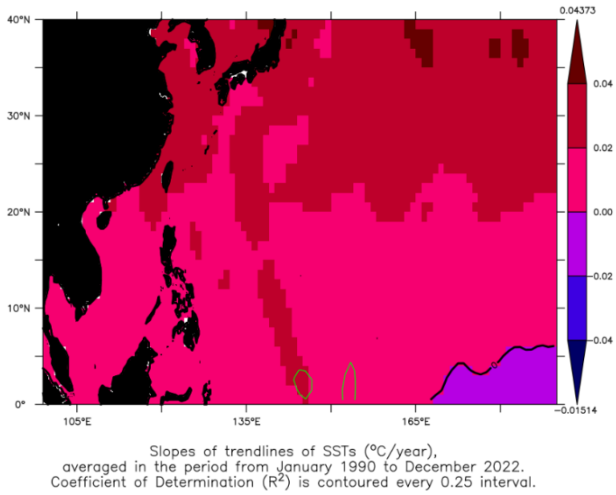

Figure 4.18 Map of slopes of the trendlines of SSTs (°C/year) in the north-west Pacific Ocean (0 °N to 40 °N, 99 °E to 170 °W), averaged in the period from January 1990 to December 2022.

The slopes of SSTs are in the range of –0.015 °C/year to 0.044 °C/year. The highest positive values of slopes of SSTs are seen along parts of the east and west coasts of Japan, and in the North Pacific Ocean near (37 °N, 165 °E) and (37

°N, 180 °E). Most of the north Pacific Ocean shows positive trends in SSTs, except near the region between 0 °N to 5 °N and 170 °E to 170 °W. The Coefficient of Determination (R^2) values are above 0.25 in some patches in the equatorial Pacific region at around 145 °E and 155 °E.

4.2.2 The Month-wise Slopes of the Trendlines of SST in the Period from January 1990 to December 2022

a. January:

The map of the slopes of the trendlines of SSTs (°C/year) in the north-west Pacific Ocean (0 °N to 40 °N, 99 °E to 170 °W), averaged in the month of January in the period from January 1990 to December 2022, is shown in Figure 4.19.

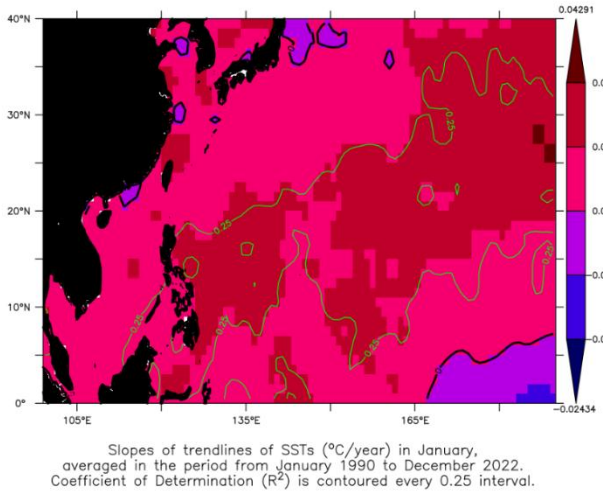

Figure 4.19 Map of slopes of the trendlines of SSTs (°C/year) in the north-west Pacific Ocean (0 °N to 40 °N, 99 °E to 170 °W), averaged in the month of January in the period from January 1990 to December 2022.

The slopes of SSTs are in the range of –0.024 °C/year to 0.043 °C/year. The highest positive values of slopes of SSTs are seen near (28 °N, 173 °W) and (26 °N, 170 °W) and the highest negative slopes are seen in the equatorial region near the longitudes between 178 °E to 170 °W. Most of the north Pacific Ocean shows positive trends in SSTs, except near the region approximately between 0 °N to 7 °N and 170 °E to 170 °W and some patches near Japan and China. The Coefficient of Determination (R^2) values are above 0.25 is widely spread in the north-west Pacific Ocean region.

b. February:

The map of the slopes of the trendlines of SSTs (°C/year) in the north-west Pacific Ocean (0 °N to 40 °N, 99 °E to 170 °W), averaged in the month of February in the period from January 1990 to December 2022, is shown in Figure 4.20.

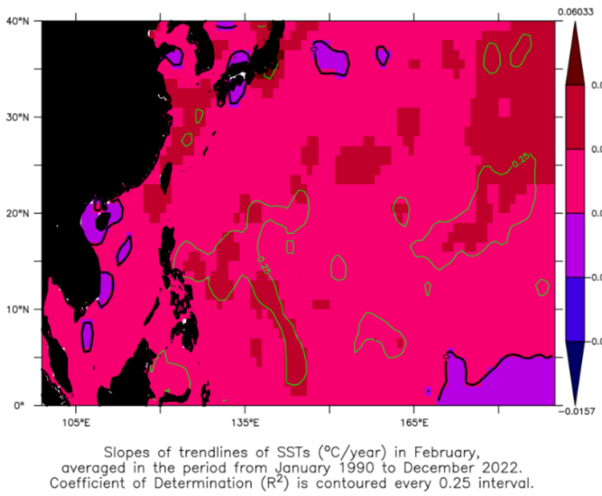

Figure 4.20 Map of slopes of the trendlines of SSTs (°C/year) in the north-west Pacific Ocean (0 °N to 40 °N, 99 °E to 170 °W), averaged in the month of February in the period from January 1990 to December 2022.

The slopes of SSTs are in the range of –0.016 °C/year to 0.060 °C/year. The highest positive values of slopes of SSTs are seen along parts of the east and west coasts of Japan. Most of the north Pacific Ocean shows positive trends in SSTs, except near the region yellow Sea, Southern part of Japan, part of Sea of Japan, part of South China Sea, 0 °N to 6 °N and 170 °E to 170 °W. The Coefficient of Determination (R^2) values are above 0.25 are in Celebes Sea, part of East China Sea, Philippine Sea.

c. *March:*

The map of the slopes of the trendlines of SSTs (°C/year) in the north-west Pacific Ocean (0 °N to 40 °N, 99 °E to 170 °W), the month of March in the period from January 1990 to December 2022, is shown in Figure 4.21.

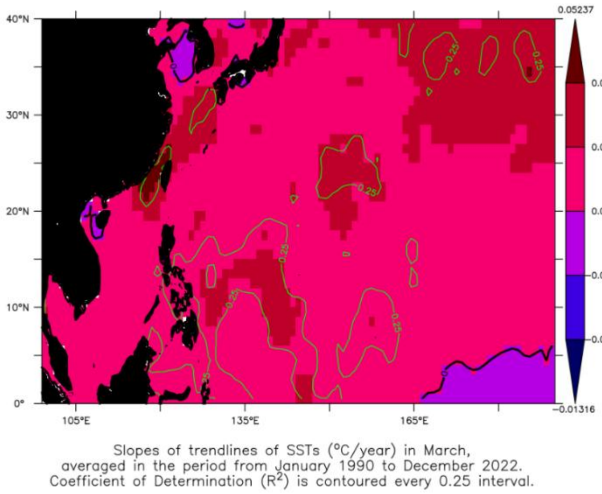

Figure 4.21 Map of slopes of the trendlines of SSTs (°C/year) in the north-west Pacific Ocean (0 °N to 40 °N, 99 °E to 170 °W), averaged in the month of March in the period from January 1990 to December 2022.

The slopes of SSTs are in the range of –0.013 °C/year to 0.052 °C/year. The highest positive values of slopes of SSTs are seen near (35 °N, 177 °W), along parts of Western coast of Taiwan. Most of the north Pacific Ocean shows positive trends in SSTs, except near the region between 0 °N to 5 °N and 165 °E to 170 °W and also in some parts of Yellow Sea, Sea of Japan, Beibu Gulf. The

Coefficient of Determination (R^2) values are above 0.25 are seen in the Pacific Ocean region at 30 °N to 40 °N and 165 °E to 170 °W, along western coast of Taiwan, parts of East China Sea.

d. April:

The map of the slopes of the trendlines of SSTs (°C/year) in the north-west Pacific Ocean (0 °N to 40 °N, 99 °E to 170 °W), the month of April in the period from January 1990 to December 2022, is shown in Figure 4.22. The slopes of SSTs are in the range of –0.016 °C/year to 0.048 °C/year. The highest positive values of slopes of SSTs are seen along coast of Fukushima. Most of the north Pacific Ocean shows positive trends in SSTs, except in parts of South China Sea, northern part of Philippines, parts of the East China Sea, Parts of the Sea of Japan, 0 °N to 5°N and 170 °E to 170 °W. The Coefficient of Determination (R^2) values are above 0.25 in some parts of Philippine Sea.

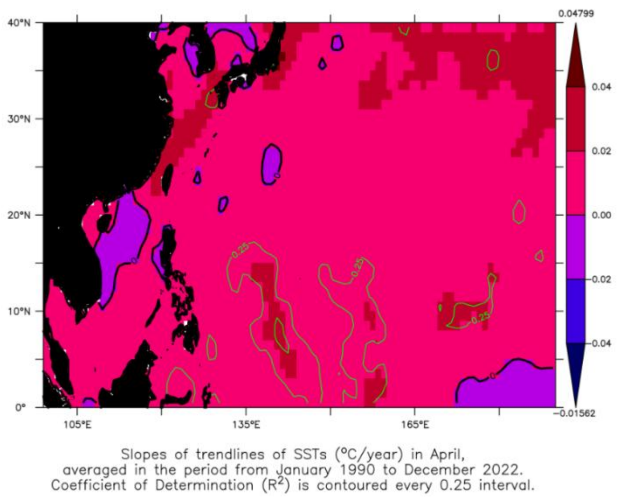

Figure 4.22 Map of slopes of the trendlines of SSTs (°C/year) in the north-west Pacific Ocean (0 °N to 40 °N, 99 °E to 170 °W), averaged in the month of April in the period from January 1990 to December 2022.

e. May:

The map of the slopes of the trendlines of SSTs (°C/year) in the north-west Pacific Ocean (0 °N to 40 °N, 99 °E to 170 °W), the month of May in the period from January 1990 to December 2022, is shown in Figure 4.23.

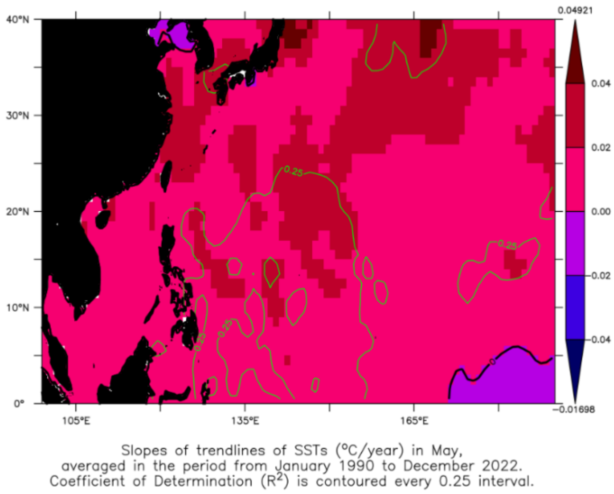

Figure 4.23 Map of slopes of the trendlines of SSTs (°C/year) in the north-west Pacific Ocean (0 °N to 40 °N, 99 °E to 170 °W), averaged in the month of May in the period from January 1990 to December 2022.

The slopes of SSTs are in the range of –0.017 °C/year to 0.049 °C/year. The highest positive values of slopes of SSTs are seen along parts of the east coasts of Japan, and in the North Pacific Ocean region near 35 °N to 40°N and 165 °E to 169 °E. Most of the north Pacific Ocean shows positive trends in SSTs, except near the region in the Bohai Sea and between 0 °N to 5 °N and 170 °E to 170 °W. The Coefficient of Determination (R^2) values are above 0.25 over the Philippine Sea, and in the North Pacific Ocean near region near bounded between the 35 °N to 40°N latitudes and 153 °E to 165 °E longitudes.

f. June:

The map of the slopes of the trendlines of SSTs (°C/year) in the north-west Pacific Ocean (0 °N to 40 °N, 99 °E to 170 °W), the month of June in the period from January 1990 to December 2022, is shown in Figure 4.24.

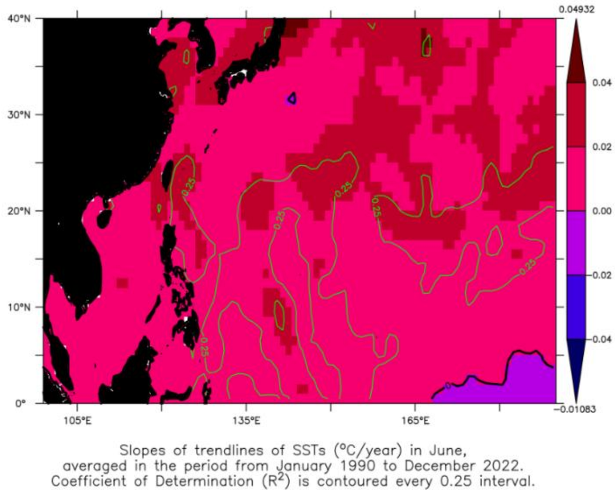

Figure 4.24 Map of slopes of the trendlines of SSTs (°C/year) in the north-west Pacific Ocean (0 °N to 40 °N, 99 °E to 170 °W), averaged in the month of June in the period from January 1990 to December 2022.

The slopes of SSTs are in the range of –0.011 °C/year to 0.049 °C/year. The highest positive values of slopes of SSTs are seen along parts of the east coasts of Japan and North Pacific Ocean near (37 °N, 165 °E). Most of the north Pacific Ocean shows positive trends in SSTs, except near the region between 0 °N to 5 °N and 170 °E to 170 °W. The Coefficient of Determination (R^2) values are above 0.25 in the Philippine Sea, North Pacific Ocean near (37 °N, 165 °E), and in the equatorial Pacific region at around 145 °E and 155 °E.

g. July:

The map of the slopes of the trendlines of SSTs (°C/year) in the north-west Pacific Ocean (0 °N to 40 °N, 99 °E to 170 °W), the month of July in the period from January 1990 to December 2022, is shown in Figure 4.25. The slopes of SSTs are in the range of –0.016 °C/year to 0.057°C/year. The highest positive values of slopes of SSTs are seen along parts of the east and west coasts of Japan, and in the North Pacific Ocean near (40 °N, 164 °E). Most of the north Pacific Ocean shows positive trends in SSTs, except near western coast of Philippines, southern parts of Japan, parts of East China Sea and between 0 °N to 5 °N and 170 °E to 170 °W. The Coefficient of Determination (R^2) values are above 0.25 are seen in the the equatorial Pacific region and at around 35 °N and 170 °W.

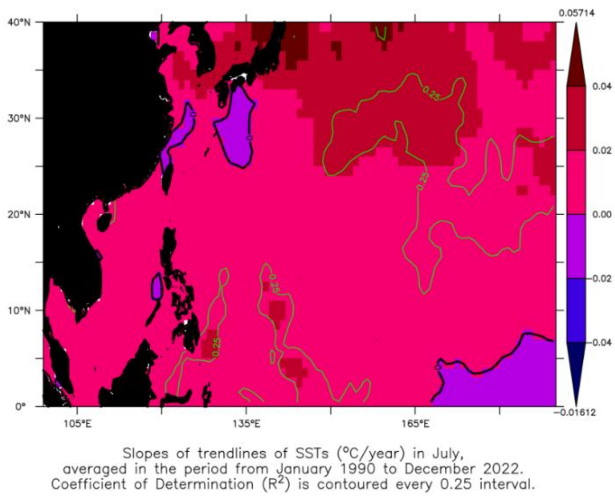

Figure 4.25 Map of slopes of the trendlines of SSTs (°C/year) in the north-west Pacific Ocean (0 °N to 40 °N, 99 °E to 170 °W), averaged in the month of July in the period from January 1990 to December 2022.

h. August:

The map of the slopes of the trendlines of SSTs (°C/year) in the north-west Pacific Ocean (0 °N to 40 °N, 99 °E to 170 °W), the month of August in the period from January 1990 to December 2022, is shown in Figure 4.26. The slopes of SSTs are in the range of –0.018 °C/year to 0.051 °C/year. The highest positive values of slopes of SSTs are seen in the the North Pacific Ocean near (35 °N to 40 °N, 150 °E to 168 °E) . Most of the north Pacific Ocean shows positive trends in SSTs, except in some parts of Beibu Gulf and near the region between 0 °N to 5 °N and 165 °E to 170 °W, parts of Bohai Sea. The Coefficient of Determination (R^2) values are above 0.25 is widely spread in the north-west Pacific Ocean.

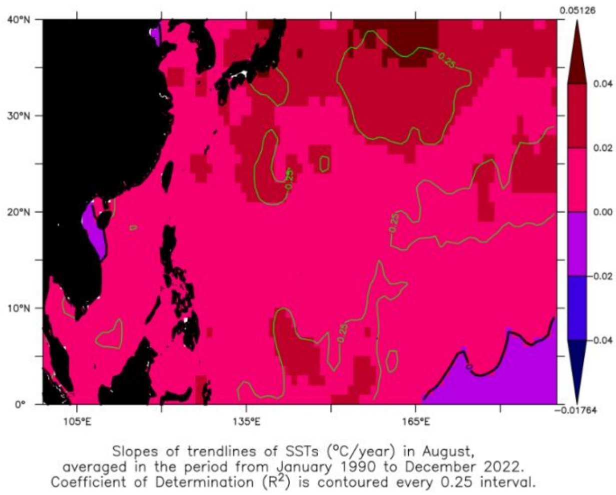

Figure 4.26 Map of slopes of the trendlines of SSTs (°C/year) in the north-west Pacific Ocean (0 °N to 40 °N, 99 °E to 170 °W), averaged in the month of August in the period from January 1990 to December 2022.

i. September:

The map of the slopes of the trendlines of SSTs (°C/year) in the north-west Pacific Ocean (0 °N to 40 °N, 99 °E to 170 °W), the month of September in the period from January 1990 to December 2022, is shown in Figure 4.27. The slopes of SSTs are in the range of –0.018 °C/year to 0.058 °C/year. The highest positive values of slopes of SSTs are seen in the North Pacific Ocean near (40 °N, 165 °E) and (40 °N, 180 °E). Most of the north Pacific Ocean shows positive trends in SSTs, except near the region between 0 °N to 5 °N and 170 °E to 170 °W and also in some parts of Sea of Japan. The Coefficient of Determination (R^2) values are above 0.25 is widely spread in the north-west Pacific Ocean region.

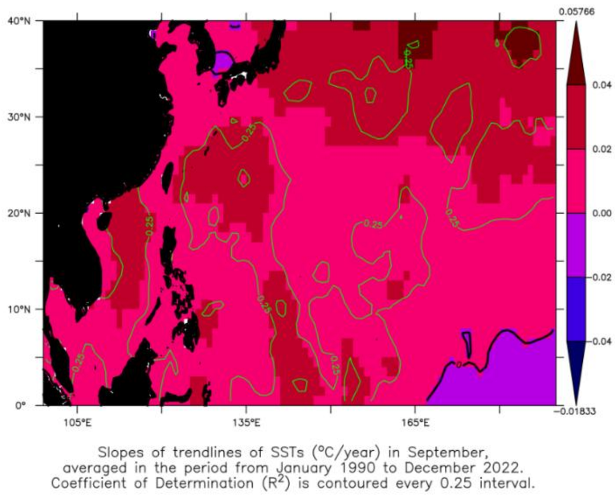

Figure 4.27 Map of slopes of the trendlines of SSTs (°C/year) in the north-west Pacific Ocean (0 °N to 40 °N, 99 °E to 170 °W), averaged in the month of September in the period from January 1990 to December 2022.

j. October:

The map of the slopes of the trendlines of SSTs (°C/year) in the north-west Pacific Ocean (0 °N to 40 °N, 99 °E to 170 °W), the month of October in the period from January 1990 to December 2022, is shown in Figure 4.28. The slopes of SSTs are in the range of –0.023 °C/year to 0.058 °C/year. The highest positive values of slopes of SSTs are seen along parts of the North Pacific Ocean near

(30°N, 40 °N) and (155 °E, 170 °W) and the highest negative slopes are seen in the equatorial region near the longitude between 178 °W to 170°W. Most of the north Pacific Ocean shows positive trends in SSTs, except near the region between 0 °N to 15 °N and 165 °E to 170 °W. The Coefficient of Determination (R^2) values are above 0.25 is widely spread in the north-west Pacific Ocean.

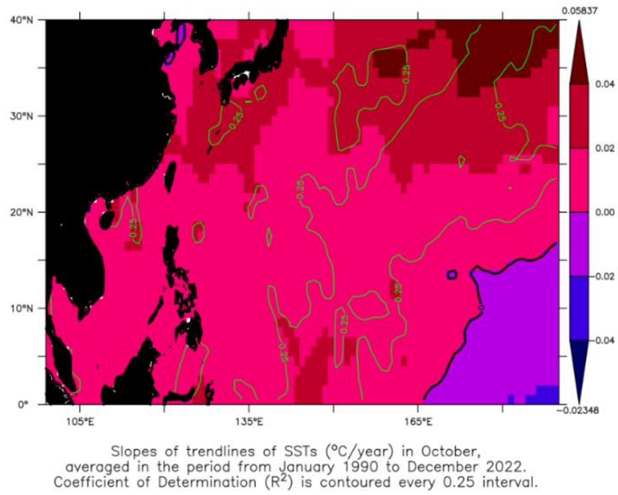

Figure 4.28 Map of slopes of the trendlines of SSTs (°C/year) in the north-west Pacific Ocean (0 °N to 40 °N, 99 °E to 170 °W), averaged in the month of October in the period from January 1990 to December 2022.

k. November:

The map of the slopes of the trendlines of SSTs (°C/year) in the north-west Pacific Ocean (0 °N to 40 °N, 99 °E to 170 °W), the month of November in the period from January 1990 to December 2022, is shown in Figure 4.29. The slopes of SSTs are in the range of –0.015 °C/year to 0.059 °C/year. The highest positive values of slopes of SSTs are seen along parts of the North Pacific Ocean near (30°N, 40 °N) and (168 °E, 170°W) and small patches in the Sea of Japan. Most of the north Pacific Ocean shows positive trends in SSTs, except near the region between 0 °N to 10 °N and 180 °E to 170 °W, small part of Yellow Sea and (40°N to 150°E), The Coefficient of Determination (R^2) values are above 0.25 is widely spread in the north-west Pacific Ocean region.

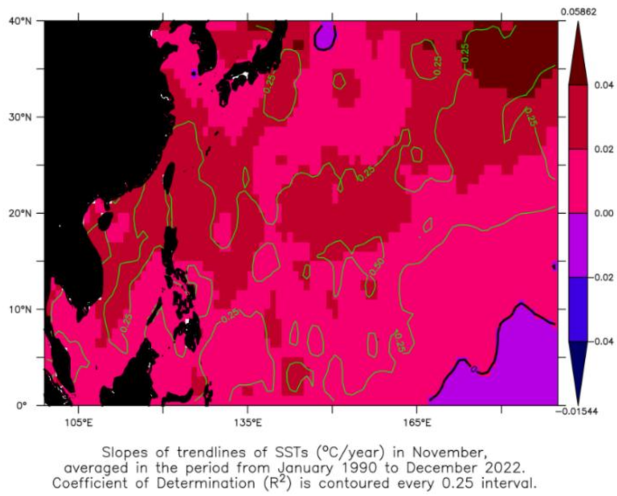

Figure 4.29 Map of slopes of the trendlines of SSTs (°C/year) in the north-west Pacific Ocean (0 °N to 40 °N, 99 °E to 170 °W), averaged in the month of November in the period from January 1990 to December 2022.

l. December:

The map of the slopes of the trendlines of SSTs (°C/year) in the north-west Pacific Ocean (0 °N to 40 °N, 99 °E to 170 °W), the month of December in the period from January 1990 to December 2022, is shown in Figure 4.30. The slopes of SSTs are in the range of –0.022 °C/year to 0.044 °C/year. The highest positive values of slopes of SSTs are seen at (35 °N, 180 °E) and the highest negative slopes are seen in the equatorial region near the longitudes between 180 °E to 170°W. Most of the north Pacific Ocean shows positive trends in SSTs, except near the region between 0 °N to 5 °N and 170 °E to 170 °W. The Coefficient of

Determination (R^2) values are above 0.25 in some patches in the equatorial Pacific region near the longitudes between 126 °E and 170 °W.

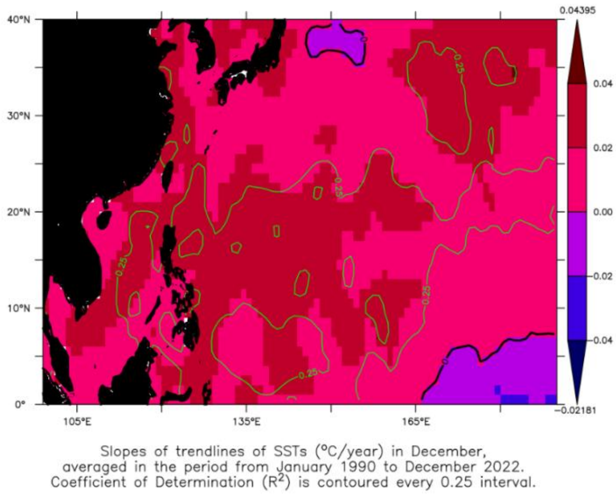

Figure 4.30 Map of slopes of the trendlines of SSTs (°C/year) in the north-west Pacific Ocean (0 °N to 40 °N, 99 °E to 170 °W), averaged in the month of December in the period from January 1990 to December 2022.

4.2.3 The Season-wise Slopes of the Trendlines of SST in the Period from January 1990 to December 2022

a. *Boreal Spring Season:*

The map of the slopes of the trendlines of SSTs (°C/year) in the north-west Pacific Ocean (0 °N to 40 °N, 99 °E to 170 °W), averaged in Boreal Spring Season for the period from January 1990 to December 2022, is shown in Figure 4.31. The slopes of SSTs are in the range of –0.013 °C/year to 0.050 °C/year. The highest positive values of slopes of SSTs are seen along parts of the east and west coasts of Japan, and in the North Pacific Ocean near (37 °N, 165 °E) and (37 °N, 180 °E). Most of the north Pacific Ocean shows positive trends in SSTs, except near the region between 0 °N to 5 °N and 170 °E to 170 °W and some parts of Yellow Sea, Sea of Japan and South China Sea. The Coefficient of Determination (R^2) values are above 0.25 in some patches in the equatorial Pacific Ocean region at around 120 °E and 180 °E and in the East China Sea.

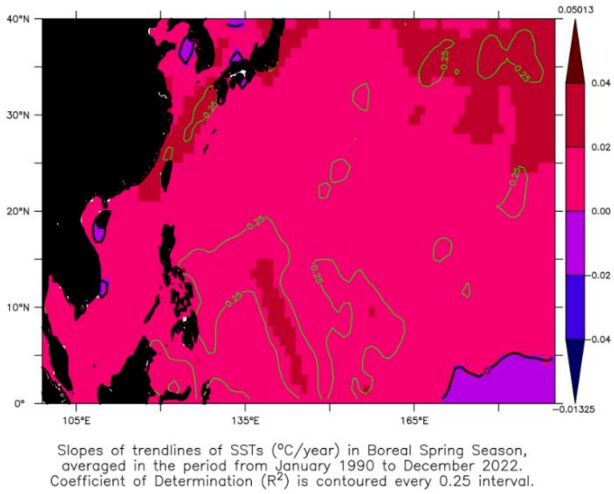

Figure 4.31 Map of slopes of the trendlines of SSTs (°C/year) in the north-west Pacific Ocean (0 °N to 40 °N, 99 °E to 170 °W), averaged in Boreal Spring Season for the period from January 1990 to December 2022.

b. Boreal Summer Season:

The map of the slopes of the trendlines of SSTs (°C/year) in the north-west Pacific Ocean (0 °N to 40 °N, 99 °E to 170 °W), averaged in Boreal Summer Season for the period from January 1990 to December 2022, is shown in Figure 4.32. The slopes of SSTs are in the range of –0.015 °C/year to 0.050 °C/year. The highest positive values of slopes of SSTs are seen along parts of the east coasts of Japan, and in the North Pacific Ocean near (37 °N, 165 °E), Small parts of Bohai Sea. Most of the north Pacific Ocean shows positive trends in SSTs, except near the region between 0.25 is widely spread in the north-west Pacific Ocean region.

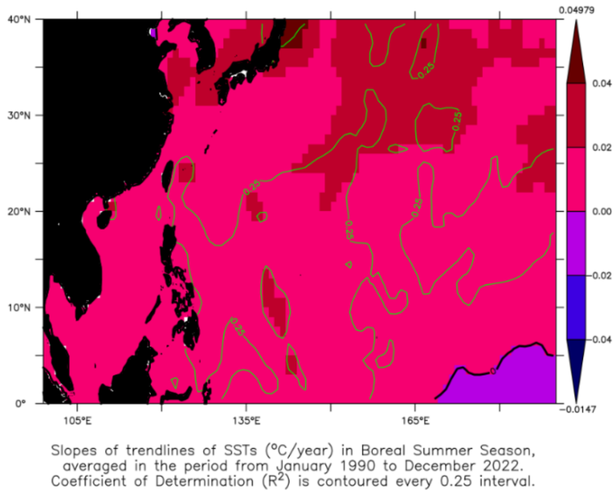

Figure 4.32 Map of slopes of the trendlines of SSTs (°C/year) in the north-west Pacific Ocean (0 °N to 40 °N, 99 °E to 170 °W), averaged in Boreal Summer Season for the period from January 1990 to December 2022.

c. *Boreal Autumn Season:*

The map of the slopes of the trendlines of SSTs (°C/year) in the north-west Pacific Ocean (0 °N to 40 °N, 99 °E to 170 °W), averaged in Boreal Autumn Season for the period from January 1990 to December 2022, is shown in Figure 4.33. The slopes of SSTs are in the range of –0.018 °C/year to 0.049 °C/year. The highest positive values of slopes of SSTs are seen along parts North Pacific Ocean near (35°N, 40 °N) and (157 °E, 175°W), Small parts of Bohai Sea. Most of the north Pacific Ocean shows positive trends in SSTs, except near the region between 0 °N to 10 °N and 170 °E to 170 °W. The Coefficient of Determination (R^2) values are above 0.25 is widely spread in the north-west Pacific Ocean region.

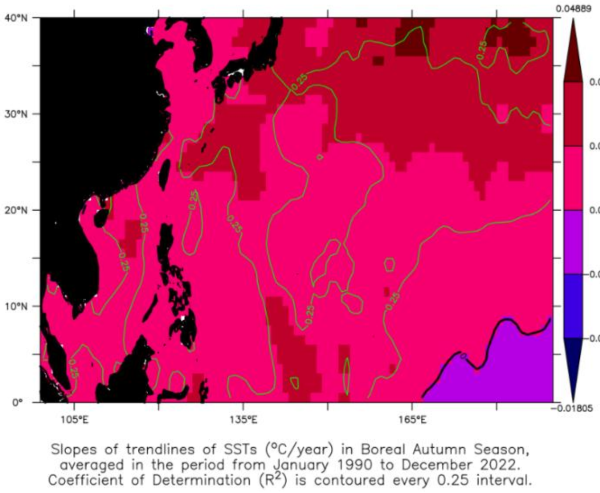

Figure 4.33 Map of slopes of the trendlines of SSTs (°C/year) in the north-west Pacific Ocean (0 °N to 40 °N, 99 °E to 170 °W), averaged in Boreal Autumn Season for the period from January 1990 to December 2022.

d. Boreal Winter Season:

The map of the slopes of the trendlines of SSTs (°C/year) in the north-west Pacific Ocean (0 °N to 40 °N, 99 °E to 170 °W), averaged in Boreal Winter Season for the period from January 1990 to December 2022, is shown in Figure 4.34. The slopes of SSTs are in the range of –0.017 °C/year to 0.043 °C/year. The highest positive values of slopes of SSTs are seen along parts North Pacific Ocean near (35°N, 177 °W). Most of the north Pacific Ocean shows positive trends in SSTs, except near the region between 0 °N to 10 °N and 170 °E to 170 °W. The Coefficient of Determination (R^2) values are above 0.25 is widely spread in the north-west Pacific Ocean region.

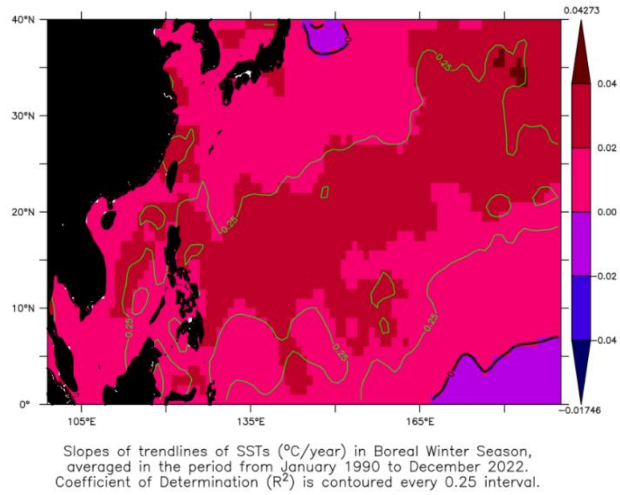

Figure 4.34 Map of slopes of the trendlines of SSTs (°C/year) in the north-west Pacific Ocean (0 °N to 40 °N, 99 °E to 170 °W), averaged in Boreal Winter Season for the period from January 1990 to December 2022.

4.3 BASIN-AVERAGED OF SEA SURFACE TEMPERATURE

4.3.1 Sea Surface Temperature Basin-averaged from January 1990 to December 2022

The plot of the basin-averaged SST in the north-west Pacific Ocean region (0 °N to 40 °N, 99 °E to 170 °W) averaged in the period from January 1990 to December 2022 is shown in Figure 4.35. The SST ranges between approximately 23.4 °C to 29 °C. The trendline of SSTs show an increasing trend, with an increase of 0.0188 °C/year. The coefficient of determination (R^2) has a value of 0.030. The averaged SST in the entire period and region gives a value of 26.174 °C.

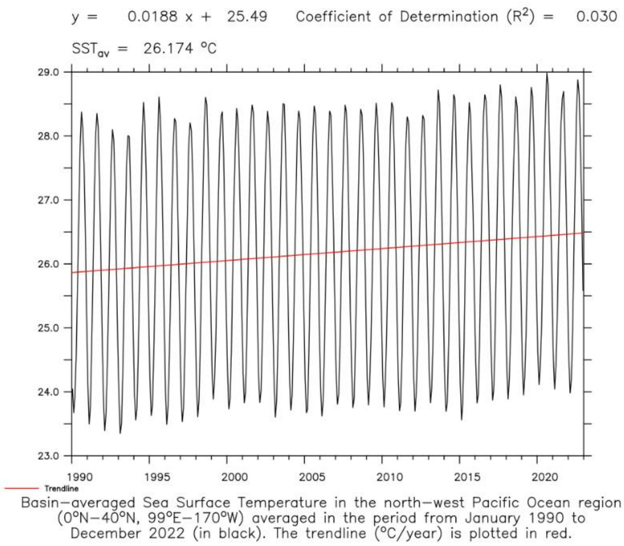

Figure 4.35 Basin-averaged Sea Surface Temperature in the north-west Pacific Ocean region (0 °N to 40 °N, 99 °E to 170 °W) averaged in the period from January 1990 to December 2022 (in black) and trendline (°C/year) in red.

4.3.2 Sea Surface Temperature Basin-Averaged Month-wise from January 1990 to December 2022

a. *January:*

The plot of the basin-averaged SST in the north-west Pacific Ocean region (0 °N to 40 °N, 99 °E to 170 °W) averaged in the month of January in the period from January 1990 to December 2022 is shown in Figure 4.36. The SST ranges between approximately 23.90 °C to 24.60 °C. The trendline of SSTs show an increasing trend, with an increase of 0.0164 °C/year. The coefficient of determination (R^2) has a value of 0.192. The averaged SST in the entire period and region gives a value of 24.237 °C.

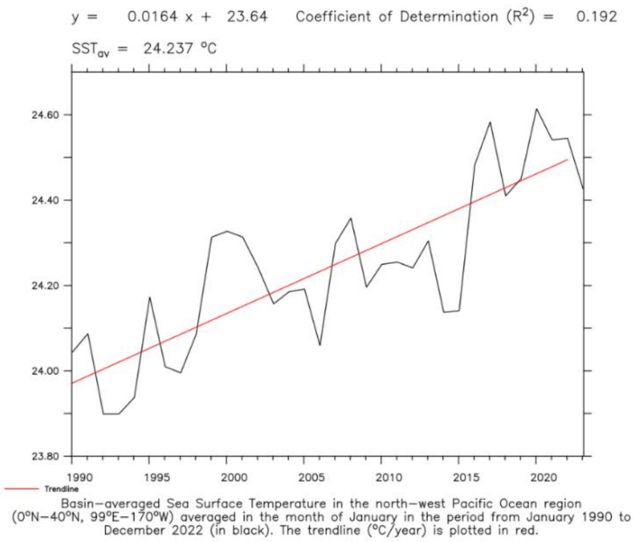

Figure 4.36 Basin-averaged Sea Surface Temperature in the north-west Pacific Ocean region (0 °N to 40 °N, 99 °E to 170 °W) averaged in the month of January in the period from January 1990 to December 2022 (in black) and trendline (°C/year) in red.

b. February:

The plot of the basin-averaged SST in the north-west Pacific Ocean region (0 °N to 40 °N, 99 °E to 170 °W) averaged in the month of February in the period from January 1990 to December 2022 is shown in Figure 4.37. The SST ranges between approximately 23.34 °C to 24.10 °C. The trendline of SSTs show an increasing trend, with an increase of 0.0141 °C/year. The coefficient of determination (R^2) has a value of 0.140. The averaged SST in the entire period and region gives a value of 23.721 °C.

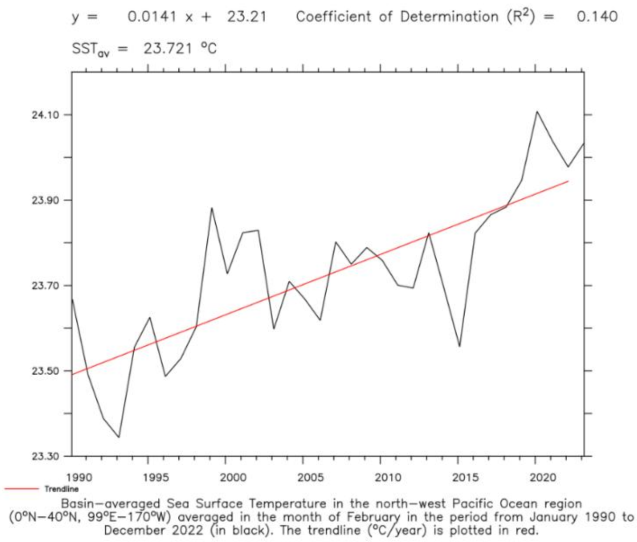

Figure 4.37 Basin-averaged Sea Surface Temperature in the north-west Pacific Ocean region (0 °N to 40 °N, 99 °E to 170 °W) averaged in the month of February in the period from January 1990 to December 2022 (in black) and trendline (°C/year) in red.

c. *March:*

The plot of the basin-averaged SST in the north-west Pacific Ocean region (0 °N to 40 °N, 99 °E to 170 °W) averaged in the month of March in the period from January 1990 to December 2022 is shown in Figure 4.38. The SST ranges between approximately 23.50 °C to 24.42 °C. The trendline of SSTs show an increasing trend, with an increase of 0.0150 °C/year. The coefficient of determination (R^2) has a value of 0.149. The averaged SST in the entire period and region gives a value of 23.948 °C.

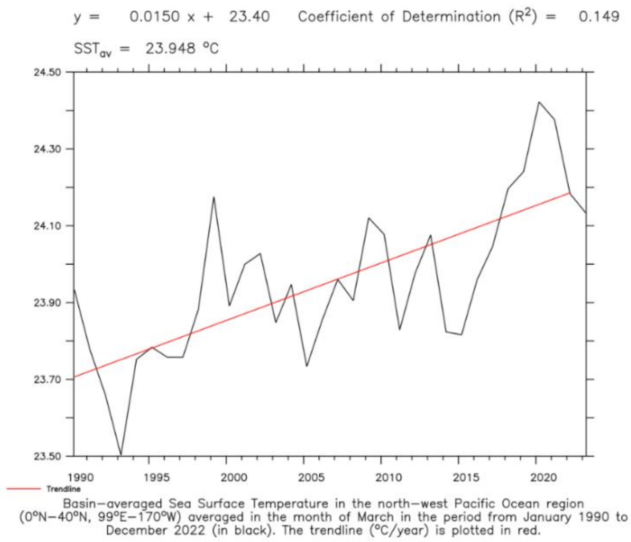

Figure 4.38 Basin-averaged Sea Surface Temperature in the north-west Pacific Ocean region (0 °N to 40 °N, 99 °E to 170 °W) averaged in the month of March in the period from January 1990 to December 2022 (in black) and trendline (°C/year) in red.

d. April:

The plot of the basin-averaged SST in the north-west Pacific Ocean region (0 °N to 40 °N, 99 °E to 170 °W) averaged in the month of April in the period from January 1990 to December 2022 is shown in Figure 4.39. The SST ranges between approximately 24.28 °C to 25.06 °C. The trendline of SSTs show an increasing trend, with an increase of 0.0120 °C/year. The coefficient of determination (R^2) has a value of 0.113. The averaged SST in the entire period and region gives a value of 23.748 °C.

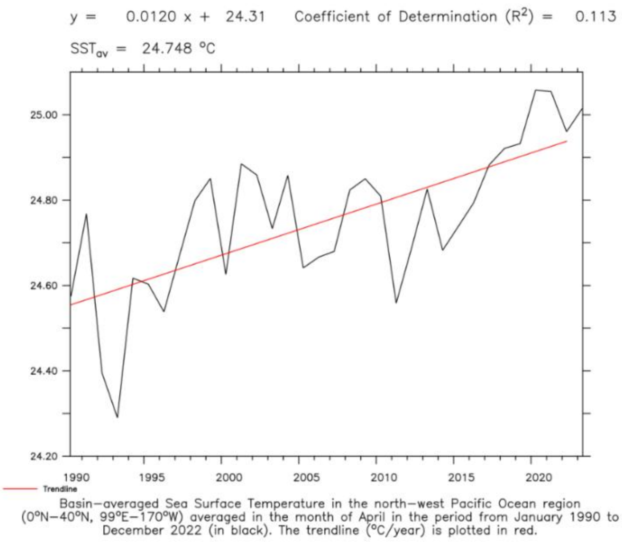

Figure 4.39 Basin-averaged Sea Surface Temperature in the north-west Pacific Ocean region (0 °N to 40 °N, 99 °E to 170 °W) averaged in the month of April in the period from January 1990 to December 2022 (in black) and trendline (°C/year) in red.

e. May:

The plot of the basin-averaged SST in the north-west Pacific Ocean region (0 °N to 40 °N, 99 °E to 170 °W) averaged in the month of May in the period from January 1990 to December 2022 is shown in Figure 4.40. The SST ranges between approximately 24.38 °C to 26.26 °C. The trendline of SSTs show an increasing trend, with an increase of 0.0155 °C/year. The coefficient of determination (R^2) has a value of 0.163. The averaged SST in the entire period and region gives a value of 25.908 °C

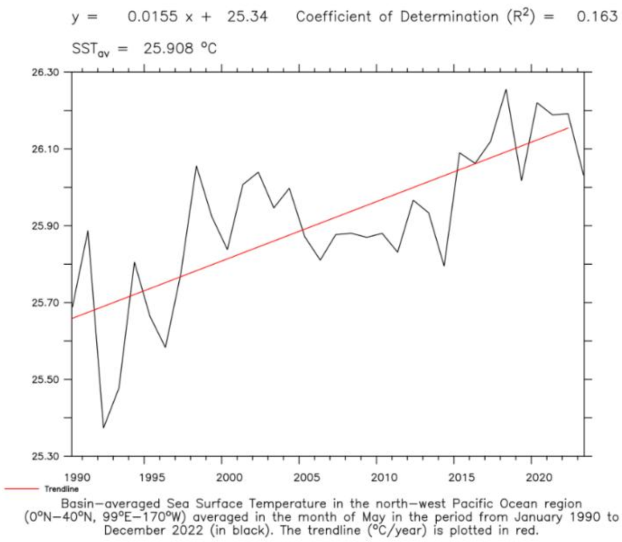

Figure 4.40 Basin-averaged Sea Surface Temperature in the north-west Pacific Ocean region (0 °N to 40 °N, 99 °E to 170 °W) averaged in the month of May in the period from January 1990 to December 2022 (in black) and trendline (°C/year) in red.

f. June:

The plot of the basin-averaged SST in the north-west Pacific Ocean region (0 °N to 40 °N, 99 °E to 170 °W) averaged in the month of June in the period from January 1990 to December 2022 is shown in Figure 4.41. The SST ranges between approximately 26.58 °C to 27.50 °C. The trendline of SSTs show an increasing trend, with an increase of 0.0153 °C/year. The coefficient of determination (R^2) has a value of 0.163. The averaged SST in the entire period and region gives a value of 27.052 °C.

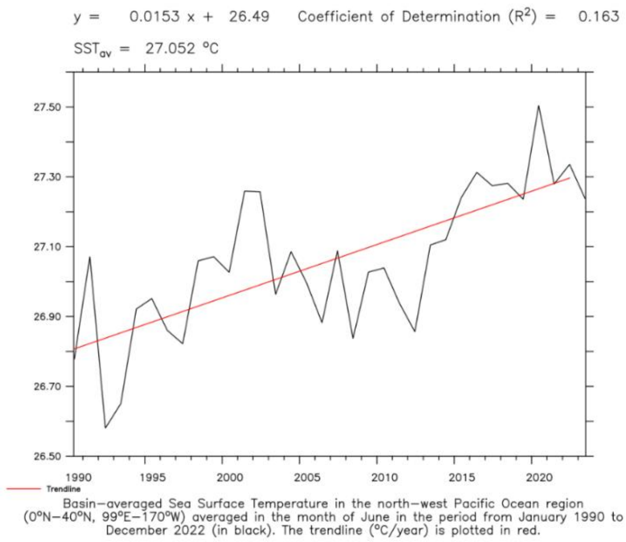

Figure 4.41 Basin-averaged Sea Surface Temperature in the north-west Pacific Ocean region (0 °N to 40 °N, 99 °E to 170 °W) averaged in the month of June in the period from January 1990 to December 2022 (in black) and trendline (°C/year) in red.

g. July:

The plot of the basin-averaged SST in the north-west Pacific Ocean region (0 °N to 40 °N, 99 °E to 170 °W) averaged in the month of July in the period from January 1990 to December 2022 is shown in Figure 4.42. The SST ranges between approximately 27.56 °C to 28.38 °C. The trendline of SSTs show an increasing trend, with an increase of 0.0133 °C/year. The coefficient of determination (R^2) has a value of 0.135. The averaged SST in the entire period and region gives a value of 28.002 °C.

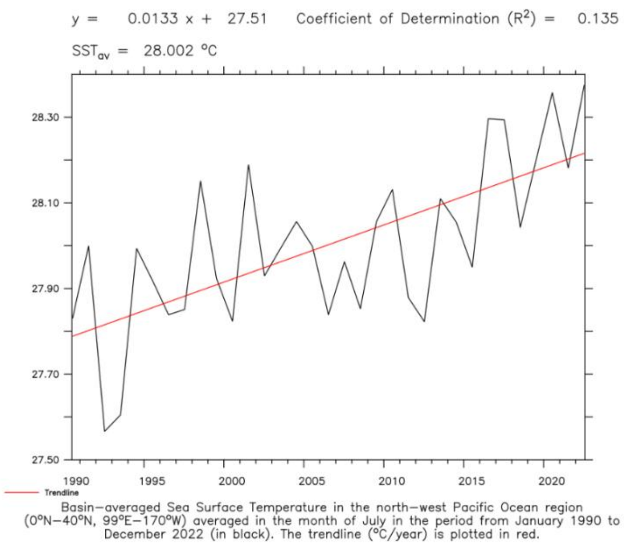

Figure 4.42 Basin-averaged Sea Surface Temperature in the north-west Pacific Ocean region (0 °N to 40 °N, 99 °E to 170 °W) averaged in the month of July in the period from January 1990 to December 2022 (in black) and trendline (°C/year) in red.

h. August:

The plot of the basin-averaged SST in the north-west Pacific Ocean region (0 °N to 40 °N, 99 °E to 170 °W) averaged in the month of August in the period from January 1990 to December 2022 is shown in Figure 4.43. The SST ranges between approximately 28.01 °C to 28.99 °C. The trendline of SSTs show an increasing trend, with an increase of 0.0152 °C/year. The coefficient of determination (R^2) has a value of 0.156. The averaged SST in the entire period and region gives a value of 28.492 °C.

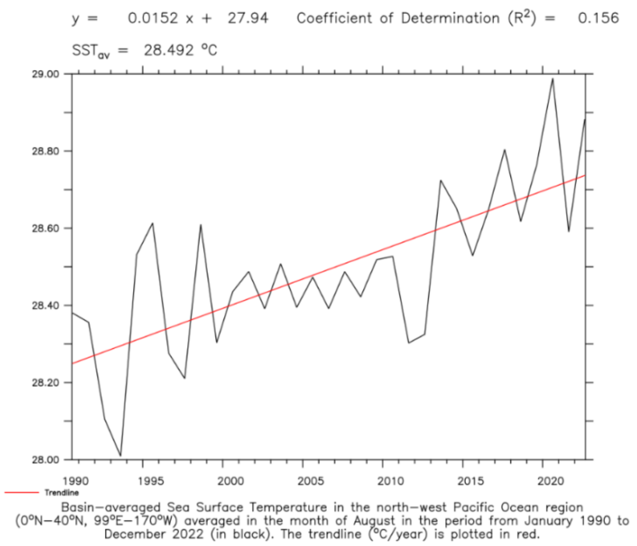

Figure 4.43 Basin-averaged Sea Surface Temperature in the north-west Pacific Ocean region (0 °N to 40 °N, 99 °E to 170 °W) averaged in the month of August in the period from January 1990 to December 2022 (in black) and trendline (°C/year) in red.

i. *September:*

The plot of the basin-averaged SST in the north-west Pacific Ocean region (0 °N to 40 °N, 99 °E to 170 °W) averaged in the month of September in the period from January 1990 to December 2022 is shown in Figure 4.44. The SST ranges between approximately 27.92 °C to 28.78 °C. The trendline of SSTs show an increasing trend, with an increase of 0.0168 °C/year. The coefficient of determination (R^2) has a value of 0.199. The averaged SST in the entire period and region gives a value of 28.352 °C.

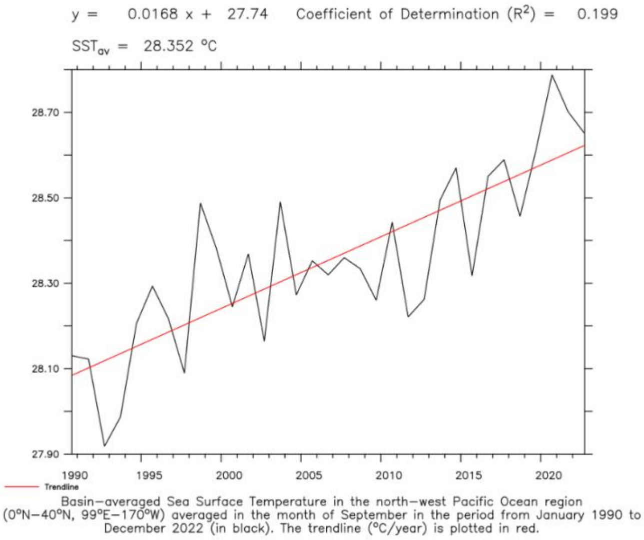

Figure 4.44 Basin-averaged Sea Surface Temperature in the north-west Pacific Ocean region (0 °N to 40 °N, 99 °E to 170 °W) averaged in the month of September in the period from January 1990 to December 2022 (in black) and trendline (°C/year) in red.

j. *October:*

The plot of the basin-averaged SST in the north-west Pacific Ocean region (0 °N to 40 °N, 99 °E to 170 °W) averaged in the month of October in the period from January 1990 to December 2022 is shown in Figure 4.45. The SST ranges between approximately 27.14 °C to 27.94 °C. The trendline of SSTs show an increasing trend, with an increase of 0.0155 °C/year. The coefficient of determination (R^2) has a value of 0.180. The averaged SST in the entire period and region gives a value of 27.617 °C.

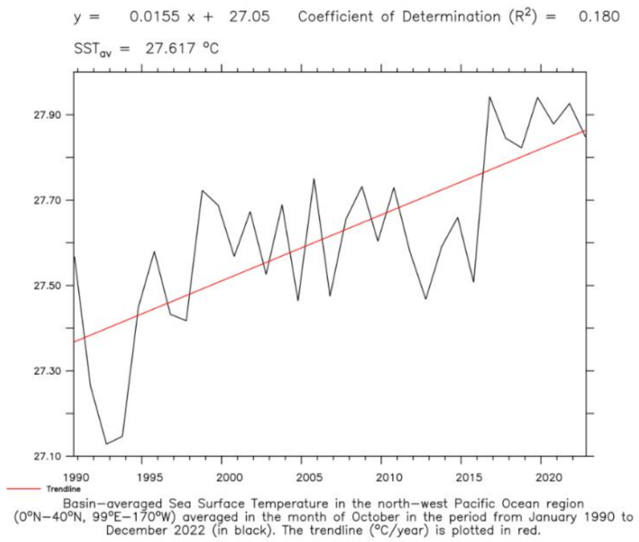

Figure 4.45 Basin-averaged Sea Surface Temperature in the north-west Pacific Ocean region (0 °N to 40 °N, 99 °E to 170 °W) averaged in the month of October in the period from January 1990 to December 2022 (in black) and trendline (°C/year) in red.

k. November:

The plot of the basin-averaged SST in the north-west Pacific Ocean region (0 °N to 40 °N, 99 °E to 170 °W) averaged in the month of November in the period from January 1990 to December 2022 is shown in Figure 4.46. The SST ranges between approximately 25.96 °C to 26.90 °C. The trendline of SSTs show an increasing trend, with an increase of 0.0180 °C/year. The coefficient of determination (R^2) has a value of 0.223. The averaged SST in the entire period and region gives a value of 26.574 °C.

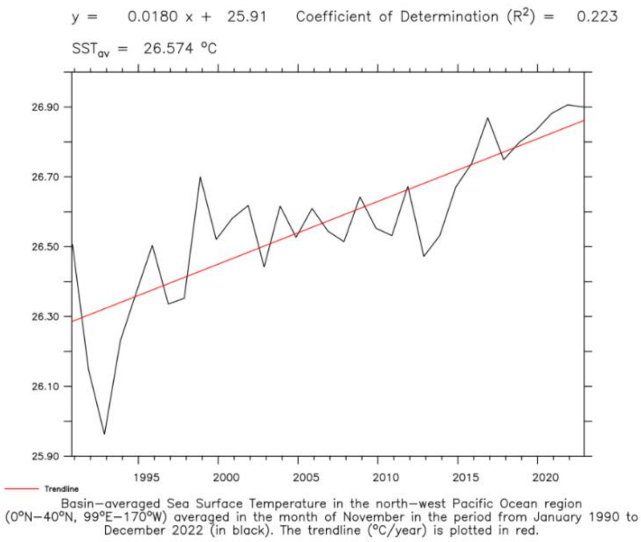

Figure 4.46 Basin-averaged Sea Surface Temperature in the north-west Pacific Ocean region (0 °N to 40 °N, 99 °E to 170 °W) averaged in the month of November in the period from January 1990 to December 2022 (in black) and trendline (°C/year) in red.

l. December:

The plot of the basin-averaged SST in the north-west Pacific Ocean region (0 °N to 40 °N, 99 °E to 170 °W) averaged in the month of December in the period from January 1990 to December 2022 is shown in Figure 4.47. The SST ranges between approximately 24.82 °C to 25.64 °C. The trendline of SSTs show an increasing trend, with an increase of 0.0173 °C/year. The coefficient of determination (R^2) has a value of 0.213. The averaged SST in the entire period and region gives a value of 25.305 °C.

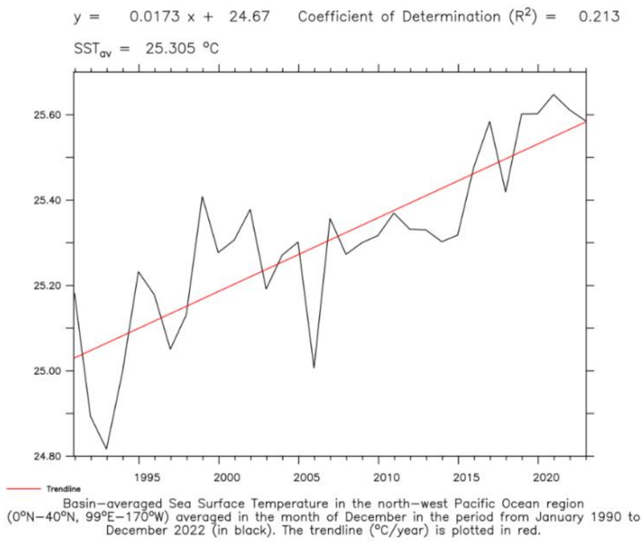

Figure 4.47 Basin-averaged Sea Surface Temperature in the north-west Pacific Ocean region (0 °N to 40 °N, 99 °E to 170 °W) averaged in the month of December in the period from January 1990 to December 2022 (in black) and trendline (°C/year) in red.

4.3.3 Sea Surface Temperature Basin-Averaged Season-wise from January 1990 to December 2022

a. Boreal Spring Season:

The plot of the basin-averaged SST in the north-west Pacific Ocean region (0 °N to 40 °N, 99 °E to 170 °W) averaged in Boreal Spring Season for the period from January 1990 to December 2022 is shown in Figure 4.48. The SST ranges between approximately 23.72 °C to 24.54 °C. The trendline of SSTs show an increasing trend, with an increase of 0.0137 °C/year. The coefficient of determination (R^2) has a value of 0.158. The averaged SST in the entire period and region gives a value of 24.145 °C.

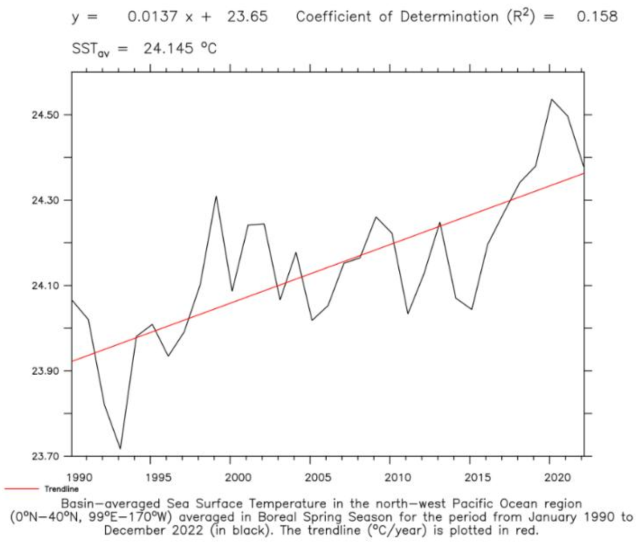

Figure 4.48 Basin-averaged Sea Surface Temperature in the north-west Pacific Ocean region (0 °N to 40 °N, 99 °E to 170 °W) averaged in Boreal Spring Season for the period from January 1990 to December 2022 (in black) and trendline (°C/year) in red.

b. Boreal Summer Season:

The plot of the basin-averaged SST in the north-west Pacific Ocean region (0 °N to 40 °N, 99 °E to 170 °W) averaged in Boreal Summer Season for the period from January 1990 to December 2022 is shown in Figure 4.49. The SST ranges between approximately 26.51 °C to 27.34 °C. The trendline of SSTs show an increasing trend, with an increase of 0.0147 °C/year. The coefficient of determination (R^2) has a value of 0.196. The averaged SST in the entire period and region gives a value of 26.987 °C.

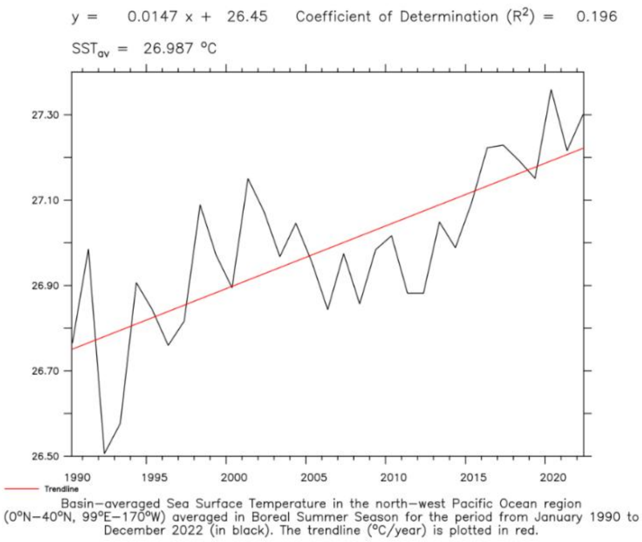

Figure 4.49 Basin-averaged Sea Surface Temperature in the north-west Pacific Ocean region (0 °N to 40 °N, 99 °E to 170 °W) averaged in Boreal Summer Season for the period from January 1990 to December 2022 (in black) and trendline (°C/year) in red.

c. Boreal Autumn Season:

The plot of the basin-averaged SST in the north-west Pacific Ocean region (0 °N to 40 °N, 99 °E to 170 °W) averaged in Boreal Autumn Season for the period from January 1990 to December 2022 is shown in Figure 4.50. The SST ranges between approximately 27.72 °C to 28.54 °C. The trendline of SSTs show an increasing trend, with an increase of 0.0159 °C/year. The coefficient of determination (R^2) has a value of 0.221. The averaged SST in the entire period and region gives a value of 28.151 °C.

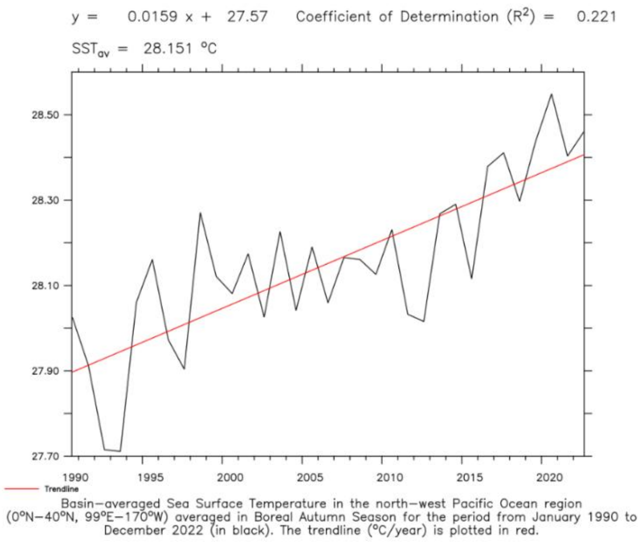

Figure 4.50 Basin-averaged Sea Surface Temperature in the north-west Pacific Ocean region (0 °N to 40 °N, 99 °E to 170 °W) averaged in Boreal Autumn Season for the period from January 1990 to December 2022 (in black) and trendline (°C/year) in red.

d. Boreal Winter Season:

The plot of the basin-averaged SST in the north-west Pacific Ocean region (0 °N to 40 °N, 99 °E to 170 °W) averaged in Boreal Winter Season for the period from January 1990 to December 2022 is shown in Figure 4.51. The SST ranges between approximately 24.88 °C to 25.68 °C. The trendline of SSTs show an increasing trend, with an increase of 0.0171 °C/year. The coefficient of determination (R^2) has a value of 0.236. The averaged SST in the entire period and region gives a value of 25.351 °C.

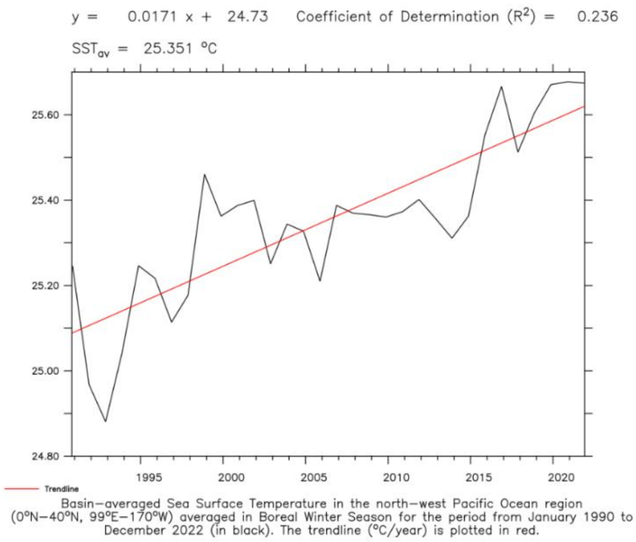

Figure 4.51 Basin-averaged Sea Surface Temperature in the north-west Pacific Ocean region (0 °N to 40 °N, 99 °E to 170 °W) averaged in Boreal Winter Season for the period from January 1990 to December 2022 (in black) and trendline (°C/year) in red.

CHAPTER 5: DISCUSSION

From Figure 4.1 it was found that the SST in the north-west Pacific Ocean have a minimum value of 13.14 °C and a maximum value of 29.77 °C, showing a range of 16.63 °C**.** The highest SST values are found in Malacca Strait, Gulf of Thailand, southern parts of South China Sea, Sulu Sea, Celebes Sea, Philippines Sea and nearly in the entire zonal band to the south of 15 °N and the lowest SST values are seen in the Bohai Sea and parts of the Sea of Japan and to the east of Japan at 40 °N. *Bao et al. (2014)* found higher SST levels in low-latitude regions compared to sub-tropical regions. *Bao et al. (2014)* used 1×1 monthly HadISST data during 1870– 2011, as used in this present study. The annual mean SST falls with increasing latitude, with high temperatures ranging from 26 °C to 28 °C in the south and low temperatures ranging from 3 °C to 6 °C in the north *(Bao et al., 2014)*. This is directly tied to solar radiation dispersion in the deep-sea region. The isotherm is oriented northeast to southwest, with a higher SST gradient along the mainland coastline. It noted that the landmass effect contributes to isotherm tilting during winter months *(Bao et al., 2014)*. In the present study, the directions of the isotherm in the regions to the west of around 135 °E longitude, is from south-west to north-east. The gradient becomes sharpest in the Boreal Spring Season after winter and the directions of the tilt is prominent (Figure 4.14). As the distance from the land-mass of Asia increases, the isotherm direction become more east-west as seen for the study region.

The interactions between the atmosphere and ocean at mid-latitudes contribute to global climate variability on an annual and longer time period. In the northern hemisphere, subtropical western boundary currents move warm water to the poles, creating a temperature differential between the surface ocean and frigid air at mid-high latitudes. This causes significant heat transfer from the water into the atmosphere. At 35 °N and 140 °E, the Kuroshio Current leaves the Japanese shore and enters the North Pacific Ocean, forming the Kuroshio Extension. As a continuation of the western boundary circulation, this extension maintains critical features such as high temperature and velocity and strong eddy turbulence *(Lebedev et al., 2003; Wang et al., 2012)*.

The Table 5.1 shows the minimum and maximum average SST range for the period from January 1990 to December 2022 in the study region. The table highlights the SST ranges of different months. However latitudinal variations cannot be deduced from this table. Among the various months, the SST range is highest in February and the least in August. The same months of February and August have the lowest and highest basin-averaged SSTs respectively (see Table 5.5). *Wu et al. (2020)* found that SST is higher near the Equator and lower at higher latitudes. In the low-latitude zone, SST is more uniformly distributed along latitudes from January to April and November to December, with greater values in the south and lower values in the north.

From May to October, the distribution of SST along the latitude is skewed, with greater values in the south-west and lower values in the north-east, which is controlled by ocean circulation *(Wu et al., 2020)*. According to *Wu et al. (2020)* the range of change of SST in different months is relatively small in low-latitude region, having values between 27 °C and 33 °C and between 5 °C to 6 °C. In the high-latitude region, the SST can be less than 3 °C at the lowest and greater than 15 °C at the highest, with a relatively large variation of more than 12 °C. SST structure inside the Western Pacific Warm Pool (WPWP) is usually overlooked because of its distinct homogeneity, but in fact it possesses a clear meridional high–low–high pattern.

Table 5.1 The month-wise minimum and maximum value of averaged SSTs obtained for the period January 1990 to December 2022, in the north-west Pacific Ocean, and also the SST range. Values obtained from Figure 4.2 to Figure 4.13.

Months	Minimum SST (°C)	Maximum SST (°C)	Range (°C)
January	02.39	29.75	27.36
February	01.98	29.66	27.68
March	03.22	29.77	26.55
April	06.81	30.12	23.31
May	11.64	30.50	18.86
June	14.57	30.18	15.61
July	18.08	29.95	11.87
August	21.66	29.82	08.16
September	20.78	29.95	09.17
October	17.78	29.86	12.08
November	13.05	30.01	16.96
December	07.01	29.90	22.89

Hu et al. (2016) found that during El Niño years, particularly extreme ones, there is a significant intensification of the SST low within the Western Pacific Warm Pool (WPWP), especially from July to October. This intensification leads to the splitting of the WPWP along the 28.50 °C isotherm. Through composite analysis and heat budget examination, they determined that this split is primarily caused by enhanced upwelling resulting from a positive wind-stress curl anomaly and the propagation of upwelling Rossby waves towards the west. While zonal advection at the eastern edge of the split region also contributes, its role is secondary. Further analysis, including results from a Matsuno-Gill Model with asymmetric cooling forcing, suggests that the WPWP split leads to notable anomalous westerly winds, thereby intensifying subsequent El Niño events. *(Hu et.al., 2016)*. The tropical and eastern North Pacific warmed but the central North Pacific experienced a large dip in SST due to an intensified Aleutian Low and surface westerlies *(Graham, 1994)*.

The tropical western Pacific often has a deeper thermocline than the tropical east Pacific due to trade winds. During El Niño occurrences, the Northern Equatorial Current's intensity decreases due to a shallower thermocline in the tropical western Pacific. This leads to a drop in Kuroshio Current velocity and volume *(Yamagata et al., 1985; Yasuda et al., 1985; Yuan et al., 2001).* During La Niña conditions, the transport of the Kuroshio Current is bolstered. This is attributed to the strengthening of trade winds and the deepening of the thermocline in the tropical western Pacific, which is associated with the Northern Equatorial Current *(Andreasen and Ravelo, 1997)*. The intensification of Pacific trade winds resulted in the upwelling of cooler water around the Equator. Because to changes in surface winds, a greater amount of heat has entered below 700 m deep over the last decade. Natural decadal climatic variability, in addition to the more widely mentioned parts of climate change, such as sea level rise, has a significant impact on global surface temperatures. The mean wind stress time series was calculated for the region encompassed by 6 °N to 6 °S latitudes and 180 °E to 150 °W longitudes. This is the zone where interannual and multidecadal Pacific Decadal Oscillation (PDO) patterns show the most regression on Pacific Ocean wind *(Kidwell et.al., 2017)*.

Table 5.2 shows that the minimum SST of about 4.13 °C is seen in the Boreal Spring season and the maximum of about 30.03 °C observed in Boreal Summer season.

Table 5.2 The season-wise minimum and maximum value of averaged SSTs obtained for the period January 1990 to December 2022, in the north-west Pacific Ocean, and also the SST range. Values obtained from Figure 4.14 to Figure 4.17.

Seasons	Minimum SST (°C)	Maximum SST (°C)	Range (°C)
Boreal Spring	04.13	29.75	25.62
Boreal Summer	15.04	30.03	14.99
Boreal Autumn	20.19	29.76	09.57
Boreal Winter	07.48	29.86	22.38

During the Boreal Spring season, the SSTs are highest in the equatorial regions and are seen at Malacca Strait, Gulf of Thailand, south-eastern parts of South China Sea, Sulu Sea, Celebes Sea, southern parts of the Philippine Sea and extends eastwards into the Pacific Ocean, covering almost the entire region equatorward of 10 °N and lowest are seen at the Bohai Sea, some parts of the Yellow Sea and parts of the Sea of Japan. During Boreal Summer season the SSTs are highest with values in the range of above 30 °C. Such values are seen in parts of the Malacca Strait and lowest are seen near the 40 °N latitude.

During the Boreal Autumn season, the SSTs are highest in the Malacca Strait, Gulf of Thailand, most parts of the South China Sea, Sulu Sea, Celebes Sea, Philippine Sea and nearly in the entire zonal band to equatorward of 25 °N and the lowest SSTs, i.e. in the range between 20 °C to 22.5 °C, are seen extending zonally at around 40 °N latitude. During Boreal Winter the SSTs are highest are seen in the Malacca Strait, most of the Gulf of Thailand, Sulu Sea, Celebes Sea and most of the Philippine Sea and the lowest temperatures are seen in the Korea Bay and the Bohai Sea. The East China Sea is likely to exhibit the largest temperature gradient compared to the South China Sea, primarily due to its complex oceanographic dynamics influenced by the Kuroshio Current and the topographical features along the coastlines of China and Japan. It is obvious that the landmass effect in the winter has contributed to the tilting of the isotherms, which was pointed out by *(Bao et al. 2014)*.

The NP-SAFZ exhibits the most significant decadal SST changes during boreal winter. Unlike in boreal winter, there is no clear maximum in SST variability along the NP-STFZ North Pacific sub-tropical oceanic frontal zones, which diminishes in summer. High variability occurs along the NP-SAFZ, North Pacific sub-arctic oceanic frontal zones spanning nearly the entire Pacific basin. The OFZ (Oceanic Frontal Zones) off Baja California and further west continues to see significant decadal fluctuation. The OFZ in the eastern equatorial Pacific is characterized by significant decadal SST variability, which extends southward and nearly completely covers the equatorial cold tongue. Compared to boreal winter, decadal variability reduces across the middle equatorial Pacific and along the SP-SAFZ, despite increased cross-frontal SST gradients in that OFZ in boreal summer. The mid-summer frontogenesis diagnosis in the NP-SAFZ (40 °N to ~45

°N) using a simple mixed layer model shows a correlation between the observed anomalous frontogenetic propensity and the calculated anomalous net force *(Nakamura and Kazmin, 2003)*. The Levitus Data suggests that the mixed layer thickness may be too shallow, resulting in poorer correspondence than in the winters. In summer, the Ekman effects are less significant due to less variations in surface westerlies *(Nakamura and Kazmin, 2003).*

The slopes of the trendlines of SST in the period from January 1990 to December 2022 are in the range of –0.015 °C/ year to 0.044 °C/ year. The highest positive values of slopes of SSTs are seen along parts of the east and west coasts of Japan, and in the North Pacific Ocean near (37 °N, 165 °E) and (37 °N, 180 °E). Most of the north Pacific Ocean shows positive trends in SSTs, except near the region between 0 °N to 5 °N and 170 °E to 170 °W. The Coefficient of Determination (R^2) values are above 0.25 in some patches in the equatorial Pacific region at around 145 °E and 155 °E. Temporal changes of SST and SST anomalies linear trend variation in the northwest Pacific, the Northern Hemisphere and the global ocean. The SST and SSTA trend are increasing due to global warming. From 1870-1910, SST decreases gradual and from 1910-1930, the SST change is minimal. From 1930 onwards steady rise in SST is seen, which continues till 2017*(Wu et.al 2020)*. PDO is an important factor of climate change of the north-west Pacific, and it has a strong correlation with ENSO *(Wu et.al 2020)*.

Table 5.3 shows that the highest negative trend is in January, and the highest positive trend is in February. Air-sea interactions contribute to the maintenance of warm *(Ando and McPhaden, 1997)* and very warm SST temperatures, resulting in positive feedback. It may also help to maintain the heat accumulation due to El Niño development *(Meinen and McPhaden 2000; Maes et al. 2005)*, and promote further eastward relocation of the Warm Pool *(Maes et al. 2002)*.

Table 5.3 The month-wise maximum and minimum values of the slopes of the trendlines of SST in the period from January 1990 to December 2022, over the north-west Pacific Ocean, obtained from Figures 4.19 to Figure 4.30.

Months	Negative Trend (°C/year)	Positive Trend (°C/year)
January	-0.024	0.043
February	-0.016	0.060
March	-0.013	0.052
April	-0.016	0.048
May	-0.017	0.049
June	-0.011	0.049
July	-0.016	0.057
August	-0.018	0.051
September	-0.018	0.058
October	-0.023	0.058
November	-0.015	0.059
December	-0.021	0.044

The potential influence of reported stratification trends on ocean-atmosphere interactions should be studied using numerical modelling. SST lows intensify before El Niño occurrences and diminish before La Niña events. During El Niño years, the Western Pacific Warm Pool (WPWP) SSTs cool and diverge from the 28.5 °C isotherm. On this occasion, it appears that the relative SST low has divided the WPWP in two *(Hu et.al., 2016)*.

As a result, the years 1982, 1986, 1990/1991, 1994, 1997, 2000, 2002, 2004, 2006, and 2009 are recognized as WPWP split years from 1982 through 2011. The split events are statistically significant at 98% confidence level. The strongest El Niño occurrences in history occurred in 1982 and 1997. WPWP-enhancing events from 1982 to 2011 include 1984, 1988/1989, 1992, 1994/1995, 1998, 2001, 2003, and 2010. Most WPWP enhancing incidents occur during La Niña times. During the composite split event, the 28/28.5°C isotherms are closed, with a lower SST area dividing the WPWP and a visible high-low-high SST structure. The SST low is weak, and the WPWP appears as a homogeneous warm water mass. Thus, the WPWP split events are nearly entirely responsible for the climatological high-low-high SST pattern *(Hu et.al., 2016)*. The WPWP during split events are roughly 0.3-0.6 °C cooler than that in non-split years, and the majority of the SSTs in the split zone are at 99% confidence level, implying that the WPWP split is statistically significant *(Hu et.al., 2016)*. The month-wise maximum and minimum values of season-wise slopes of the trendlines of SST in the period from January 1990 to December 2022, in the north-west Pacific Ocean (Table 5.4).

A substantial high-low-high SST structure is revealed within the boreal summer-autumn WPWP. During El Niño years, the SST low intensifies and splits the 28.50 °C isotherm defined WPWP, resulting in a WPWP split event. Horizontal currents, such as NEC (North Equatorial Current), NECC (North Equatorial Counter-current), and Mindanao Current, are amplified during the WPWP split event, resulting in negative zonal advection and greater cooling *(Hu et.al., 2016)*.

Table 5.4 The season-wise maximum and minimum values of the slopes of the trendlines of SST in the period from January 1990 to December 2022, over the north-west Pacific Ocean, obtained from Figures 4.31 to Figure 4.34.

Seasons	Negative Trend (°C/year)	Positive Trend (°C/year)
Boreal Spring	-0.013	0.050
Boreal Summer	-0.015	0.050
Boreal Autumn	-0.018	0.049
Boreal Winter	-0.017	0.043

No typhoon formed in July 2020 for the first time, according to the Digital Typhoon database, which may have reduced upper ocean cooling *(Emanuel, 1999; Wang et al., 2016)*. Furthermore, elevated surface temperatures are linked to abnormally warm underlying water temperatures below 50 metres depth. According to a high-resolution regional ocean reanalysis for 1993-2020 *(Miyazawa et al., 2019)* and a long-term global ocean reanalysis for 1955-2019 *(Ishii et al., 2017)*, deep ocean temperatures have gradually increased since the mid-twentieth century, but they suddenly increased in 2018 and persisted until 2020, owing to oceanic interannual variability. These variables may work together to cause this record-high SST event. This heated temperature, however, is likely to occur as frequently as reported regardless of internal variability mechanisms, as anthropogenic forcing has altered the climate mean state. The frequency of these catastrophes is predicted to grow as global temperatures continue to increase. Apply composite analysis to the linked physical processes, followed by a heat budget analysis in the split region to study the quantitative contributions of various physical processes.

Anomalous divergence and upwelling form in the zone between North Equatorial Counter current (NECC) and North Equatorial Current (NEC) which may lead to the formation of the WPWP divide. Vertical advections are most likely responsible for the divide in the WPWP. As previously stated, another essential factor in regulating SST change is the sea surface heat flux. Warming and cooling events in the western North Pacific, along with local wind stress curl, are thought to play an important role in the ENSO phase shift *(Wang et al. 1999).* Warm waters provide the atmosphere with water vapor and heat, releasing latent heat and resulting in convection and high rainfall exceeding 2-3 m per year *(Delcroix et al. 1996; Chen et al. 2004)*. Waters warmer than 28.5 °C include both low and high salinity waters. Warm seas are limited to the western tropical Pacific, whereas low-salinity waters cover the whole tropical Pacific. Furthermore, it has been demonstrated that the position of the equatorial convergence zone located at the eastern margin of the Warm Pool, which is essential for ENSO events, correlates to the position of the 34.6 and 34.8 isohalines *(Maes et al. 2004)*.

In the northern section of the tropical basin, it can reach up to 1.2 °C per 50 years and exceed five standard deviations of the interannual signal in 50 years. It is weaker or even zero in the eastern equatorial band, reinforcing the zonal SST gradient, as shown by *Cane et al. (1997)*. An exception is a cooling (from 0.12 °C to 0.25 °C per 50 years, depending on the SST product) in a finger-like section of the central northern tropical Pacific that enters the Warm Pool. Given the presence of decadal variability, the trend derived by linear regression over a shorter time period may be influenced by both decadal fluctuations and lower frequency changes *(McPhaden and Zhang, 2004; Zhang and McPhaden, 2006)*.

The ocean surface covered by seas warmer than 29 °C doubled from the beginning to the conclusion of the period in both products, and waters warmer than 29 °C in 1990 to 2000 increased to cover the same area as waters warmer than 28.5 °C 40-years earlier. The area covered by waters warmer than 29.5 °C expanded by 4 to 6 times (from 0.8 or 1.5 million km^2 to 6.5 million km^2 depending on the SST product), and waters warmer than 30 °C, which were occasional 50-years ago in both products, became a common feature of the Warm Pool waters *(Cravatte et al., 2009)*. The strengthening of the Pacific trade winds led to the emergence of colder water along the equator. Over the past decade, a higher proportion of heat has been absorbed into depths exceeding 700 meters due to alterations in surface wind patterns. Natural fluctuations over decades significantly impact global surface temperatures, alongside more commonly discussed climate change factors like rising sea levels. Researchers analyzed the mean wind stress over the area spanning from 6°N to 6°S and 180° to 150°W, a region where interannual and multidecadal climate phenomena such as the Interdecadal Pacific Oscillation (IPO) or Pacific Decadal Oscillation (PDO) exhibit the strongest correlation with Pacific Ocean winds *(Kidwell et.al., 2017).* During El Niño and La Niña, a moderately significant trend in zonal SST gradients emerges early in the Northern Hemisphere spring (March to May), as well as in the late summer (July to September). However, these SST trends in the zonal gradient do not clearly represent an ENSO Modoki-like dipole because they are only connected with significant positive SST trends in the eastern or western Pacific, with no corresponding strong negative trends. The zonal SST gradient shows no notable trends throughout the boreal winter months, when ENSO events generally mature. Given the prevalence of positive SST trends across much of the equatorial Pacific Ocean, utilizing fixed SST anomaly criteria to characterize ENSO events should be revisited *(L'Heureux et.al., 2012)*.

The SST basin-averaged from January 1990 to December 2022 showed that there is an increasing trend in the north-west Pacific Ocean (see Table 5.5). All the seasons also show an increasing trend in the north-west Pacific Ocean. There is global warming occurring in the world *(Laufkötter et al., 2020)*. The results of the basin-averaged trends of all the months and seasons in the north-west Pacific concur with the warming trends being reported world-wide. At the onset of an El Niño event, there is an emergence of atypical westerly winds in the equatorial region, impacting the event's severity in two main ways. Firstly, these abnormal westerly winds in the western Pacific Ocean near the equator can intensify eastward ocean currents, facilitating the transfer of warm water to the eastern Pacific Ocean and driving the movement of the Western Pacific Warm Pool (WPWP) eastward. Additionally, they generate eastward-propagating downwelling equatorial Kelvin waves, which deepen the thermocline and raise temperatures in the eastern equatorial Pacific Ocean. Conversely, anomalous westerly winds in the central-eastern equatorial Pacific Ocean can dampen equatorial upwelling, leading to positive anomalies in SST *(Wang et al., 1999).* Linear regression analysis conducted over a shorter timeframe may be influenced by both decadal oscillations and longer-term changes in frequency *(McPhaden and Zhang, 2004; Zhang and McPhaden, 2006)*.

The basin-averaged SST in the north-west Pacific Ocean region (0 °N to 40 °N, 99 °E to 170 °W) averaged in the period from January 1990 to December 2022 is shown in Table 5.5.

Table 5.5 The values of north-west Pacific Ocean (0 °N to 40 °N, 99 °E to 170 °W) basin-averaged SST, slopes of the trendlines, intercepts and coefficient of determination (R^2) month-wise and in the entire study period, from January 1990 to December 2022, obtained from Figures 4.35 to Figure 4.47.

Average/ Months	SST average (°C)	Slope of Trendline (°C/year)	Intercept of Trendline	Coefficient of Determination (R^2)
Annual Average	26.174	0.0188	25.49	0.030
January	24.237	0.0164	23.64	0.192
February	23.721	0.0141	23.21	0.140
March	23.948	0.0150	23.40	0.149
April	24.748	0.0120	24.31	0.113
May	25.908	0.0155	25.34	0.163
June	27.052	0.0153	26.49	0.163
July	28.002	0.0133	27.51	0.135
August	28.492	0.0152	27.94	0.156
September	28.352	0.0168	27.74	0.199
October	27.617	0.0155	27.05	0.180
November	26.574	0.0180	25.91	0.223
December	25.305	0.0173	24.67	0.213

In Table 5.5 also show the monthly basin-average slopes of trendlines of SSTs. The averaged SST from January to February shows decreasing followed by increasing in SST averaged from April to August and then further decreases. The highest slope of trendline is seen in November and lowest seen in April. The highest coefficient of determination is seen in November and lowest is seen in April.

Table 5.6 The values of north-west Pacific Ocean (0 °N to 40 °N, 99 °E to 170 °W) basin-averaged SST, slopes of the trendlines, intercepts and coefficient of determination (R^2) season-wise in the period from January 1990 to December 2022, obtained from Figures 4.48 to Figure 4.51.

Seasons	SST average (°C)	Slope of Trendline (°C/year)	Intercept of Trendline	Coefficient of Determination (R^2)
Boreal Spring Season	24.145	0.0137	23.65	0.158
Boreal Summer Season	26.987	0.0147	26.45	0.196
Boreal Autumn Season	28.151	0.0159	27.57	0.221
Boreal Winter Season	25.351	0.0171	24.73	0.236

The minimum SSTs in the north-west Pacific Ocean occur in February due to reduced solar radiation, colder air temperatures, and potential influence from cold ocean currents or upwelling. Conversely, the warmest SSTs are observed in August, driven by increased solar insolation, warmer air temperatures, and potential dominance of warm ocean currents. These seasonal variations in SSTs are influenced by factors such as solar energy input, atmospheric conditions, ocean currents, seasonal mixing, and geographical features. The minimum temperature basically occurs in February and the warmest occurs in August. The fluctuation range of SST in Bohai Sea is the largest, basically between 5 and 22 °C, from 18 to 27 °C in the East China Sea, and the smallest fluctuations are in the South China Sea, maintained at a range of 26 to 29 °C *(Wu et al., 2020)*. In August 2020, the northwestern Pacific (120 °E to 180 °E, 20 °N to 35 °N) witnessed a record high SST. Because of anthropogenic forcing, the risk of such warm SST events occurring between 2001 and 2020 has increased from 0.0 % and 0.1 % to 5.5 % and 8.5 %, respectively *(Hayashi et al., 2021)*.

Using CMIP6 multi-model ensembles, researchers discovered that from the twentieth century to the present, anthropogenic GHG (greenhouse gas) emissions enhanced the risk of the highest recorded warm NWPac SST, which occurred in August 2020. Without anthropogenic forcing, it was unlikely that regional record high warm SST would occur in the early 21st century. They confirmed that anthropogenic warming in the NWPac region has been observable since the 2010s, independent of internal variability. Until now, this warming signal has been difficult to discern from internal variability because anthropogenic aerosol forcing cancels out the warming trend. As a result of human-caused global warming, the 2020 record warm SST in the NWPac happened once every 12 to 18 years between 2001 and 2020, which is consistent with previous observations. This change in likelihood is consistent with trends in maritime heatwaves in other regions *(Laufkötter et al., 2020)*.

The Table 5.6 show seasonal basin-average SSTs and also slopes of trendlines of SSTs. The highest averaged SST seen in Boreal Autumn season and lowest is seen in Boreal Spring Season. The highest slope of trendline is seen in Boreal Winter season and lowest seen in Boreal Spring season. The highest coefficient of determination is seen in Boreal Winter season and lowest is seen in Boreal spring season. Temperatures have risen by 0.032 °C to 0.035 °C every decade from 1854 to 2017, throughout all seasons. The last 30 years' seasonal pattern indicates a stronger warming trend than the previous 164 years. Winter has experienced the most significant warming (0.146 °C and 0.124 °C/decade, respectively) over the previous 30 years, whereas spring has seen the least increase *(Wu et.al., 2020)*.

CHAPTER 6: CONCLUSION

The SST map in the north-west Pacific Ocean (0 °N to 40 °N, 99 °E to 170 °W), averaged in the period from January 1990 to December 2022, is shown in Figure 4.1. The SSTs have a minimum value of 13.14 °C and a maximum value of 29.77 °C. The basin-averaged SST in the north-west Pacific Ocean, in the entire period from January 1990 to December 2022 is 26.174 °C. The SST is high in low latitude regions compared to high latitudes. The highest basin-averaged SSTs are seen in the Boreal Autumn Season with a value of 28.151 °C and the lowest basin-averaged SSTs are seen in the Boreal Spring Season with a value of 24.145 °C. The basin-averaged SST is highest (28.492 °C) in August and the lowest (23.721 °C) in February. This shows the thermal inertia of the ocean, which lags the summer and winter solstices by a couple of months in reaching their maximum and minimum value. The isotherm pattern is oriented northeast-southwest till 135 °E, with a higher SST gradient along the mainland coastline.

The basin-averaged SST in the north-west Pacific Ocean shows positive trends (0.0188 °C/year) in the entire study period. All the months and seasons show increasing trends in SSTs. However, the rates of increase between the months and seasons are different and the highest increasing trends are seen in the Boreal Winter Season (0.0171 °C/year) and in the month of November (0.0180 °C/year). The least increasing trend was seen in the Boreal Spring Season (0.0137 °C/year) and in the month of April (0.0120 °C/year). Spatially, different parts of the north-west Pacific Ocean show different slopes of trendlines. The sub-tropical regions show a larger increasing trend than the tropical regions. Some parts of the equatorial North Pacific Ocean near the 180° longitude shows a cooling trend.

CHAPTER 7: REFERENCES

1. Andreasen, D., & Ravelo, A. C. (1997). Tropical Pacific Ocean thermocline depth reconstructions for the Last Glacial Maximum. *Paleoceanography*, *12*(3), 395–413. d.o.i.: https://doi.org/10.1029/97pa00822

2. Ando, K., & McPhaden, M. J. (1997). Variability of surface layer hydrography in the tropical Pacific Ocean. *Journal of Geophysical Research*, *102*(C10), 23063–23078. d.o.i.: https://doi.org/10.1029/97jc01443

3. Ault, T. R., Cole, J. E., Evans, M. N., Barnett, H., Abram, N. J., Tudhope, A. W., & Linsley, B. K. (2009). Intensified decadal variability in tropical climate during the late 19th century. *Geophysical Research Letters*, *36*(8). d.o.i.: https://doi.org/10.1029/2008gl036924

4. Bao, B., & Ren, G. (2014). Climatological characteristics and long-term change of SST over the marginal seas of China. *Continental Shelf Research*, *77*, 96–106. d.o.i.: https://doi.org/10.1016/j.csr.2014.01.013

5. Buckley, M. W., Ponte, R. M., Forget, G., & Heimbach, P. (2014). Low-frequency SST and upper-ocean heat content variability in the North Atlantic. *Journal of Climate*, 27, 4996– 5018. d.o.i.: https://doi.org/10.1175/JCLI-D-13-00316.1

6. Bulgin, C. E., Merchant, C. J., & Ferreira, D. (2020). Tendencies, variability and persistence of SST anomalies. *Scientific Reports*, *10*(1). d.o.i.: https://doi.org/10.1038/s41598-020-64785-9

7. Cane, M. A., Clement, A. C., Kaplan, A., Kushnir, Y., Pozdnyakov, D., Seager, R., Zebiak, S. E., & Murtugudde, R. (1997). Twentieth-Century Sea

surface temperature trends. *Science*, *275*(5302), 957–960. d.o.i.: https://doi.org/10.1126/science.275.5302.957

8. Chen, G., Fang, C., Zhang, C., & Chen, Y. (2004). Observing the coupling effect between warm pool and "rain pool" in the Pacific Ocean. *Remote Sensing of Environment*, *91*(2), 153–159. d.o.i.: https://doi.org/10.1016/j.rse.2004.02.010

9. Chen, Z., Wen, Z., Wu, R., Lin, X., & Wang, J. (2016). Relative importance of tropical SST anomalies in maintaining the Western North Pacific anomalous anticyclone during El Niño to La Niña transition years. *Climate Dynamics*, *46*(3–4), 1027–1041. d.o.i: https://doi.org/10.1007/s00382-015-2630-1

10. Chelton, D. B., & Xie, S. (2010). Coupled Ocean-Atmosphere interaction at oceanic mesoscales. *Oceanography*, *23*(4),69. d.o.i: https://doi.org/10.5670/oceanog.2010.05

11. Cravatte, S., Delcroix, T., Zhang, D., McPhaden, M. J., & Leloup, J. (2009). Observed freshening and warming of the western Pacific Warm Pool. *Climate Dynamics*, *33*(4), 565–589. d.o.i.: https://doi.org/10.1007/s00382-009-0526-7

12. D'Mello, J. R., & Prasanna Kumar, S. (2016). Why is the Bay of Bengal experiencing a reduced rate of sea surface warming? *International Journal of Climatology*, *36*(3), 1539–1548. d.o.i.: https://doi.org/10.1002/joc.4414

13. Delcroix, T., Hénin, C., Porte, V., & Arkin, P. A. (1996). Precipitation and sea-surface salinity in the tropical Pacific Ocean. *Deep Sea Research Part I: Oceanographic Research Papers*, *43*(7), 1123–1141. d.o.i.: https://doi.org/10.1016/0967-0637(96)00048-9

14. Diamond, M., & Bennartz, R. (2015). Occurrence and trends of eastern and central Pacific El Niño in different reconstructed SST data sets. *Geophysical Research Letters*, *42*(23). d.o.i.: https://doi.org/10.1002/2015gl066469

15. Emanuel, K. (1999). Thermodynamic control of hurricane intensity. *Nature*, *401*(6754), 665–669. d.o.i.: https://doi.org/10.1038/44326

16. England, M. H., McGregor, S., Spence, P., Meehl, G. A., Timmermann, A., Cai, W., Gupta, A. S., McPhaden, M. J., Purich, A., & Santoso, A. (2014). Recent intensification of wind-driven circulation in the Pacific and the ongoing warming hiatus. *Nature Climate Change*, *4*(3), 222–227. d.o.i.: https://doi.org/10.1038/nclimate2106

17. Graham, N. E. (1994). Decadal-scale climate variability in the tropical and North Pacific during the 1970s and 1980s: observations and model results. *Climate Dynamics*, *10*(3), 135–162. d.o.i.: https://doi.org/10.1007/bf00210626

18. Gray, W. M. (1998). The formation of tropical cyclones. *Meteorology and Atmospheric Physics*, *67*(1–4), 37–69. d.o.i.:https://doi.org/10.1007/bf01277501

19. Griffies, S. M., Winton, M., Anderson, W., Benson, R., Delworth, T. L., Dufour, C. O., Dunne, J., Goddard, P. B., Morrison, A. K., Rosati, A., Wittenberg, A. T., Yin, J., & Zhang, R. (2015). Impacts on ocean heat from transient mesoscale eddies in a hierarchy of climate models. *Journal of Climate*, *28*(3), 952– 977. d.o.i.: https://doi.org/10.1175/jcli-d-14-00353.1.

20. Hayashi, M., Shiogama, H., Emori, S., Ogura, T., & Hirota, N. (2021). The Northwestern Pacific warming record in August 2020 occurred under anthropogenic forcing. *Geophysical Research Letters*, *48*(1). d.o.i.: https://doi.org/10.1029/2020gl090956

21. Huang, B., Banzon, V. F., Freeman, E., Lawrimore, J. H., Liu, W., Peterson, T. C., Smith, T. M., Thorne, P., Woodruff, S. D., & Zhang, H. (2015). Extended Reconstructed Sea Surface Temperature Version 4 (ERSST.V4). Part I: Upgrades and Intercomparisons. *Journal of Climate*, *28*(3), 911–930. d.o.i.: https://doi.org/10.1175/jcli-d-14-00006.1.

22. Hurrell, J., & Trenberth, K. E. (1999). Global Sea Surface Temperature Analyses: Multiple problems and Their Implications for Climate Analysis, *Research Gate*. d.o.i.: https://doi.org/10.1175/1520-0477(1999)080

23. Hu, S., Hu, D., Guan, C., Xing, N., Li, J., & Feng, J. (2016). Variability of the western Pacific warm pool structure associated with El Niño. *Climate Dynamics*, *49*(7–8), 2431–2449. d.o.i.: https://doi.org/10.1007/s00382-016-3459-y.

24. Hu, H., Wu, Q., & Wu, Z. (2018). Influences of two types of El Niño event on the Northwest Pacific and tropical Indian Ocean SST anomalies. *Journal of Oceanology and Limnology*, *36*(1), 33–47. d.o.i.: https://doi.org/10.1007/s00343-018-6296-5

25. Ishii, M., Fukuda, Y., Hirahara, S., Yasui, S., Suzuki, T., & Sato, K. (2017). Accuracy of Global Upper Ocean Heat Content Estimation Expected from Present Observational Data Sets. *SOLA*, *13*(0), 163-167. d.o.i.: https://doi.org/10.2151/sola.2017-030

26. Jia, W., Chang, F., Li, T., Sun, H., Cui, Y., & Liu, T. (2020). The evolution of the Kuroshio Current over the last 5 million years since the Pliocene: Evidence from planktonic foraminiferal faunas. *Science China Earth Sciences*, *63*(11), 1714–1729. d.o.i.: https://doi.org/10.1007/s11430-019-9641-9.

27. Kidwell, A., Han, L., Jo, Y., & Yan, X. (2017). Decadal Western Pacific Warm Pool variability: A Centroid and heat Content study. *Scientific Reports*, *7*(1). d.o.i.: https://doi.org/10.1038/s41598-017-13351-x

28. L'Heureux, M., Collins, D. C., & Hu, Z. (2012). Linear trends in sea surface temperature of the tropical Pacific Ocean and implications for the El Niño-Southern Oscillation. *Climate Dynamics*, *40*(5–6), 1223–1236. d.o.i.: https://doi.org/10.1007/s00382-012-1331-2

29. Latif, M. (2006). On North Pacific multidecadal climate variability. *Journal of Climate*, *19*(12), 2906–2915. d.o.i.: https://doi.org/10.1175/jcli3719.1

30. Li, G., Li, C., Ya, T., & Bai, T. (2014). The interdecadal changes of south pacific sea surface temperature in the mid-1990s and their connections with ENSO. *Advances in Atmospheric Sciences*, *31*(1), 66–84. d.o.i.: https://doi.org/10.1007/s00376-013-2280-3

31. Li, X., Zong, Y., Zheng, Z., Huang, G., & Xiong, H. (2017). Marine deposition and sea surface temperature changes during the last and present interglacials in the west coast of Taiwan Strait. *Quaternary International*, *440*, 91–101. d.o.i.: https://doi.org/10.1016/j.quaint.2016.05.023

32. Liu, C., Sun, Q., Xing, Q., Liang, Z., Deng, Y., & Zhu, L. (2017). Spatio-temporal variability in sea surface temperatures for the Yellow Sea based on MODIS dataset. *Ocean Science Journal*, *52*(1), 1–10. d.o.i.: https://doi.org/10.1007/s12601-017-0006-7

33. Laufkötter, C., Zscheischler, J., & Frölicher, T. L. (2020). High-impact marine heatwaves attributable to human-induced global

warming. *Science*, *369*(6511), 1621–1625. d.o.i.: https://doi.org/10.1126/science.aba0690

34. Lebedev, K. B., Yaremchuk, M., Mitsudera, H., Nakano, I., & Yuan, G. (2003). Monitoring the Kuroshio Extension with Dynamically Constrained Synthesis of the Acoustic Tomography, Satellite Altimeter and in situ Data. *Journal of Oceanography*, *59*(6), 751–763. d.o.i.: https://doi.org/10.1023/b:joce.0000009568.06949.c5

35. Luo, D., Diao, Y., & Feldstein, S. B. (2011). The Variability of the Atlantic Storm Track and the North Atlantic Oscillation: A Link between Intraseasonal and Interannual Variability. *Journal of the Atmospheric Sciences*, *68*(3), 577–601. d.o.i.: https://doi.org/10.1175/2010jas3579.1

36. Maes, C., Picaut, J., & Bélamari, S. (2002). Salinity barrier layer and onset of El Niño in a Pacific coupled model. *Geophysical Research Letters*, *29*(24). d.o.i.: https://doi.org/10.1029/2002gl016029

37. Maes, C., Picaut, J., Kuroda, Y., & Ando, K. (2004). Characteristics of the convergence zone at the eastern edge of the Pacific warm pool. *Geophysical Research Letters*, *31*(11). d.o.i.: https://doi.org/10.1029/2004gl019867

38. Maes, C., Picaut, J., & Bélamari, S. (2005). Importance of the salinity barrier layer for the buildup of el niño. *Journal of Climate*, *18*(1), 104–118. d.o.i.: https://doi.org/10.1175/jcli-3214.1

39. McPhaden, M. J. (1993). TOGA-TAO and the 1991–93 El Niño Southern Oscillation event. *Oceanography (Washington, D.C.)*, *6*(2), 36–44. d.o.i.: https://doi.org/10.5670/oceanog.1993.12

40. McPhaden, M. J., & Zhang, D. (2004). Pacific Ocean circulation rebounds. *Geophysical Research Letters*, *31*(18). d.o.i.: https://doi.org/10.1029/2004gl020727

41. Meinen, C. S., & McPhaden, M. J. (2000). Observations of warm water volume changes in the Equatorial Pacific And their relationship to El Niño and La Niña. *AMETSOC*. d.o.i.: https://doi.org/10.1175/1520-0442(2000)013

42. Mei, W., Xie, S., Primeau, F., McWilliams, J. C., & Pasquero, C. (2015). Northwestern Pacific typhoon intensity controlled by changes in ocean temperatures. *Science Advances*, *1*(4). d.o.i.: https://doi.org/10.1126/sciadv.1500014

43. Minnett, P. J. (2014). Sea surface temperature. In *Springer eBooks* (pp. 754–759). d.o.i.: https://doi.org/10.1007/978-0-387-36699-9_166

44. Miyazawa, Y., Kuwano-Yoshida, A., Doi, T., Nishikawa, H., Narazaki, T., Fukuoka, T., & Sato, K. (2019). Temperature profiling measurements by sea turtles improve ocean state estimation in the Kuroshio-Oyashio Confluence region. *Ocean Dynamics*, *69*(2), 267–282. d.o.i.: https://doi.org/10.1007/s10236-018-1238-5

45. Nakamura, H., & Kazmin, A. S. (2003). Decadal changes in the North Pacific oceanic frontal zones as revealed in ship and satellite observations. *Journal of Geophysical Research*, *108*(C3), 3078. d.o.i.: https://doi.org/10.1029/1999jc000085.

46. Nakamura, H., Lin, G., & Yamagata, T. (1997). Decadal climate variability in the North Pacific during the recent decades. Bulletin of the *American Meteorological Society*, 78, 2215–2225. d.o.i.: https://doi.org/10.1175/1520-0477(1997)078<2215:DCVITN>2.0.CO;2

47. Nonaka, M., Nakamura, H., Tanimoto, Y., Kagimoto, T., & Sasaki, H. (2005). Decadal variability in the Kuroshio–Oyashio extension simulated in an Eddy-Resolving OGCM. *Journal of Climate*, *19*(10), 1970–1989. d.o.i.: https://doi.org/10.1175/jcli3793.1

48. Ogawa, F., Nakamura, H., Nishii, K., Miyasaka, T., & Kuwano-Yoshida, A. (2012). Dependence of the climatological axial latitudes of the tropospheric westerlies and storm tracks on the latitude of an extratropical oceanic front. *Geophysical Research Letters*, *39*(5). d.o.i.: https://doi.org/10.1029/2011gl049922

49. Pachauri, R. K., Allen, M. R., Barros, V. R., Broome, J., Cramer, W., Christ, R., Church, J. A., Clarke, L., Dahe, Q. D., Dasqupta, P., Dubash, N. K., Edenhofer, O., Elgizouli, I., Field, C. B., Forster, P., Friedlingstein, P., Fuglestvedt, J., Gomez-Echeverri, L., Hallegatte, S., . . . Van Ypersele, J. (2014). Climate change 2014 synthesis report. contribution of working groups I, II, and III to the fifth assessment report of the Intergovernmental Panel on Climate Change. The UWA Profiles and Research Repository.

50. Pan, X., Wong, G. T., Ho, T., Tai, J., Liu, H., Liu, J., & Shiah, F. (2018). Remote sensing of surface [nitrite + nitrate] in river-influenced shelf-seas: The northern South China Sea Shelf-sea. *Remote Sensing of Environment*, *210*, 1–11. d.o.i.: https://doi.org/10.1016/j.rse.2018.03.012

51. Qiu, B. (2001). Kuroshio and Oyashio currents. In *Elsevier eBooks* (pp. 1413–1425). d.o.i.: https://doi.org/10.1006/rwos.2001.0350

52. Qiu, B., & Chen, S. (2012). Multidecadal sea level and gyre circulation variability in the northwestern Tropical Pacific Ocean. *Journal of Physical Oceanography*, *42*(1), 193–206. d.o.i.: https://doi.org/10.1175/jpo-d-11-061.1

53. Ritchie, E. A., & Holland, G. J. (1999). Large-Scale Patterns Associated with Tropical Cyclogenesis in the Western Pacific. *AMETSOC*. d.o.i.: https://doi.org/10.1175/1520-0493(1999)127.

54. Robinson, C. J. (2016). Evolution of the 2014-2015 sea surface temperature warming in the central west coast of Baja California, Mexico, recorded by remote sensing. *Geophysical Research Letters*, *43*(13), 7066–7071. d.o.i.: https://doi.org/10.1002/2016gl069356

55. Schneider, N., A. J. Miller, and D. W. Pierce (2002): Anatomy of North Pacific decadal variability. *J. Climate*, 15, 586–605. d.o.i: https://doi.org/10.1175/1520-0442(2002)015%3C0586:AONPDV%3E2.0.C.

56. Schneider, N., & Cornuelle, B. D. (2005). The forcing of the Pacific decadal oscillation. *Journal of Climate*, *18*(21), 4355–4373. d.o.i.: https://doi.org/10.1175/jcli3527.1

57. Shakun, J. D., & Shaman, J. (2009). Tropical origins of North and South Pacific decadal variability. *Geophysical Research Letters*, *36*(19). d.o.i.: https://doi.org/10.1029/2009gl040313

58. Skirving, W., Enríquez, S., Hedley, J. D., Dove, S., Eakin, C. M., Mason, R. a. B., De La Cour, J. L., Liu, G., Høegh-Guldberg, O., Strong, A. E., Mumby, P. J., & Iglesias-Prieto, R. (2018). Remote Sensing of Coral Bleaching Using Temperature and Light: Progress towards an Operational Algorithm. *Remote Sensing*, *10*(2), 18. d.o.i.: https://doi.org/10.3390/rs10010018

59. Smith, C. A., Compo, G. P., & Hooper, D. K. (2014). Web-Based Reanalysis Intercomparison Tools (WRIT) for analysis and comparison of reanalyses and other datasets. *Bulletin of the American Meteorological Society*, *95*(11), 1671–1678. d.o.i.: https://doi.org/10.1175/bams-d-13-00192.1

60. Song, D., Duan, Z., Zhai, F., & He, Q. (2018). Surface diurnal warming in the East China Sea derived from satellite remote sensing. *Journal of Oceanology and Limnology*, *36*(3), 620–629. d.o.i:https://doi.org/10.1007/s00343-018-7035-7

61. Stuecker, M. F., Jin, F., Timmermann, A., & McGregor, S. (2015). Combination mode dynamics of the anomalous Northwest Pacific anticyclone. *Journal of Climate*, *28*(3), 1093–1111. d.o.i.: https://doi.org/10.1175/jcli-d-14-00225.1

62. Takakura, T., Kawamura, R., Kawano, T., Ichiyanagi, K., Tanoue, M., & Yoshimura, K. (2018). An estimation of water origins in the vicinity of a tropical cyclone's center and associated dynamic processes. *Climate Dynamics*, *50*(1–2), 555–569. d.o.i.: https://doi.org/10.1007/s00382-017-3626-9

63. Tang, D., Kester, D. R., Zhaoding, W., Ji, L., & Kawamura, H. (2003). AVHRR satellite remote sensing and shipboard measurements of the thermal plume from the Daya Bay, nuclear power station, China. *Remote Sensing of Environment*, *84*(4), 506–515. d.o.i.: https://doi.org/10.1016/s0034-4257(02)00149-9

64. Trenberth, K. E., & Hurrell, J. W. (1994). Decadal atmosphere-ocean variations in the Pacific. *Climate Dynamics*, *9*(6), 303–319. d.o.i.:https://doi.org/10.1007/bf00204745

65. Wang, B., Barcilon, A., & Fang, Z. (1999). Stochastic dynamics of El Niño–Southern oscillation. *AMETSOC*. d.o.i.: https://doi.org/10.1175/1520-0469(1999)056

66. Wang, C., Zou, L., & Zhou, T. (2018). SST biases over the Northwest Pacific and possible causes in CMIP5 models. *Science China Earth Sciences*, *61*(6), 792–803. d.o.i.: https://doi.org/10.1007/s11430-017-9171-8

67. Wang, G., Wu, L., Johnson, N. C., & Zheng, L. (2016). Observed three- dimensional structure of ocean cooling induced by Pacific tropical cyclones. *Geophysical Research Letters*, *43*(14), 7632–7638. d.o.i.: https://doi.org/10.1002/2016gl069605

68. Wang, L., Li, T., & Zhou, T. (2012). Intraseasonal SST Variability and Air–Sea Interaction over the Kuroshio Extension Region during Boreal Summer. *Journal of Climate*, *25*(5), 1619–1634. d.o.i.: https://doi.org/10.1175/jcli-d-11-00109.1

69. Wills, R. C. J., Battisti, D. S., Proistosescu, C., Thompson, L., Hartmann, D. L., & Armour, K. (2019). Ocean circulation signatures of North Pacific decadal variability. *Geophysical Research Letters*, 46, 1690–1701. d.o.i.: https://doi.org/10.1029/2018GL080716

70. Wills, R. C. J., Schneider, T., Wallace, J. M., Battisti, D. S., & Hartmann, D. L. (2018). Disentangling global warming, multidecadal variability, and el niño in Pacific temperatures. *Geophysical Research Letters*, *45*(5), 2487–2496. d.o.i.: https://doi.org/10.1002/2017gl076327

71. Wu, Z. Y., Jiang, C., Chen, J., Long, Y., Deng, B., & Liu, X. (2019 a). Three-Dimensional Temperature Field Change in the South China Sea during Typhoon Kai-Tak (1213) Based on a Fully Coupled Atmosphere–Wave–Ocean Model. *Water*, *11*(1), 140. d.o.i.: https://doi.org/10.3390/w11010140

72. Wu, Z. Y., Jiang, C., Conde, M., Chen, J., & Deng, B. (2020). The long-term spatiotemporal variability of sea surface temperature in the northwest Pacific and China offshore. *Ocean Science*, *16*(1), 83–97. d.o.i.: https://doi.org/10.5194/os-16-83-2020

73. Wu, Z. Y., Jiang, C., Conde, M., Deng, B., & Chen, J. (2019 b). Hybrid improved empirical mode decomposition and BP neural network model for the prediction of sea surface temperature. *Ocean Science*, *15*(2), 349–360. d.o.i.: https://doi.org/10.5194/os-15-349-2019

74. Xiao, M., Zhang, Q., & Singh, V. P. (2015). Influences of ENSO, NAO, IOD and PDO on seasonal precipitation regimes in the Yangtze River basin, China. *International Journal of Climatology*, *35*(12), 3556–3567. d.o.i.: https://doi.org/10.1002/joc.4228

75. Xu, L., He, S., Li, F., Ma, J., & Wang, H. (2018). Numerical simulation on the southern flood and northern drought in summer 2014 over Eastern China. *Theoretical and Applied Climatology*, *134*(3–4), 1287–1299. d.o.i.: https://doi.org/10.1007/s00704-017-2341-0

76. Xue, X., Chen, W., Chen, S., & Feng, J. (2017). PDO modulation of the ENSO impact on the summer South Asian high. *Climate Dynamics*, *50*(3–4), 1393–1411. d.o.i.: https://doi.org/10.1007/s00382-017-3692-z

77. Yamagata, T., Shibao, Y., & Umatanit, S. (1985). Interannual variability of the Kuroshio Extension and its relation to the Southern Oscillation/El Niño. *Journal of the Oceanographical Society of Japan*, *41*(4), 274–281. d.o.i.: https://doi.org/10.1007/bf02109276

78. Yang, J., Gong, P., Fu, R., Zhang, M., Chen, J., Liang, S., Xu, B., Shi, J., & Dickinson, R. E. (2013). The role of satellite remote sensing in climate change studies. *Nature Climate Change*, *3*(10), 875–883. d.o.i.: https://doi.org/10.1038/nclimate1908

79. Yang, L., Chen, S., Wang, C., Wang, D., & Wang, X. (2017). Potential impact of the Pacific Decadal Oscillation and sea surface temperature in the

tropical Indian Ocean–Western Pacific on the variability of typhoon landfall on the China coast. *Climate Dynamics*, *51*(7–8), 2695–2705. d.o.i.: https://doi.org/10.1007/s00382-017-4037-7

80. Yasuda, I., Yoon, J. H., & Suginohara, N. (1985). Dynamics of the Kuroshio large meander. *Journal of the Oceanographical Society of Japan*, *41*(4), 259–273. d.o.i.: https://doi.org/10.1007/bf02109275

81. Yuan, Y., Liu, Y., & Su, J. (2001). Variability of the Kuroshio in the East China Sea during El- Nino to La- NiÑa phenomenon of 1997 and 1998. *Chinese Journal of Geophysics*, *44*(2), 196–207. d.o.i.: https://doi.org/10.1002/cjg2.132

82. Zhang, C., Li, H., Liu, S., Shao, L., Zhao, Z., & Liu, H. (2015). Automatic detection of oceanic eddies in reanalyzed SST images and its application in the East China Sea. *Science China Earth Sciences*, *58*(12), 2249–2259. d.o.i.: https://doi.org/10.1007/s11430-015-5101-y

83. Zhang, D., & McPhaden, M. J. (2006). Decadal variability of the shallow Pacific meridional overturning circulation: Relation to tropical sea surface temperatures in observations and climate change models. *Ocean Modelling*, *15*(3–4), 250–273. d.o.i.: https://doi.org/10.1016/j.ocemod.2005.12.005

84. Zheng, J., Wu, Q., Guo, Y., & Zhao, S. (2016). The Impact of Summertime North Indian Ocean SST on Tropical Cyclone Genesis over the Western North Pacific. *SOLA*, *12*(0), 242–246. d.o.i.: https://doi.org/10.2151/sola.2016-048

Web-pages referred

1. https://www.britannica.com/place/Pacific-Ocean, accessed on 1/12/2023

2. https://www.epa.gov/climate-indicators/climate-change-indicators-sea-surface-temperature, accessed on 19/12/2023

3. https://www.iucn.org/resources/issues-brief/ocean-warming, accessed on 31/12/2023

4. https://neo.gsfc.nasa.gov/, accessed on 30/12/2023

5. https://coastwatch.pfeg.noaa.gov/erddap/griddap/erdHadISST.html, accessed on 07/12/2023.

6. https://ecowatch.noaa.gov/thematic/sea-surface-temperature, accessed on 25/12/2023

7. https://ferret.pmel.noaa.gov/Ferret/, accessed on 21/03/2024

8. https://www.remss.com/measurements/sea-surface-temperature/, accessed on 10/12/2023

9. https://skybrary.aero/articles/western-pacific-warm-pool, accessed on 3/1/2023

10. https://en.wikipedia.org/wiki/Pacific_Ocean, accessed on 6/12/2023

11. https://en.wikipedia.org/wiki/Sea_surface_temperature, accessed on 11/12/2023.